

# **Development of novel trispecific immunoligands (triplebodies) to retarget natural killer cells against chronic lymphocytic leukemia**

**Inaugural-Dissertation**

zur

Erlangung des Doktorgrades

der Mathematisch-Naturwissenschaftlichen Fakultät

der Universität zu Köln

vorgelegt von

**Maulik Vyas**

aus Ahmedabad (Indien)

Copy-Star Druck & Werbung, Köln

Köln, 2017

Berichterstatter:  
(Gutachter)

1st Gutachter:

Prof. Dr. Peter Nürnberg

2nd Gutachterin:

Prof. Dr. Elke Pogge von Strandmann

Tag der mündlichen Prüfung: 30th November, 2016

## Table of contents

1. <b>Zusammenfassung</b> .....	6
2. <b>Abstract</b> .....	7
3. <b>Introduction</b> .....	8
3.1. Chronic lymphocytic leukemia (CLL).....	8
3.1.1. Current therapeutic options for CLL.....	9
3.1.2. Promising immunotherapeutic approaches for CLL.....	10
3.2. Natural killer (NK) cells.....	11
3.2.1. Activating and inhibitory receptors on NK cells.....	12
3.3. NK cell mediated surveillance in CLL patients is defective.....	15
3.4. NK cells can be retargeted against CLL cells.....	16
3.5. Mono-targeting trispecific immunoligand (triplebody) - ULBP2-aCD19-aCD19.....	18
3.6. Antigen loss variants in leukemia result in therapy resistance and tumor relapse.....	19
3.7. Dual-targeting trispecific immunoligand (triplebody) – ULBP2-aCD19-aCD33.....	20
3.8. Synergy among multiple activating receptors on NK cells for enhanced effector functions.....	22
3.9. Dual-activating trispecific immunoligand (triplebody) – ULBP2-aCD19-aNKR.....	23
3.10. Specific aims of this thesis.....	24
4. <b>Materials and Methods</b> .....	25
4.1. Cell culture.....	25
4.1.1. Drosophila Schneider 2 (S2) cells.....	25
4.1.2. Human derived cell lines and primary CLL cells.....	25
4.1.3. Primary natural killer (NK) cells: Purification and culturing.....	26
4.2. Cloning of Drosophila and mammalian expression vectors.....	27
4.2.1. Generation of pAc5.1/V5-His_ULBP1 and pAc5-STABLE1-neo_ULBP1-GFP for constitutive expression of ULBP1 in Drosophila Schneider 2 cells.....	27
4.2.2. Generation of expression vectors for expression and secretion of bispecific immunoligands and trispecific immunoligands (triplebodies) in HEK293T and CHO cells.....	29
4.3. Transfection of cloned constructs into Drosophila and mammalian cells.....	30
4.3.1. Calcium phosphate-based transfection of Schneider-2 cells.....	30
4.3.2. Lipid-based transfection of mammalian cells.....	31

4.4.	Detection of expressed proteins in both expression systems .....	32
4.4.1.	Surface expression of ULBP1 on Schneider-2 cells .....	32
4.4.2.	Western blot .....	32
4.4.3.	Specificity assessment of immunoligands: Flow cytometry and ELISA.....	33
4.5.	Flow cytometry based investigation of NK cell effector functions .....	35
4.5.1.	Analysis of NK cell effector functions in response to NKG2D and/or CD16 stimulation by Schneider-2 cells .....	35
4.5.2.	NK cell cytotoxicity and degranulation by immunoligands.....	36
4.5.3.	NK cell IFN $\gamma$ and TNF $\alpha$ secretion by immunoligands .....	38
4.6.	Animal study .....	39
4.6.1.	Role of ULBP2-aCD19-aCD19 in restriction of xenografted tumor growth in NSG mice....	39
4.7.	Software and statistics.....	40
5.	<b>Results</b> .....	41
5.1.	NKG2D stimulation requires IL2 and IL15 priming for efficient execution of NK cell effector functions .....	41
5.2.	A mono-targeting triplebody ULBP2-aCD19-aCD19 enhances NK cell dependent killing of CLL cell line – MEC1.....	48
5.3.	ULBP2-aCD19-aCD19 mediates NK cell dependent killing of primary CLL cells in allogeneic setting	55
5.4.	ULBP2-aCD19-aCD19 overcomes soluble inhibitory factors in the serum of CLL patients.....	57
5.5.	ULBP2-aCD19-aCD19 mediates NK cell dependent killing of primary CLL cells in autologous setting	59
5.6.	ULBP2-aCD19-aCD19 shows promising anti-tumor activity in immuno-deficient mouse model (NSG)	63
5.7.	A dual-targeting triplebody ULBP2-aCD19-aCD33 can simultaneously bind to all three target antigens and retains specificity for antigen loss variants .....	66
5.8.	ULBP2-aCD19-aCD33 enhances NK cell dependent killing of CD19/CD33 double positive cell lines as well as antigen loss variants.....	71
5.9.	Resting NK cells can be activated by CD16 stimulation which can be further enhanced by NKG2D co-stimulation.....	75
5.10.	A dual-activating triplebody ULBP2-aCD19-aNKR can retarget resting and freshly isolated NK cells against target cells .....	77
6.	<b>Discussion</b> .....	83

6.1. IL15 priming, either alone or in combination with IL2, is required for NKG2D-dependent NK cell effector functions.....	83
6.2. Triplebodies show better NK-cell-dependent killing of CLL and MLL target cells compared to bispecific counterparts.....	85
6.3. ULBP2-aCD19-aCD19 retargets NK cells against primary CLL cells in both, allogeneic and autologous settings.....	87
6.4. ULBP2-aCD19-aCD19 shows significant <i>in vivo</i> activity - Implications for its clinical utility against CLL .....	88
6.5. Dual-targeting and dual-activating triplebodies - Novel formats to improve clinical outcome in CLL.....	90
6.6. Future perspectives .....	91
6.7. Conclusion.....	92
<b>References</b> .....	93
<b>Abbreviations</b> .....	98
<b>Acknowledgment</b> .....	101
<b>Erklärung</b> .....	103
<b>Lebenslauf</b> .....	104

## 1. Zusammenfassung

Die chronisch lymphatische Leukämie vom B-Zell Typ (B-CLL oder CLL) beschreibt eine maligne Transformation von reifen B-Lymphozyten und ist gekennzeichnet durch eine Anhäufung von CD19<sup>+</sup> CD5<sup>+</sup> monoklonalen B-Zellen. Zur Behandlung der CLL werden zurzeit Chemoimmunotherapie und die neuerdings zugelassenen Kinase-Inhibitoren verwendet. Trotz erheblicher Fortschritte auf dem Gebiet der CLL Therapie, bleibt die Krankheit, auch aufgrund vieler rezidivierender Krankheitsverläufe, unheilbar. Natürliche Killerzellen (NK Zellen) sind in CLL Patienten intrinsisch wirksam, können aber dennoch nicht zuverlässig gegen maligne B-Zellen rekrutiert werden. Lösliche Liganden für den aktivierenden NK-Zell Rezeptor NKG2D (Natural-killer group 2 member D) sind hauptsächlich an der Inhibition der NK-Zellaktivität in der CLL beteiligt. Aus diesem Grund sind neue Immunotherapien, die zu einer NK-Zell aktivierung gegen maligne Zellen führen von großer Bedeutung.

Zu diesem Zweck habe ich rekombinante trispezifische Immunoliganden (Triplebodies) in drei verschiedenen Varianten entwickelt, die alle die NK-Zell Reaktivierung gegen CLL-Zellen zum Ziel haben. Unter autologen und allogenen Bedingungen haben wir erfolgreich den Triplebody ULBP2-aCD19-aCD19 genutzt um NK-Zellen gegen die CD19<sup>+</sup> CLL Zelllinie und gegen primäre Spendertumorzellen zu rekrutieren. Weiterhin haben wir die signifikante in vivo Wirksamkeit dieses Triplebodies im immunodefizienten Mausmodell (NSG mouse) nachgewiesen. Der Triplebody ULBP2-aCD19-aCD33, der die Tumorzellen gleich an zwei verschiedenen Clustern bindet, wurde speziell entwickelt um auch bei Antigenverlust auf Tumorzellen im Krankheitsverlauf wirksam zu sein. Die duale Spezifität dieses Triplebodies führte zur Eliminierung von CD19<sup>+</sup>CD33<sup>+</sup> Tumorzellen sowie CD19<sup>loss</sup> und CD33<sup>loss</sup> Varianten.

Um die NK-Zell Aktivierung zu verstärken wurde die dritte Variante, ein dual-aktivierender Triplebody (ULBP2-aCD19-aNKR) entwickelt. Neben NKG2D stimuliert dieser Triplebody zusätzlich NKR (ein NK-Zell Rezeptor), einen weiteren wichtigen Rezeptor auf NK Zellen mit zytotoxischer Aktivität. Dies verstärkt die anti-Tumoraktivität gegen CLL Zellen erheblich. Die klinische Relevanz der drei Triplebody-Varianten wird im Kontext der CLL diskutiert.

## 2. Abstract

Chronic lymphocytic leukemia of B cells (B-CLL or CLL) involves malignant transformation of mature B lymphocytes and is characterized by accumulation of CD19<sup>+</sup> CD5<sup>+</sup> monoclonal B cells. Chemo-immunotherapy and recently approved kinase inhibitors are currently used for the treatment of CLL patients. Despite significant advances in the field, many patients relapse and CLL remains an incurable disease. Natural Killer (NK) cells in CLL patients are intrinsically potent but fail to be activated against malignant B cells. Soluble ligands for the Natural-killer group 2 member D (NKG2D), an activating receptor on NK cells, are one of the main players in inhibiting NK cell activity in CLL. To this end, novel immunotherapies that can harness NK cells to kill CLL cells are warranted.

Here, I developed recombinant trispecific immunoligands (triplebodies) in three different formats but with a common aim to retarget NK cells against CLL. A mono-targeting triplebody ULBP2-aCD19-aCD19 utilized an NKG2D ligand ULBP2 to successfully retarget NK cells against CD19<sup>+</sup> CLL cell line and primary tumor cells in both, allogeneic and autologous settings. Further, significant *in vivo* potency of this triplebody was observed in immunodeficient (NSG) mouse model. A dual-targeting triplebody ULBP2-aCD19-aCD33 was specifically generated to target antigen loss variants in cancer. Dual specificity of this triplebody was functional and could eliminate CD19<sup>+</sup>CD33<sup>+</sup> tumor cells as well as CD19<sup>loss</sup> and CD33<sup>loss</sup> tumor variants.

Finally, the third format – a dual activating triplebody ULBP2-aCD19-aNKR was developed to enhance the activation of NK cells. NKR is another major activating receptor on NK cells and stimulation of this receptor by the triplebody greatly improved the NK cell effector functions. Clinical implications and foreseeable challenges for all three triplebodies are discussed in the context of CLL.

## 3. Introduction

### 3.1. Chronic lymphocytic leukemia (CLL)

Chronic lymphocytic leukemia of B cells (B-CLL or CLL) is a disease involving malignant transformation of B lymphocytes and is the most commonly occurring leukemia in western countries, with more prevalence in males than in females (1.7 males for every female) [1, 2]. B lymphocytes originate from hematopoietic stem cells (HSCs) in the bone marrow where they also mature and constitute the humoral arm of the adaptive immune system [3]. Mature B cells express B cell receptor and migrate through secondary lymphoid organs such as lymph nodes and spleen where they can be activated upon antigen encounter to generate and secrete antibodies in normal conditions [4]. Typically, CLL affects mature B lymphocytes within peripheral blood, bone marrow, spleen or lymph nodes and can be characterized by progressive outgrowth and accumulation of CD19 and CD5 double positive monoclonal B cells [1, 4]. CLL is considered a disease of adults, mainly because the median age when CLL is diagnosed in the USA and Europe is 70 years with only 6% of total diagnosed cases below 50 years [1]. However, incidence of very early stage CLL with no clinical symptoms in younger patients is predicted to increase owing to increased awareness and frequent blood testing [5].

In most cases, CLL patients do not show any apparent signs or symptoms and a routine blood test in most cases leads to the diagnosis [1, 6]. However, patients at very advanced stage can also be presented with enlarged lymph nodes (adenopathy), enlarged spleen (splenomegaly) and bone marrow infiltration [1]. Based on these aspects, two widely accepted staging systems were developed to classify patients within different stages of disease progression. While, the Rai system of staging CLL patients is more used in the USA, here in Europe, the Binet staging system is more preferred [7, 8]. As part of Binet staging, all patients (with adenopathy) are classified according to the areas of enlarged lymph nodes, anemia (low red blood cells) and thrombocytopenia (low platelets) [1, 8]. Binet A stage represents up to 2 enlarged

lymph node areas and no anemia and thrombocytopenia; Binet B stage represents 3 or more enlarged lymph node areas and no anemia and thrombocytopenia [1, 8]. Patients with anemia and/or thrombocytopenia irrespective of enlarged lymph nodes are classified into Binet C stage [1, 8]. These staging systems hold valuable prognostic information and are routinely used to decide the treatment options for patients [1, 6]. The University Hospital of Cologne is an active part of the German CLL study group (DCLLSG) and routinely treats many CLL patients according to the Binet staging, both, outside and within this study group. In this study, samples from several CLL patients that were staged by Binet system were collected and used for the experiments.

### **3.1.1. Current therapeutic options for CLL**

Most CLL patients at Binet A and B stages and with inactive and asymptomatic disease do not undergo any treatment [6, 9]. Treatment is only initiated for patients at advanced (Binet C) stage or with active and symptomatic disease [6, 9]. In recent years, therapeutic options for CLL have advanced considerably with approval of two novel CD20 targeting humanized antibodies (obinutuzumab and ofatumumab) and kinase inhibitors such as ibrutinib and idelalisib [1]. Ibrutinib is a selective and irreversible inhibitor of Bruton's tyrosine kinase (BTK) while idelalisib inhibits  $\delta$ -isoform of phosphoinositide 3-kinase (PI3K) [10, 11]. Patients with good physical condition receive a "gold standard" first-line chemo-immunotherapy regimen consisting a purine analogue fludarabine, cyclophosphamide and anti-CD20 chimeric antibody rituximab [1, 12].

In addition to the Binet staging, several genetic aberrations also provide prognostic and therapeutic indications [13, 14]. Loss of function of tumor suppressor TP53, by either deletion of the short arm of chromosome 17 (del(17p) or mutations in TP53 gene, is associated with resistance to genotoxic therapy that cannot be overcome by anti-CD20 antibodies [15, 16]. These patients are treated with novel kinase inhibitor, ibrutinib or idelalisib with or without rituximab [1]. Although, approval of these novel kinase

inhibitors has dramatically improved the care of unfit and poor risk (del(17p)) as well as relapsed CLL patients, many patients fail to respond and relapse following ibrutinib and idelalisib therapy. While, the mechanisms behind the resistance to idelalisib are not yet known, several acquired mutations have been recently identified in CLL patients that account for the resistance to BTK inhibitor ibrutinib [17-19].

Alternatively, hematopoietic stem cell transplantation (HSCT) is the only known curative therapeutic option for CLL patients with sustained minimal residual disease (MRD) negativity in up to half of the HSCT treated CLL patients [20]. Importantly, previously defined poor-risk factors such as del(17p) and resistance to chemo-immunotherapy do not affect the patients' response to HSCT. Despite such favorable prospects, most CLL patients do not qualify for this option due to old age and lack of fitness, while some patients that undergo HSCT suffer from chronic graft versus host disease (GvHD) [20]. Therefore, novel therapies that are milder yet effective are warranted for such treatment refractory and other elderly and unfit patients.

### **3.1.2. Promising immunotherapeutic approaches for CLL**

Over the last 30 years, researchers all over the globe have continuously explored the field of cancer immunotherapy, which is defined by the National Cancer Institute (NCI) as "...a type of biological therapy that uses substances to stimulate or suppress the immune system to help the body fight cancer". Much of its success is attributed to therapies against hematological malignancies and for many cancers including CLL, some sort of immunotherapy is now being considered as a first-line therapeutic option [21]. For CLL, above mentioned FDA approved anti-CD20 antibodies (rituximab, obinutuzumab or ofatumumab), anti-CD52 antibody alemtuzumab and other promising anti-CD19 antibodies (MEDI-551 and XmAb5574) that are currently in clinical trials are prime examples in this context. To this end, natural killer cells (NK cells) serve as an important effector population in CLL patients that mediate antibody-dependent cell mediated cytotoxicity (ADCC) response by these clinically successful antibodies

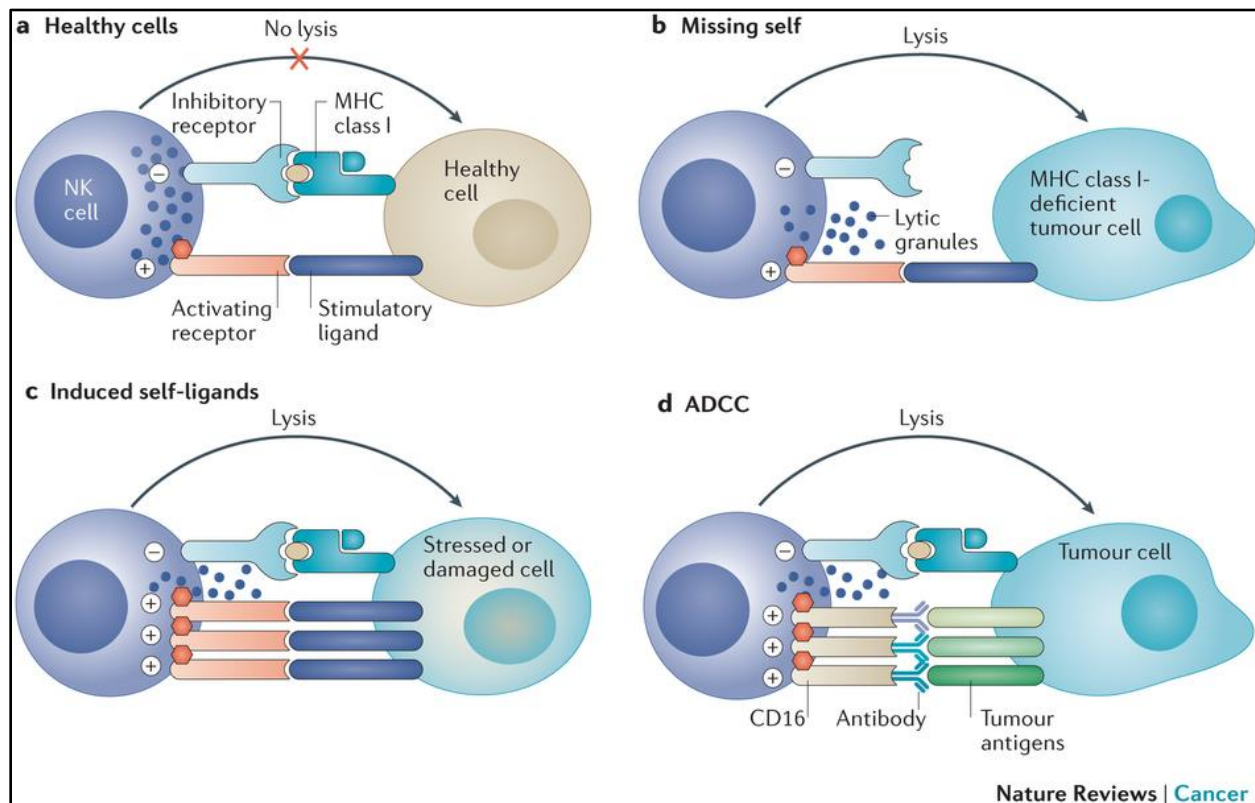
to kill cancer cells [22]. Moreover, much of the graft versus leukemia (GvL) effect of potentially curative allogeneic HSCT is also attributed to NK cell population within this graft making NK cell-based cancer immunotherapy as an attractive field of research [23, 24].

### 3.2. Natural killer (NK) cells

Natural killer (NK) cells were first identified in mice more than 30 years ago in 1975 by two independent researches named Rolf Kiessling and Ronald Herberman [25, 26], and later in the humans by Hugh Pross and Mikael Jondal [27]. These seminal studies identified NK cells as an immune cell population, which unlike T and B lymphocytes can mount a “natural” cytotoxic response against tumor cells from different donors (i.e. foreign or non-self) without pre-sensitization. Of note, my PhD work only involved working with human derived NK cells and hence, human NK cells are denoted simply as “NK cells” throughout this thesis. From more than three decades of intense work on NK cells, we now know that NK cells, along with B and T lymphocytes, are derived from the common lymphoid progenitor cells in the bone marrow. They are primarily found in bone marrow, peripheral blood and spleen but can also migrate to tonsils, thymus and uterus [24]. NK cells are classically defined as CD56 positive but do not express pan T-cell marker CD3. Further, CD56<sup>+</sup>/CD3<sup>-</sup> NK cells can be divided into two subpopulations depending upon the surface expression of CD56 [24]. While, the CD56<sup>low</sup>/CD16<sup>+</sup> NK cell subset is primarily cytotoxic and accounts for 90% of NK cells found in peripheral blood, the CD56<sup>bright</sup>/CD16<sup>-</sup> subset is predominantly located within lymph nodes and exert immune regulatory functions by producing cytokines such as IFN $\gamma$  and TNF $\alpha$  [24].

### 3.2.1. Activating and inhibitory receptors on NK cells

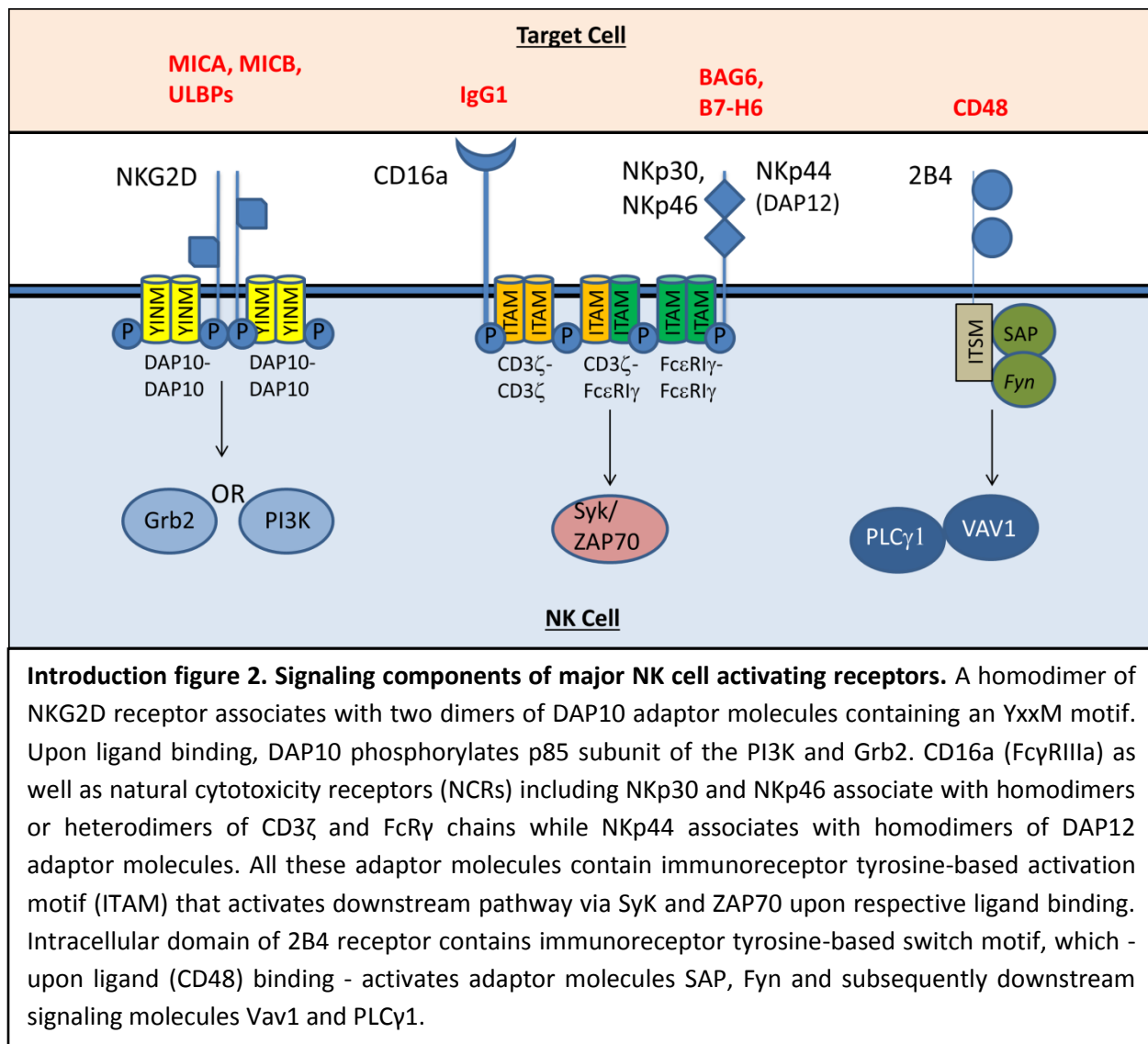
NK cells express a diverse array of activating and inhibitory receptors and, as shown in the introduction figure 1 (taken from [28]), a dynamic balance between the signaling from these two sets of receptors determine the fate of NK cell activation [29].



**Introduction figure 1. Activation of NK cells is regulated by activating and inhibitory signals.** (A) NK cells are tolerant towards healthy cells that express self MHC-I molecules and very low or no activating ligands. (B and C) Loss of expression of MHC-I molecules on virally infected or tumor cells ("Missing self") or overexpression of activating ligands on stressed or tumor cells even in the presence of self MHC-I ("Induced self-ligands") leads to the activation of NK cells. (D) NK cells can also be activated by stimulation of CD16 receptor by tumor-antigen specific antibodies in a process known as antibody-dependent cell mediated cytotoxicity (ADCC).

Killer-cell immunoglobulin-like receptors (KIRs) and CD94/NKG2A are inhibitory receptors on NK cells which upon binding to their respective ligands, HLA-A/B/C and HLA-E, send an inhibitory signal to NK cells via intracellular tyrosine-based inhibitory motif (ITIM) that results in NK cell tolerance to the “self-normal” cells [24]. Viral infection or malignant transformation of cells downregulate the HLA molecules in order to escape T cell response, but in turn, alert the NK cells to mount a killing response (also known as “missing-self” hypothesis). Moreover, stressed or transformed cells can also upregulate certain stress-induced proteins on the cell surface which serve as natural ligands for activating receptors on NK cells. In what is known as “induced-self” hypothesis, expression of ligands on target cells for NK-cell activating receptors can overcome the tolerance and activate NK cells despite the presence of same levels of self-HLA molecules [24, 29].

Several diverse activating receptors are expressed on NK cells. Some of the characterized activating receptors on NK cells include 2B4, DNAM-1 and NKG2C/CD94. One important set of receptors from the immunoglobulin superfamily are called natural cytotoxicity receptors (NCRs) and include NKp30, NKp44 and NKp46 [24]. Cell surface expression of NKp44 can only be induced in response to NK cell activation [30], while expression of NKp46 is constitutive and restricted to NK cells, making it a valuable NK cell marker [31]. Recently, proliferating cell nuclear antigen (PCNA) and mixed lineage leukemia 5 (MLL5) have been identified as natural ligands for NKp44 [32, 33], and vimentin is identified as a ligand for NKp46 [34]. NKp30 is the most studied NCR in the context of cancer immunology. BCL2-associated athanogene 6 (BAG6/BAT3) and B7 family member B7-H6 are recently discovered natural ligands for NKp30. BAG6, when expressed on the surface of exosomes, can activate NK cells via NKp30 to induce target cell killing of tumor cells and immature DCs [35, 36]. Expression of B7-H6 is more tumor-specific and is found on the surface of cells or extracellular vesicles (exosomal fractions) [37, 38].



One of the most potent and clinically utilized activating receptor on NK cells is low affinity Fc receptor FcyRIIIa or CD16a, which induces strong antibody-dependent cell mediated cytotoxicity (ADCC) response upon binding to the Fc portion of IgG antibody (Introduction figure 1d). Most clinically used antibodies for CLL and many other malignancies take advantage of CD16a receptor on NK cells [39]. NKG2D is a homodimeric type II transmembrane protein belonging to the family of C-type lectin-like receptors. Various stress-induced proteins such as MICA, MICB and UL16-binding proteins (ULBP1-6) are natural ligands for NKG2D and expressed upon infection and malignant transformation [40].

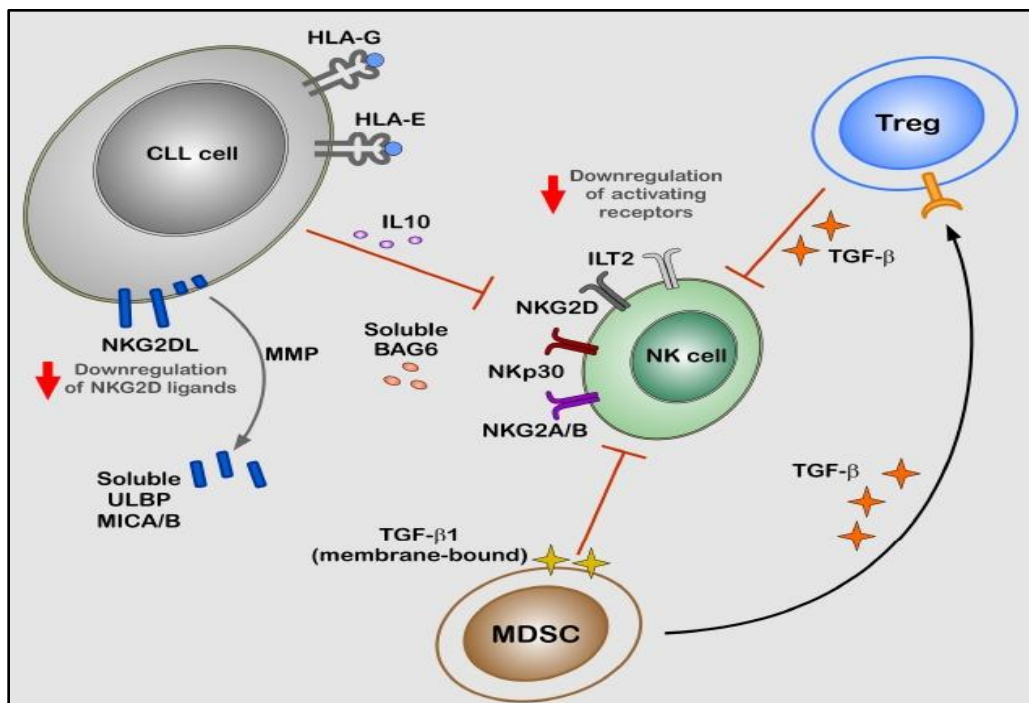
As shown in the introduction figure 2, these diverse activating receptors on NK cells associate with distinct adaptor molecules to signal for NK cell induced killing of target cells via perforin and granzyme dependent apoptosis. Of note, NK cells can also induce the extrinsic apoptosis pathway in target cells via death ligands namely tumor necrosis factors alpha (TNF $\alpha$ ), TNF-related apoptosis-inducing ligand (TRAIL) or CD95L (Fas ligand) [24].

### 3.3. NK cell mediated surveillance in CLL patients is defective

NK cells are equipped with multiple attack mechanisms and should eliminate any malignant B cells before they progress to CLL. However, CLL cells do escape NK cells and possibly other potent immune cells by mechanisms which are not yet completely understood [41]. There have been many studies to analyze the possible defects in the cross-talk between malignant B cells and NK cells in CLL patients and all studies could confirm the inability of NK cells to kill CLL cells from the same patients in an autologous setting (introduction figure 3; adapted from [41]).

The expression level of NKG2D, CD16, NKp46, DNAM-1 and 2B4 on NK cells were unaltered between CLL patients and healthy age-matched controls. However, the expression of NKp30 was found to be slightly but significantly downregulated on NK cells from CLL patients [42, 43]. Many ligands for activating and inhibitory receptors were also assessed on CLL cells which appeared to be the more probable reason for NK cell resistance. Veuillen *et al* showed that CLL cells downregulated the surface expression of NKG2D ligands ULBP1, ULBP2, MICA and MICB in order to escape NK cell response, while HLA-E, a ligand for an inhibitory receptor CD94/NKG2A, was overexpressed [44]. Previously, our lab has shown that the high levels of soluble ligands MICA/B, ULBP2 (NKG2D ligands) and BAG6 (NKp30 ligand) as well as other soluble factors in CLL plasma hampered the NK cell cytotoxicity [43]. BAG6 is an NKp30 ligand which activates NKp30 receptor when expressed on the exosomes but inhibits it in soluble form [35]. Additionally, soluble NKG2D ligands in CLL can also be used as prognostic markers [45]. In tumor cells,

matrix metalloproteinases can shed the ligands from the surface of cell or exosomal membrane and thereby evade immune stimulation [46]. In addition to these functional changes in both NK and CLL cell compartments, few studies have identified the low number of NK cells in CLL patients as a main reason for defective NK surveillance [47, 48].



**Introduction figure 3. Factors contributing in NK cell evasion of CLL cells.** Overexpression of inhibitory ligands (HLA-E) and/or downregulation or proteolytic shedding (by MMPs) of activating ligands (for NKG2D and NKp30 receptors) on CLL cells allow NK cell escape. Soluble factors such as IL10, TGF $\beta$  and ligands for activating NK cell receptors can inhibit NK cells, possibly by downregulating the correspondent receptors on the surface of NK cells.

### 3.4. NK cells can be retargeted against CLL cells

Researchers have worked on different therapeutic strategies to empower NK cells against malignancies including CLL. Checkpoint blockade is one such strategy that involves blocking of the inhibitory receptors on immune cells to reverse the immune suppression by tumor cells. Recent success in blocking of inhibitory receptors on T cells such as CTLA-4 and PD-1 by FDA approved antibodies (checkpoint

inhibitors) has led to the development of novel checkpoint inhibitors for NK cells [49, 50]. Two promising antibodies blocking NK cell inhibitory receptors KIR (Lirilumab, Innate Pharma) and CD94/NKG2A (IPH2201, Innate Pharma) are currently in clinical trials (NCT01714739 and NCT02331875, respectively) [51]. Alternatively, a few studies particularly focused on expanding NK cell population to increase the above mentioned low NK:CLL ratio in CLL patients [47, 52]. To this end, advances in the field of adoptive NK cell transfer have been reviewed and suggested the use of NK cells from different sources such as haploidentical donors and NK cell lines (e.g. NK-92) [53, 54].

We and others have utilized recombinant DNA technology to generate mAb-based bispecific and trispecific constructs in different formats to activate NK cells. I have reviewed the progress in the field of constructs activating, both, T and NK cells against cancer and also suggested two terms to clearly distinguish different formats of such constructs [55]. The term '**immunoligand**' is used for recombinant constructs, which utilize natural ligands for the activating immune receptors fused to tumor-specific single chain fragment variable (scFv) part. While "**immunoconstruct**" can be considered as recombinant constructs that utilize antibody-derived components to target both immune cells and target cells. Several bispecific and trispecific immunoconstructs have been studied, all with an anti-CD16 scFv moiety to activate NK cells (via CD16a receptor), while, NK cells were specifically retargeted against various tumor entities by respective scFv moieties against tumor antigens such as CD30, CD33, CD123, and CD19 [56-61].

We particularly focused on developing recombinant immunoligands containing human NKG2D ligand ULBP2 fused to tumor antigen specific scFv. The idea is that these immunoligands will bind specifically to the tumor antigens and will coat the tumor cells with ULBP2 ligand. This will turn the otherwise NK cell resistant tumor cells visible to NK cells for attack. The first immunoligand ULBP2-BB4 retargeted NK cells (by ULBP2) against CD138<sup>+</sup> multiple myeloma cells (by BB4 scFv) (cell lines and primary patient tumor

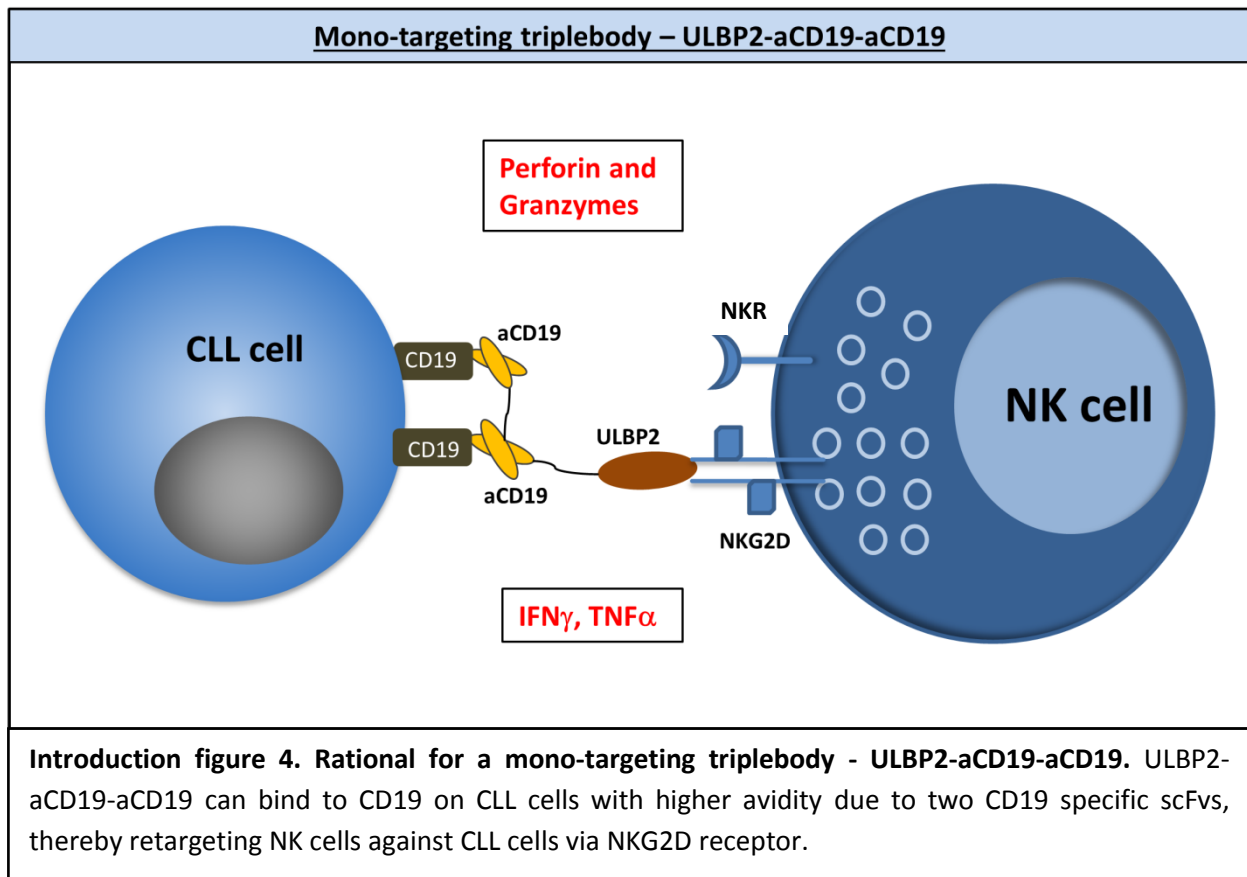
cells) and also showed significant antitumor activity in a xenograft mouse model [62]. Subsequently, two additional immunoligands in similar formats but targeting different tumor antigens [CEA and prostate-specific membrane antigen (PSMA)] also validated our approach [63, 64]. CEA and PSMA are tumor-specific antigens with frequent overexpression on colon and prostate cancers, respectively. Recently, other groups also developed NKG2D targeting immunoligands, albeit using an alternative NKG2D ligand MICA. This CD20 (7D8 scFv) specific immunoligand MICA-7D8 could also retarget NK cells against CD20<sup>+</sup> lymphoma cells thereby validating this approach [65].

As reviewed above, CLL cells frequently downregulate or shed ligands for activating NK receptors including NKG2D as a mean to evade NK cell response. Therefore, our immunoligand-based strategy to coat CLL cells with ULBP2, a natural ligand for NKG2D, should re-sensitize them for NK cell mediated immune response. To this end, following the encouraging results with bispecific immunoligands, one aim of this thesis was to generate the trispecific immunoligand containing ULBP2 to activate and retarget NK cells against CLL cells.

### **3.5. Mono-targeting trispecific immunoligand (triplebody) - ULBP2-aCD19-aCD19**

The term “mono-targeting triplebody” represents a trispecific immunoligand but targeting a single antigen on cancer cells. ULBP2-aCD19-aCD19 contained ULBP2 and two CD19 specific scFvs in a single polypeptide chain separated by a glycine-serine linker to confer the flexibility to each arm.

CD19, a transmembrane glycoprotein, is expressed on various B cell malignancies corresponding to different stages of B cell maturation including CLL. Expression of CD19 is found to be very low on healthy B cells while is undetectable on hematopoietic stem cells making it an attractive target for immunotherapy [55]. CD19 antigen is clinically validated by a FDA approved bispecific T cell engager (BiTE<sup>®</sup>) Blinatumomab [66] as well as by promising anti-CD19 antibodies and CD19 specific CAR-T cell therapy against CLL [1, 55].



As shown in the introduction figure 4, it is expected that ULBP2-aCD19-aCD19 will bind specifically to CD19 antigens on CLL cells allowing free ULBP2 ligand on the surface of CLL cells to interact with the NKG2D receptor on NK cells, thereby, bringing NK cells in the close proximity of CLL cells. This way NK cells can be activated to specifically kill CLL cells and to secrete cytokines such as IFN $\gamma$  and TNF $\alpha$ .

### 3.6. Antigen loss variants in leukemia result in therapy resistance and tumor relapse

Cancer, though originating from a single cell, consists of a pool of heterogeneous cell clones with diverse genetic and phenotypic makeup. During the course of progression, tumor cell clones negative for the expression of a particular tumor antigen can be naturally selected and may outgrow the clones that express that antigen or the heterogeneous clones can simply coexist [67]. In such cases, targeted

immunotherapies specific for a single tumor antigen, including mAb or immunoligand-based therapies, can be partially successful but may give rise to antigen negative tumor relapse.

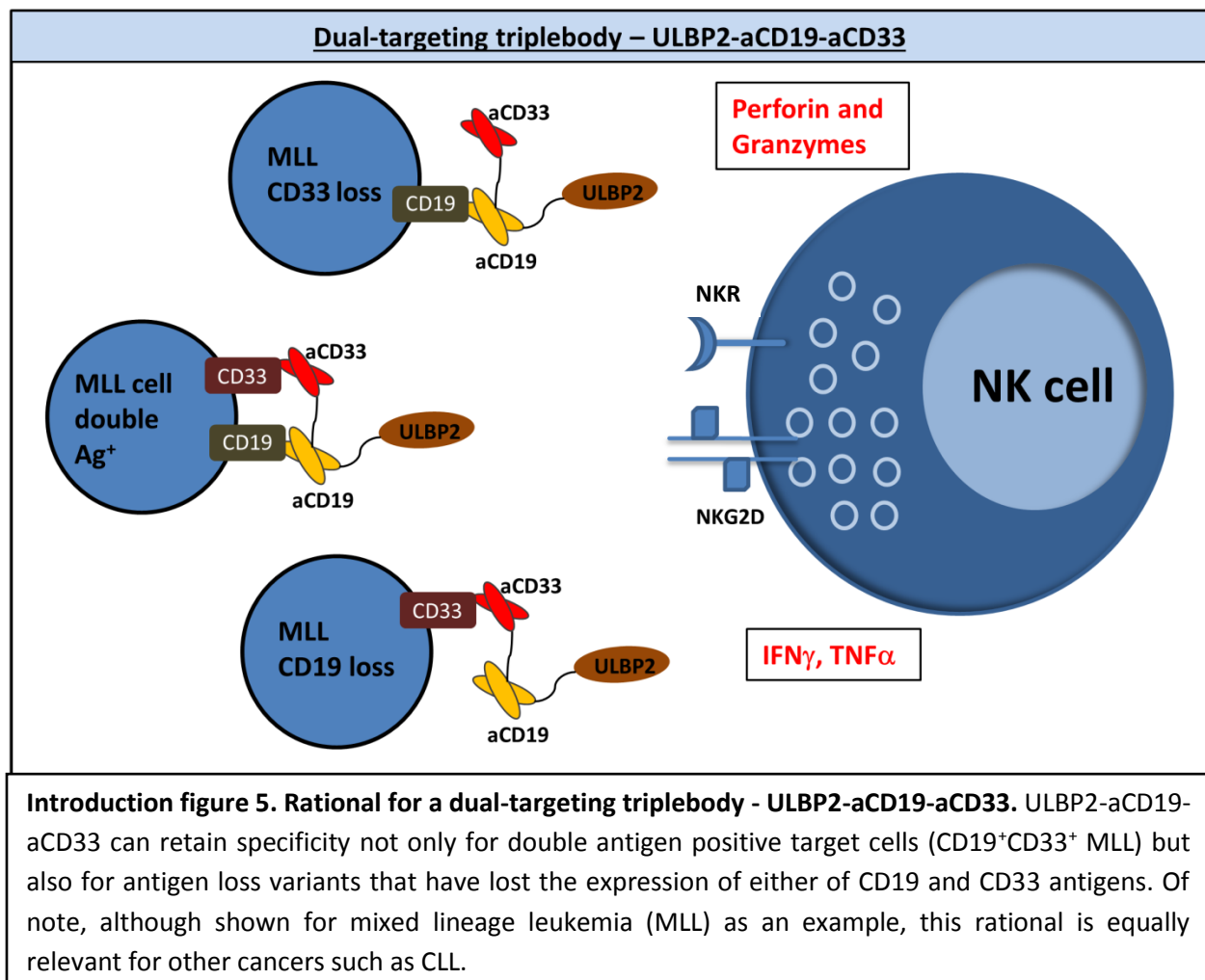
Additionally, there are reports suggesting the direct role of targeted therapies in antigen loss on tumor cells. CLL and mixed lineage leukemia (MLL) both have been studied in this regard. Mostly, mAb therapies against CLL have caused surface antigens to be lost from the cell surface [68-71]. Mixed lineage leukemia (MLL) is childhood leukemia with a very poor prognosis due to rearrangements of the mixed lineage leukemia (MLL) gene on chromosome 11q23 and characteristically expresses a typical lymphoid marker CD19 and a myeloid marker CD33 [72]. Recently, few cases of B cell acute lymphoid leukemia (B-ALL) with MLL rearrangements were reported, where CD19 directed CAR T cell therapy resulted in the relapse of clonally related acute myeloid leukemia with typical myeloid expression patterns, a phenomenon termed as a lineage switch [72].

Taken together, tumor relapses involving antigen loss variants are often more aggressive and difficult to manage which needs to be addressed in designing novel immunotherapies to move ahead in the direction of complete cancer cure. Thus, taking advantage of the triplebody format, dual-targeting trispecific immunoligands (triplebodies) were designed in this project.

### **3.7. Dual-targeting trispecific immunoligand (triplebody) – ULBP2-aCD19-aCD33**

The term “dual-targeting triplebody” represents a trispecific immunoligand targeting two distinct antigens on cancer cells. ULBP2-aCD19-aCD33 contained ULBP2 as a natural ligand and a CD19 specific and a CD33 specific scFv in a single polypeptide chain separated by a glycine-serine linker to confer the flexibility to each arm. The lymphoid antigen CD19 was already introduced above (in chapter 3.5) and the sialic acid binding transmembrane receptor CD33, which is typically expressed by myeloid cells, is also a clinically validated antigen [73].

In this thesis, ULBP2-aCD19-aCD33 was developed to assess whether dual specificities can eliminate antigen loss variants where a mono-targeting approach would fail (introduction figure 5). Mixed lineage leukemia (MLL) with dual expression of CD19 and CD33 was used as a model in this regard, but this approach is applicable to any other cancer type including equally relevant CLL.



### 3.8. Synergy among multiple activating receptors on NK cells for enhanced effector functions

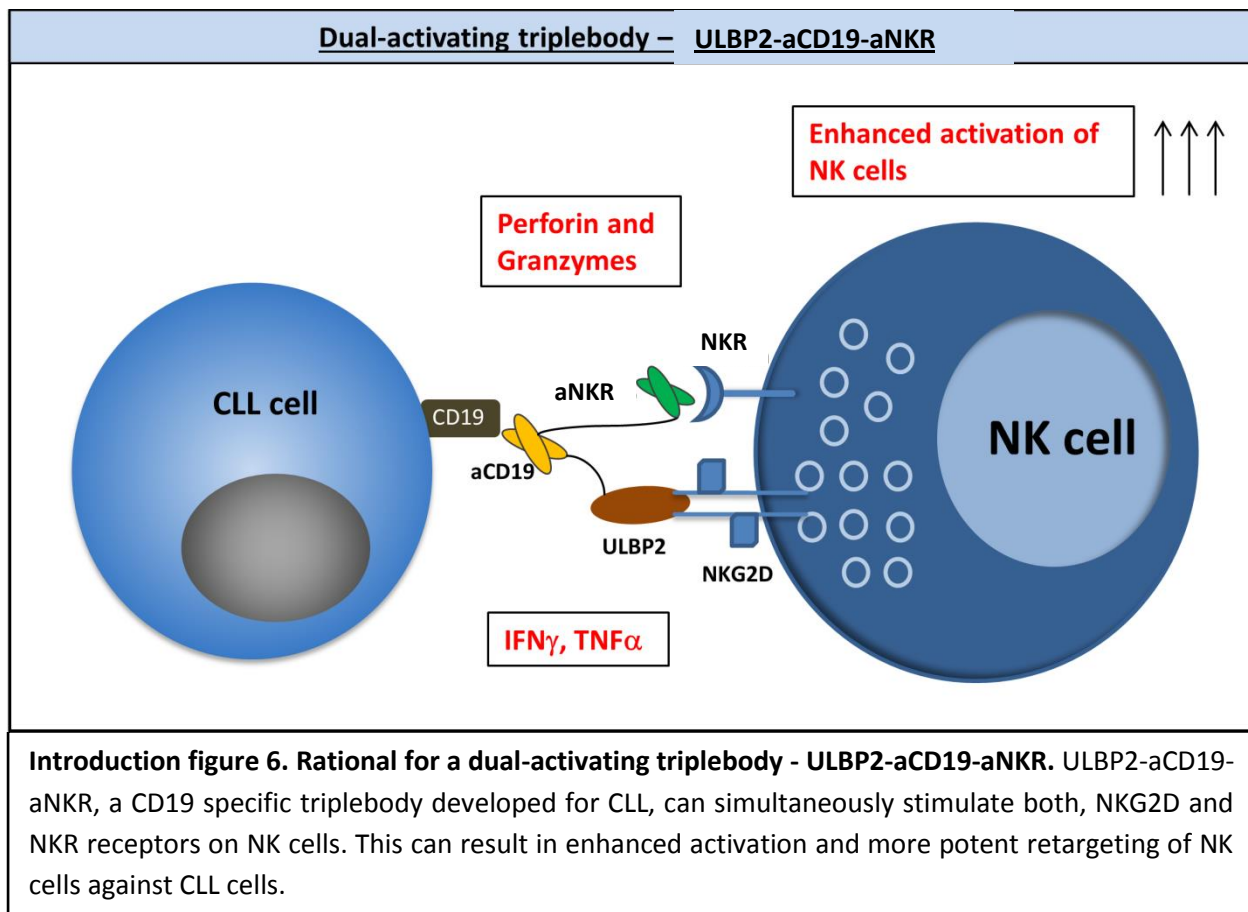
As already shown before, NK cells can be retargeted by multiple activating receptors, many of which utilize distinct adaptor molecules and signaling components to activate NK cells. To assess an individual role of a single activating receptor on NK cell in response to target cells is not straightforward, as typical target cells such as tumor cells often express several known and unknown NK cell ligands. To address these specific questions, Eric Long's group developed a *Drosophila* expression system with regulated expression of a single or a combination of NK cell ligands without the interference of any other known or unknown NK cell ligands [74]. *Drosophila* Schneider-2 (S2) cell line, derived from a late stage embryo of *Drosophila melanogaster*, do not express any ligands for human NK cells and are easy to transfect and culture and therefore, served as a useful system to study NK cell activation [74, 75].

Synergy among activating receptors such as NKG2D, LFA-1, CD16 and 2B4 was explored in resting NK cells using transfected Schneider-2 cells expressing respective human NK ligands. Interestingly, this approach revealed that receptors can signal independently in resting NK cells but this is in most cases not sufficient to trigger all functional aspects such as adhesion, granule polarization and degranulation, which are all essential for cytotoxicity [76, 77]. For example, LFA-1 engagement triggers adhesion and granule polarization while CD16 activation signals for degranulation – only synergistic activation of both can mediate cytotoxicity by resting NK cells [78]. Similarly, synergistic activation of NKG2D and 2B4 receptors can induce resting NK cells to kill the target cells while individual stimulation of NKG2D or 2B4 is not sufficient [76].

Schneider-2 cells were also used in this thesis to address the role of cytokine priming on NKG2D stimulation alone or in combination with CD16a stimulation on NK cells.

### 3.9. Dual-activating trispecific immunoligand (triplebody) – ULBP2-aCD19-aNKR

The term “dual-activating triplebody” represents a trispecific immunoligand with two arms activating distinct receptors on NK cells and one scFv against a single tumor antigen. ULBP2-aCD19-aNKR contained a CD19 specific scFv moiety flanked by ULBP2, a natural ligand for NKG2D, and NKR activating scFv, all in a single polypeptide chain separated by a glycine-serine linker to confer the flexibility to each arm (introduction figure 6).



### 3.10. Specific aims of this thesis

Taken together, CLL is a relevant disease for the development of novel NK cell based immunotherapies. Our idea is to coat (opsonize) CLL cells with NK cell activating ligands in the form of different triplebodies to re-sensitize them for NK cell surveillance. Antigen loss from tumor cells, via natural or therapy induced mechanisms, is particularly addressed in this regard. Triplebodies in three different formats will be studied in this thesis to address the following topics.

- i. To assess whether priming of NK cells with different cytokines (IL2, IL12, IL15, IL18) can modulate NKG2D receptor induced NK cell effector functions. To this end, Schneider-2 cells expressing ULBP1 (NKG2D ligand) are used.
- ii. To develop a mono-targeting triplebody ULBP2-aCD19-aCD19 to retarget NK cells via NKG2D receptor against CLL cell line and primary CLL cells. Particularly, to assess the ability of ULBP2-aCD19-aCD19 to overcome NK cell inhibitory factors in CLL patients' serum. To test the tumor limiting effects of ULBP2-aCD19-aCD19 in an immunodeficient xenograft mouse model.
- iii. To develop a dual-targeting triplebody ULBP2-aCD19-aCD33 with a view to retarget NK cells against antigen loss variants in cancer. To use CD19<sup>+</sup>CD33<sup>+</sup> MLL cells as targets in order to test the proof-of-principle that can also be applied to other cancers such as CLL.
- iv. ULBP2-aCD19-aNKR was developed to assess whether activation of NKR in addition to NKG2D receptor on NK cell confers any advantage in terms of NK cell cytotoxicity and cytokine secretion in response to CLL cells

## 4. Materials and Methods

### 4.1. Cell culture

#### 4.1.1. *Drosophila* Schneider 2 (S2) cells

The Schneider 2 (S2) cell line was derived from a late stage embryo (20-24 days old) of *Drosophila melanogaster* and shares many characteristics from a macrophage-like lineage [75]. A frozen aliquot of Schneider 2 cells was provided in DES®-Blasticidin support kit (Cat. Nr. K515001, ThermoFisher Scientific). Schneider 2 cells were cultured in Schneider's *Drosophila* medium (Cat. Nr. 21720-024, ThermoFisher Scientific) supplemented with 10% fetal bovine serum (Invitrogen). Schneider 2 cells were grown at 27°C without CO<sub>2</sub> as a suspension cell line and cells were passaged every 2-3 days. Cells were regularly checked for mycoplasma contamination by polymerase chain reaction (PCR) and only cell lines negative for mycoplasma contamination were used for experiments.

#### 4.1.2. Human derived cell lines and primary CLL cells

Human embryonic kidney-derived cell line 293T (HEK293T), chinese hamster ovary cell line CHO, chronic B cell leukemia cell line MEC1, pro-B ALL-derived cell line SEM, pre-B phenotypic cell line BV173 and acute myeloid leukemia cell line HL60 were purchased from DSMZ. HEK293T and CHO were cultivated in Dulbecco's MEM medium (Invitrogen), SEM was cultivated in Iscove's MDM (Cat. Nr. 12440053, Invitrogen) while MEC1, HL60 and BV173 were cultivated in RPMI-1640 medium (Cat. Nr. 61870010, Invitrogen). All cells were cultivated at 37°C and in 5% CO<sub>2</sub> atmosphere. Mediums for the cell lines were supplemented with 10% (vol/vol) heat-inactivated fetal calf serum (Invitrogen) and 50 µg/mL penicillin, 50 µg/mL streptomycin and 2 mM L-glutamine.

Peripheral blood from chronic lymphocytic leukemia patients (CLL) was collected by CLL biobank, University Hospital Cologne and B cells were purified on the same day. Freshly purified CLL were

received from the CLL biobank and were cultured overnight in Panserin 411S (Cat. Nr. P04-7411S1, Pan-Biotech, Germany). Sampling of blood samples (CLL patients and healthy donors for NK cell purification (next)) was approved by the local ethics committee of the University of Cologne under reference numbers 11-140 and 08-275, and donors provided written consent in accordance with the Declaration of Helsinki.

**Table: Cell lines**

Cell line	Origin
<b>Drosophila Schneider-2</b>	Late stage (20–24 hours old) <i>Drosophila Melanogaster</i> embryos
<b>HEK293T</b>	Human embryonic kidney
<b>CHO</b>	Ovary of the Chinese hamster
<b>MEC1</b>	Peripheral blood of a chronic B-cell leukemia (B-CLL) patient
<b>HL60</b>	Acute promyelocytic leukemia patient
<b>BV173</b>	B cell precursor leukemia cells from the peripheral blood of a patient with chronic myeloid leukemia (CML) in blast crisis
<b>SEM</b>	B cell precursor leukemia cells from the peripheral blood of a patient at relapse of acute lymphoblastic leukemia (ALL)

#### 4.1.3. Primary natural killer (NK) cells: Purification and culturing

Buffy coats from healthy donors were provided by the blood bank of University Hospital Cologne. Blood sampling was approved by the local ethics committee of the University of Cologne under reference numbers 11-140 and 08-275. Peripheral blood mononuclear cells (PBMCs) were isolated from the buffy

coats by Ficoll-Paques density gradient centrifugation. These PBMC preparations were used to purify NK cells by negative selection using NK cell isolation kit (Miltenyi) and auto-MACS Pro Separator (Miltenyi, Bergisch-Gladbach, Germany) according to manufacturer's instructions. In brief, depending upon the desired number of NK cells, specific number of PBMC were stained with a cocktail of primary antibody (specific for all immune cells but NK cells in PBMC) and magnetic beads coupled secondary antibody. The preparation was washed and run through the magnetic column to isolate non-labeled NK cells from the antibody bound other immune cells (negative selection). Purified polyclonal NK cells were cultivated overnight at 37°C in 5% CO<sub>2</sub> atmosphere in Iscove's Modified Dulbecco's Medium (IMDM) + GlutaMAX™ (Invitrogen) supplemented with 10% (vol/vol) heat-inactivated fetal calf serum (Invitrogen) and 50 µg/mL penicillin, 50 µg/mL streptomycin and recombinant cytokine(s). Purified NK cells were primed by different cytokines depending upon the specific requirement of an experiment. Resting NK cells were incubated with recombinant human IL2 (10 U/ml). Additionally, NK cells were also primed by individual or combinations of following cytokines (also indicated in the respective legends of the figures): recombinant human IL2 (200 U/ml); IL15 (10 ng/ml); IL12 (10 ng/ml); IL18 (100 ng/ml).

## **4.2. Cloning of *Drosophila* and mammalian expression vectors**

### **4.2.1. Generation of pAc5.1/V5-His\_ULBP1 and pAc5-STABLE1-neo\_ULBP1-GFP for constitutive expression of ULBP1 in *Drosophila* Schneider 2 cells**

A *Drosophila* constitutive vector pAc5.1/V5-His\_ULBP1 was a kind gift by Dr. Yenan Bryceson (Karolinska Institute, Sweden) after we bought an empty pAc5.1/V5-His vector from Invitrogen (Cat. Nr. V411020) as it was a part of license agreement. pAc5.1/V5-His is a 5.4 kb expression vector and contains the *Drosophila* actin 5C (Ac5) promoter that allows high level, constitutive expression of desired protein in *Drosophila* cells. pAc5.1/V5-His vector contains an ampicillin resistance gene for selection of transformants in *E. coli*. However, it does not contain other selectable markers for selection of stably

transfected *Drosophila* cells and hence, the selection vector (pCoHygro or pCoBlast) needs to be co-transfected to achieve stable cell lines exhibiting constitutive expression of the protein of interest. Moreover, it also contains C-terminal V5 epitope (Gly-Lys-Pro-Ile-Pro-Asn-Pro-LeuLeu-Gly-Leu-Asp-Ser-Thr) and polyhistidine (6xHis) tag for detection and purification of the expressed protein.

Initial small amount of pAc5.1/V5-His\_ULBP1 was used for transformation of competent *recA*, *endA* *E.coli* strain TOP10 (One Shot® TOP10 chemically competent *E.coli*; Cat. Nr. C404010; Invitrogen). Transformation was done by mixing 1 ng of plasmid DNA with 100 µl of competent TOP10 cells on ice for 30 min followed by heat shock at 42°C for 90 sec and 2 min cooling on ice. Transformed bacteria were spread onto 2YT agar plates with 100 µg/ml ampicillin concentration. 2YT-medium was prepared by dissolving 16 g Bacto Tryptone, 10 g Bacto Yeast and 5 g NaCl in 1 liter of ddH<sub>2</sub>O. To prepare 2YT agar, 15g agar was dissolved in 1 liter of 2YT-medium. The plates were incubated at 37°C and on next day one clone was picked from the plate and 2YT medium was inoculated. This maxiprep sample was incubated at 37°C in shaker incubator for overnight. Following day, plasmid DNA was isolated from the maxiprep sample as instructed in manufacturer's protocol (NucleBond Xtra® Maxiprep Kit; Cat. Nr. 740414.50, MN). Plasmid DNA was eluted ddH<sub>2</sub>O and was stored at -20°C for further use. A selection vector pCoBlast (DES®-Blasticidin support kit (Cat. Nr. K515001, ThermoFisher Scientific)) is a 3.9 kb vector containing a *Drosophila* copia promoter for high-level, constitutive expression of the blasticidin resistance gene (*bsd*) and was generated in same way and was stored at -20°C for further use.

Another variant of above described *Drosophila* constitutive expression vector is pAc5-STABLE1-neo which allows multicistronic expression of GFP and Neomycin resistance gene under Ac5 promoter. Moreover, it also allows N-terminal or C-terminal fusion of desired gene sequence to GFP to generate GFP-fused protein of interest. Plasmid pAc5-STABLE1-neo was a gift from Rosa Barrio & James Sutherland (Addgene plasmid # 32425). ULBP1 cDNA was PCR amplified from pAc5.1/V5-His\_ULBP1

vector to replace the restriction enzyme sites and was later cloned into pAc5-STABLE1-neo vector at the N-terminal part of GFP sequence to generate pAc5-STABLE1-neo\_ULBP1-GFP.

**Table: Plasmids**

Plasmid	Protein Product	Promoter	Tags
pAc5.1_ULBP1	ULBP1	Drosophila Ac5	-
pAc5_STABLE1_ULBP1	ULBP1-GFP	Drosophila Ac5	GFP
pL(aCD19scFv)	Anti CD19 scFv	CMV	6xHis
pL(aCD33scFv)	Anti CD33 scFv	CMV	6xHis
pL(ULBP2-aCD19)	ULBP2-aCD19	CMV	6xHis; c-Myc
pL(ULBP2-aCD33)	ULBP2-aCD33	CMV	6xHis; c-Myc
pL(ULBP2-aCD19-aCD19)	ULBP2-aCD19-aCD19	CMV	6xHis; c-Myc
pL(ULBP2-aCD19-aCD33)	ULBP2-aCD19-aCD33	CMV	6xHis; c-Myc
pL(ULBP2-aCD19-aNKR)	ULBP2-aCD19-aNKR	CMV	6x His; c-Myc

#### 4.2.2. Generation of expression vectors for expression and secretion of bispecific immunoligands and trispecific immunoligands (triplebodies) in HEK293T and CHO cells

A total of three different formats of triplebody and their respective bispecific counterparts were generated in this project. A mono-targeting triplebody ULBP2-aCD19-aCD19 and its bispecific counterpart ULBP2-aCD19 was generated with view to enhance the avidity for the target cells. A dual-targeting triplebody ULBP2-aCD19-aCD33 was generated to specifically target antigen loss variants where ULBP2-aCD19 and ULBP2-aCD33 served as its bispecific counterparts. A dual-activating triplebody ULBP2-aCD19-aNKR was generated to enhance the activation of NK cells. A blocking construct – aCD19 single chain (scFv) lacked ULBP2 and was used to block CD19 antigen in some experiments. Cloning of a bispecific immunoligand ULBP2-BB4 has been described in detail previously and was used as a backbone

for the following clonings [62]. Human CD19-specific scFv (derived from 4G7 hybridoma, mouse IgG1), Human CD33-specific scFv and Human NKR-specific scFv (derived from XYZ hybridoma, mouse IgG1) were kind gifts by Dr Georg Fey (University of Erlangen-Nuremberg, Erlangen, Germany). The sequence of CD19- and CD33-specific scFv was optimized for improved expression and secretion in eukaryotic system (OptimumGene™ algorithm, Genscript Ltd.). Optimized aCD19scFv and aCD33scFv were cut at SfiI and NotI restriction sites and were cloned into the eukaryotic expression vector pL (ULBP2-BB4) to generate pL (ULBP2-aCD19) and pL (ULBP2-aCD33), respectively. Expression vector pL (previously designated as pMS) was described previously. In brief, pL is a derivative of the pSecTag2 plasmid (Invitrogen) that contains the IVS/IRES-EGFP sequence of the pIRES-EGFP plasmid (Clontech). Cloning of control constructs pL (aCD19) and pL (aCD33) was accomplished by PCR amplifying each scFv, thereby adding NheI site followed by human Ig kappa (Igk) light-chain signal peptide in front of aCD19 and aCD33 scFv sequence, respectively, and cloning of each resulting PCR product into an empty pL vector. Finally, to generate all three triplebodies, aCD19, aCD33 and aNKR scFvs were PCR amplified from their respective backbones to replace SfiI by NotI restriction site at the 5' end to generate each scFv sequence flanked by NotI sites. Each PCR product (scFv sequence) was cloned into a linearized pL (ULBP2-aCD19) to generate pL (ULBP2-aCD19-aCD19), pL (ULBP2-aCD19-aCD33) and pL (ULBP2-aCD19-aNKR).

### **4.3. Transfection of cloned constructs into Drosophila and mammalian cells**

#### **4.3.1. Calcium phosphate-based transfection of Schneider-2 cells**

To generate stable Schneider-2 cell line expressing ULBP1, cells were co-transfected by an expression vector pAc5.1/V5-His\_ULBP1 for constitutive expression of ULBP1 and a selection vector pCoBlast for selection of stably transfected cells in 19:1 ratio using calcium phosphate transfection kit (ThermoFisher Scientific) according to manufacturer's protocol. In brief,  $3 \times 10^6$  cells were seeded in a single well of a 6-well plate in complete Schneider's Drosophila medium and on following day a mixture of solution A (2M

CaCl<sub>2</sub> + 19µg pAc5.1\_ULBP1 + 1µg pCoBlast) and a solution B (2x Hepes Buffered Saline (HBS)) was added dropwise to the cells and cells were further cultured for 2 days before analyzing the transient expression of ULBP1 and starting the Blasticidin selection. For selection of ULBP1 positive stable clones, cells were cultured for 2-3 weeks in presence of 25 µg/ml Blasticidin and cell surface expression of ULBP1 was monitored by FACS. A stable ULBP1 expressing Schneider-2 cell line (S2-ULBP1) was generated when ≈100% population was found to be positive for cell surface expression of ULBP1. Once selected, S2-ULBP1 cell line was maintained in complete Schneider's Drosophila medium with 25 µg/ml Blasticidin and surface expression of ULBP1 was regularly monitored before experiments to maximize reproducibility.

#### 4.3.2. Lipid-based transfection of mammalian cells

For expression of cloned constructs, HEK293T cells were transfected using Lipofectamine 2000 (Invitrogen) according to manufacturer's instructions. In brief, 4 µg of plasmid DNA and 10 µl of Lipofectamine were mixed to allow DNA-lipid complex formation. Once, incubated together the mixture was used to transfect 1 x 10<sup>6</sup> HEK293T cells in a 6 well tissue-culture plate (pre-seeded on the previous day). Two days after transfection, cells were transferred to a 75 cm<sup>2</sup> medium flask (T75, Sarstedt) and were grown in RPMI-1640 + GlutaMAX™ (Invitrogen) supplemented with 200 µg/ml Zeocin (Invitrogen) for selection of stable clones. Following 2–3 weeks of selection and cultivation, stably transfected polyclonal clones were visible under fluorescence microscope, as all cloned constructs were expressed simultaneously with enhanced green fluorescent protein (EGFP) encoded by a bicistronic mRNA. For more efficient productivity, transfected HEK293T cells were further cultivated in serum-free CD293 medium (Invitrogen) and supernatant was collected every 2 to 3 days for up to one month. The constructs which contained ULBP2 at the N-terminal were secreted into the S/N due to the inherent leader sequence of ULBP2 protein while the secretion of the blocking constructs aCD19scFv and

aCD33scFv was facilitated by Igk-leader sequence at the N-terminal. The purification of His-tagged recombinant constructs was achieved by immobilized metal affinity chromatography (IMAC) using Ni-NTA Sepharose (Qiagen) according to manufacturer's protocol and constructs were eluted in elution buffer containing 250 mM imidazole. Subsequently, eluted constructs were dialyzed in PBS buffer.

#### **4.4. Detection of expressed proteins in both expression systems**

##### **4.4.1. Surface expression of ULBP1 on Schneider-2 cells**

Both, ULBP1-expressing and wild type Schneider-2 cells were washed and resuspended in FACS buffer (PBS containing 0.2 % BSA and 0.2 % NaN<sub>3</sub>) at 1x10<sup>6</sup> cells/ml. 1x10<sup>5</sup> cells were stained with either relevant isotype antibody or mouse anti-human ULBP1 antibody for 30 min on ice. After thoroughly washing the unbound antibody, specifically bound primary antibody was detected by secondary phycoerythrin (PE) labeled antibody on ice in the dark. For exclusion of dead cells, 7-AAD (BioLegend) was added prior to measurement and only negative cells were included in analysis. FACS was performed on Gallios (Beckman Coulter).

##### **4.4.2. Western blot**

Purified bispecific immunoligands and triplebodies were mixed with Laemmli sample buffer (250mM Tris pH 7, 10% SDS, 50% Glycerol, 100mM DTT, 0,01% Bromophenol blue) and cooked at 95°C for 5 min and were subsequently loaded onto 10% SDS-polyacrylamide gels. The samples were separated for 1:30 hours at constant 150 V and were transferred to the nitrocellulose membrane for further 1:30 hours at constant 0.35 Amp. Blots were overnight blocked at 4°C by 5 % non-fat milk (in 1x PBST) and on next day were incubated with primary c-Myc tag specific antibody (in 5 % milk) and HRP-tagged secondary antibody for 1 hour each. Proteins were detected with ECL (Thermo Scientific) using the digital Intas ChemoCam Imager.

#### 4.4.3. Specificity assessment of immunoligands: Flow cytometry and ELISA

Specificity of immunoligands to the respective target antigens (CD19 and/or CD33) was assessed by flow-cytometry (FACS). To this end, MEC1 (CD19<sup>+</sup>), HL60 (CD19<sup>-</sup>), BV173 (CD19<sup>+</sup>CD33<sup>+</sup>) and SEM (CD19<sup>+</sup>CD33<sup>+</sup>) cell lines were mainly used for following experiments. For all FACS-based specificity experiments,  $1 \times 10^5$  cells resuspended in FACS buffer (PBS containing 0.2 % BSA and 0.2 % NaN<sub>3</sub>) were used per tube. Cells were then incubated with 10 µg/ml of a bi- or tri-specific immunoligand for 30 min on ice. Depending upon the experiment, CD19 and/or CD33 antigens were blocked on the cell line by addition of 20 µg/ml blocking constructs (aCD19scFv or aCD33scFv, respectively) prior to the incubation with the respective immunoligand in order to confirm the specificity of the latter. After thorough washing, bound immunoligands were stained by either mouse antibody against c-Myc tag (present on immunoligands) or by recombinant human NKG2D-Fc receptor that could bind to free ULBP2 moiety of immunoligand. Staining by NKG2D-Fc receptor could further confirm the ability of immunoligands to bind tumor antigen and NKG2D receptor simultaneously. Finally, PE-labeled anti-mouse antibody or AF647-labeled anti-Fc antibody could detect the c-Myc specific mAb or NKG2D-Fc receptor, simultaneously. Further, a CD19<sup>+</sup>/CD33<sup>-</sup> cell line MEC1 was used to assess the simultaneous binding ability of a dual-targeting immunoligand ULBP2-aCD19-aCD33.

Here, recombinant human receptors NKG2D-Fc and CD33-FLAG (or DDK) were used in the same tube to detect CD19 antigen bound immunoligand. AF647-labeled anti-Fc antibody and PE-labeled FLAG (DDK) specific antibody provided the signals. For exclusion of dead cells, 7-AAD (BioLegend) was added prior to measurement and only negative cells were included in analysis. FACS was performed on a FACSCalibur (Becton Dickinson) or Gallios (Beckman Coulter).

**Table: Antibodies**

Antibody	Antigen	Isotype	Label*	Application Concentration	Supplier (Clone) (Cat. Nr.)
<b>LEAF™ anti-NKG2D</b>	Human NKG2D	Mouse IgG1	-	NKG2D blocking 20 µg/ml	BioLegend (1D11) (320810)
<b>FITC-anti-NKG2D</b>	Human NKG2D	Mouse IgG1	FITC	FACS 1:100 dilution	BioLegend (1D11) (320810)
<b>FITC-anti-CD69</b>	Human CD69	Mouse IgG1	FITC	FACS; Activation assay 1:50 dilution	BioLegend (FN50) (310904)
<b>BV421-anti-CD56</b>	Human CD56	Mouse IgG1	BV421	Functional assays 1:100 dilution	BioLegend (HCD56) (318328)
<b>AF647-anti-NKp46</b>	Human NKp46	Mouse IgG1	AF647	FACS 1:100 dilution	BioLegend (9E2) (331910)
<b>PE-anti-CD107a</b>	Human CD107a	Mouse IgG1	PE	Degranulation assay 1:100 dilution	BioLegend (1D4B) (121612)
<b>AF647-anti-IFNγ</b>	Human IFNγ	Mouse IgG1	AF647	IFNγ assay 1:100 dilution	BioLegend (4S.B3) (502516)
<b>FITC-anti-TNFα</b>	Human TNFα	Mouse IgG1	FITC	TNFα assay 1:100 dilution	BioLegend (Mab11) (502906)
<b>Anti-ULBP1</b>	Human ULBP1	Mouse IgG2a	-	FACS 10 µg/ml	Bamomab (AUMO2) (AUMO2-500)

\*FITC, Fluorescein isothiocyanate; PE, Phycoerythrin; BV421, Brilliant Violet™ 421; AF647, Alexa Fluor® 647; PB, Pacific Blue™ ; HRP, Horseradish peroxidase.

Further, binding of ULBP2-aCD19 and ULBP2-aCD19-aCD19 to NKG2D receptor was also checked by ELISA. Recombinant human NKG2D-Fc receptor was coated at 100ng per well of a 96-well flat-bottom MaxiSorp™ plate. 10 µg/ml of immunoligand was added to each well whereby pre-blocking of NKG2D receptor by anti-NKG2D antibody (clone 1D11) confirmed the specificity. Finally, HRP-conjugated anti c-Myc antibody could detect the bound immunoligand when the 1-step™ Ultra TMB-ELISA substrate (ThermoFisher Scientific) was added.

**Table: Antibodies (cont.)**

Antibody	Antigen	Isotype	Label*	Application Concentration	Supplier (Clone) (Cat. Nr.)
<b>Anti-c-Myc</b>	c-Myc tag	Mouse IgG1	-	FACS (10 µg/ml) Western blot (1:5000)	Prepared in house (800 µg/ml)
<b>HRP-anti-cMyc</b>	c-Myc tag	Mouse IgG1	HRP	ELISA 1:5000 dilution	Life Technologies (R951-25)
<b>AF647-anti-Fc</b>	Human IgG	Mouse IgG2a	AF647	FACS 1:100 dilution	BioLegend (HP6017) (409320)
<b>PE-anti-DDK/FLAG</b>	FLAG/ DDK tag	Rat IgG2a	PE	FACS 1:100 dilution	BioLegend (L5) (637310)
<b>PB-anti-CD3</b>	Human CD3	Mouse IgG1	PB	FACS 1:100 dilution	BioLegebd (HIT3a) (300330)
<b>AF647-anti-CD20</b>	Human CD20	Mouse IgG2b	AF647	FACS 1:100 dilution	BioLegend (2H7) (302318)
<b>PB-anti-CD5</b>	Human CD5	Mouse IgG2a	PB	FACS 1:100 dilution	BioLegend (L17F12) (364024)
<b>Goat anti-mouse Ab</b>	Mouse IgG	Goat polyclonal IgG	PE	FACS 1:100 dilution	BioLegend (Poly4053) (405307)
<b>Goat anti-mouse Ab</b>	Mouse IgG	Goat polyclonal IgG	HRP	Western blot and ELISA 1:10,000 dilution	Cell Signalling (7076p2)
<b>Isotype control Ab</b>	-		FITC, PE, AF647	FACS	

\*FITC, Fluorescein isothiocyanate; PE, Phycoerythrin; BV421, Brilliant Violet™ 421; AF647, Alexa Fluor® 647; PB, Pacific Blue™ ; HRP, Horseradish peroxidase.

#### 4.5. Flow cytometry based investigation of NK cell effector functions

##### 4.5.1. Analysis of NK cell effector functions in response to NKG2D and/or CD16 stimulation by Schneider-2 cells

Purified  $2.5 \times 10^4$  (resting or cytokine primed) NK cells were incubated with  $2.5 \times 10^4$  Schneider-2 cells in “U” bottom 96-well plate for 6 hours for activation and cytokine assays and for 6 hours for degranulation assay. Schneider-2 cells expressing ULBP1 or coated with rabbit polyclonal serum were

used as target cells to activate NKG2D or CD16a receptor on NK cells, respectively. At the end of the respective incubations, samples were stained with BV421™-labeled anti-human CD56 antibody to discriminate CD56-positive NK cells from CD56-negative Schneier-2 cells. NK cell activation was assessed by an additional FITC-labeled antibody staining for NK cell activation marker CD69. NK cell degranulation was assessed by flow cytometric analysis of the cell surface expression of the lysosomal protein CD107a. The last 4 hours of degranulation assay was carried out in presence of 2  $\mu$ M monensin (BioLegend) and PE-labeled anti-human CD107a mAb because CD107a that has been externalized by NK cells upon degranulation is rapidly reinternalized. Similarly, last 4 hours of cytokine assay was carried out in presence of Brefeldin A (BFA) at a final concentration of 5  $\mu$ g/ml as Brefeldin A is a protein transport inhibitor that leads to accumulation of most cytokines at the Golgi Complex/Endoplasmic Reticulum. For intracellular staining of IFN $\gamma$  and TNF $\alpha$  in NK cells, cells were fixed and permeabilized using Cytofix/Cytoperm™ kit (BD Bioscience) according to the protocol and were subsequently stained with Alexa Fluor® 647-labeled anti-IFN $\gamma$  and FITC-labeled anti-TNF $\alpha$  antibodies.

#### **4.5.2. NK cell cytotoxicity and degranulation by immunoligands**

Flow cytometry based NK cell cytotoxicity assays involved MEC1, HL60, BV173, SEM and primary malignant B cells from CLL patients at different stages. These target cells were labeled with lipophilic membrane dye DiR (Invitrogen) according to manufacturer's instructions. Purified NK cells primed with different cytokines (See figure legends for details) were co-incubated with labeled target cells in "U" bottom 96-well plates at indicated E:T ratios with or without indicated immunoligands for 3 hours. At the end of co-culture, cells were stained with 7-AAD (BioLegend) and measured by flow cytometry (Gallios, Beckman Coulter). Gating on 7-AAD-positive population within DiR-positive population indicated dead target cells in percentage (%). Further, allogeneic toxicity assays with primary CLL cells were also done as above mentioned but in presence of 20% serum from CLL patients with known levels

of soluble NKG2D ligands. This was done to assess whether immunoligands can overcome the NK cell inhibitory effects of CLL serum *in vitro*.

Toxicity assays involving mono-targeting triplebody (ULBP2-aCD19-aCD19) against MEC1 and HL60 cell lines as well as primary CLL cells utilized 10 nM of immunoligands while toxicity assays against BV173 and SEM cell lines involving a dual-targeting triplebody (ULBP2-aCD19-aCD33) included 100 nM of immunoligands. Dual-activating triplebody (ULBP2-aCD19-aNKR) was not purified and crude concentrated S/N with undefined amount of triplebody was used for the experiments. Experiments confirming the role of NKG2D in immunoligand mediated toxicity involved pre-blocking of NKG2D receptor on purified NK cells by 20 µg/ml anti-NKG2D antibody (clone 1D11).

For autologous cytotoxicity assay using patient's innate NK:CLL ratio, PBMC were isolated from the peripheral blood of CLL patients similarly as described above for healthy donors. Percentage of NK, CLL and T cells were determined for each patient and accordingly PBMC were cultured in 96-well "U" bottom plates either alone or in presence of 10 nM ULBP2-aCD19-aCD19 for 48 hours. At the end of the incubation, cells were stained by AF647-labeled anti-CD20 and Pacific Blue-labeled anti CD5 antibodies. Fixed amount of counting beads (ThermoFisher, Cat Nr C36950) and 7-AAD dye were added in each sample and relative CLL cell count and 7-AAD-positive dead cells were determined by gating for CD20<sup>+</sup>/CD5<sup>+</sup> CLL cells.

Flow cytometry based NK cell degranulation assay was also performed additionally. Target cell line (See figure legend) and purified NK cells were co-incubated in "U" bottom 96-well plates at 2.5:1—E:T ratio with or without ULBP2-aCD19-aCD19 (10 nM) or ULBP2-aCD19-aCD33 (100 nM) for 6 hours. After 2 hours of incubation, monensin (BioLegend) was added at a final concentration of 2 mM in every well and co-culture was continued for 4 hours. PE-labeled anti-human CD107a mAb was present in the medium throughout the 6 hours incubation period. At the end of the incubation, cells were stained with AF647-

labeled anti-NKp46 and BV421-labeled anti-CD56 antibodies for 30 min on ice. Cells were then washed thrice with PBS containing 0.2 % BSA and 0.2 % NaN<sub>3</sub> and were measured by flow cytometry. Gating on CD107a-positive cells within NKp46/CD56 double positive NK population revealed degranulated NK cells.

#### 4.5.3. NK cell IFN $\gamma$ and TNF $\alpha$ secretion by immunoligands

To detect the IFN $\gamma$  secretion from NK cells in response to dual-targeting triplebody (ULBP2-aCD19-aCD33) and its bispecific counterparts, purified and IL2 (200 U/ml) and IL15 (10 ng/ml) primed NK cells from healthy donors were cultured for 48 hours in 96 well MaxiSorp™ plates pre-coated with 10  $\mu$ g/ml of immunoligands. In case of mono-targeting triplebody (ULBP2-aCD19-aCD19), purified NK cells were co-cultured with MEC1 cells in a 96 well “U” bottom plate at 1:1 (E:T) ratio in presence of 10 nM immunoligands for 24 hours. . After 48 or 24 hours respectively, S/N was collected by spinning down the cells in 500  $\mu$ l eppendorf tubes and was frozen at -20°C until further use. Subsequently, SN was used to detect and measure IFN $\gamma$  by ELISA (Human IFN $\gamma$  ELISA MAX™ standard, Biolegend) according to manufacturer’s protocol. In brief, on day 1 MaxiSorp™ plate was coated with appropriately diluted capture antibody and was incubated at 4°C overnight. Next day, the plate was washed off the capture antibody and was blocked using assay diluent (1% BSA in PBS) for 1 hour at room temperature (RT). SN diluted 1:20 and 1:100 with assay diluent was incubated in appropriate wells for 2 hours at RT. After thorough washing, detection antibody and subsequently HRP-avidin was added to the wells. Finally, 1-step™ Ultra TMB-ELISA substrate (ThermoFisher Scientific) was added to visualize the IFN $\gamma$  bound antibody. Human IFN $\gamma$  standard (500 pg/ml – 7.8 pg/ml) was used to quantify IFN $\gamma$  in SN.

## 4.6. Animal study

### 4.6.1. Role of ULBP2-aCD19-aCD19 in restriction of xenografted tumor growth in NSG mice

21 five week old and female NOD *scid* gamma (NSG™) mice were purchased from Jackson laboratories and were maintained under sterile conditions. MEC1 cells were resuspended in Hank's Buffered Salt Solution (HBSS) and  $5 \times 10^6$  MEC1 cells in 100 $\mu$ l were injected subcutaneously (s.c.) into the flank of each mouse. This was considered as day 0. Following MEC1 cells engraftment, all 21 mice were randomly distributed within three groups (7 mice in each group). On day 2, PBMC were isolated from the buffy coats of healthy donors using Ficoll-Paques density gradient centrifugation as stated above. On the same day, each of the 7 mice in "Group 3" received freshly isolated  $4 \times 10^5$  PBMC in HBSS + 15  $\mu$ g ULBP2-aCD19-aCD19 by a single intravenous (i.v.) injection into a tail vein. While, 3 mice within the "Group 2" received freshly isolated  $4 \times 10^5$  PBMC in HBSS alone, the remaining 4 mice received freshly isolated  $4 \times 10^5$  PBMC in HBSS + 15  $\mu$ g ULBP2-aPSMA. ULBP2-aPSMA was used as a non-relevant immunoligand as it is against Prostate-Specific Membrane Antigen (PSMA) which is absent from MEC1 cells, human PBMC population and mice tissue. This group served as a control for the group treated with PBMC + a mono-targeting triplebody (ULBP2-aCD19-aCD19). The first group (7 mice) was left untreated and served as a control for the both treatment groups. Tumor development was measured periodically and the tumor volume was determined by the formula: (length x width x height)/2. The animals were sacrificed by cervical dislocation when the tumor volume reached 1,000 mm<sup>3</sup> or at the end of the study period (until day 52) in case of no tumor sign. Animal experiments were approved from local authorities (State Northrhine-Westfalia, LANUV, approval no. 84-02.04.2012.A216).

#### 4.7. Software and statistics

FlowJo x was used to analyze the data of flow cytometry and imageJ was used to generate the confocal image. DNASTar was used to design cloning strategies and to analyze plasmid sequences. Microsoft office 2010 was used to prepare the figures and to write the thesis. Graphpad Prism 6 (San Diego, CA) was used for statistical analyses.

Student's t-test was used to compare two groups in NK cell functional assays in response to Schneider-2 cells as target cells. Paired t-test was performed to compare two groups in NK cell functional assays in response to immunoligand against the same target cells. For comparisons involving three or more groups, one-way ANOVA test was performed and p values were corrected by Tukey's multiple comparisons test. Kaplan–Meier survival at fixed time points was compared using log rank (Mantel–Cox) test. In all experiments, error bars are presented as standard error of the mean (SEM). A two tailed  $p < 0.05$  indicated statistical significance and ns (not significant),  $p > 0.05$ ; \*,  $p < 0.05$ ; \*\*,  $p < 0.05$ ; \*\*\*,  $p < 0.01$ .

## 5. Results

### 5.1. NKG2D stimulation requires IL2 and IL15 priming for efficient execution of NK cell effector functions

To assess the ability of NKG2D stimulation to facilitate NK cell activation and various effector functions, I used *Drosophila* Schneider-2 cells stably transfected with pAc5.1/V5-His\_ULBP1 to express ULBP1 ligand on the cell surface. ULBP1 is one of several ligands for the activating receptor NKG2D on human NK cells as well as CD8<sup>+</sup> T cells and  $\gamma/\delta$  T cells.

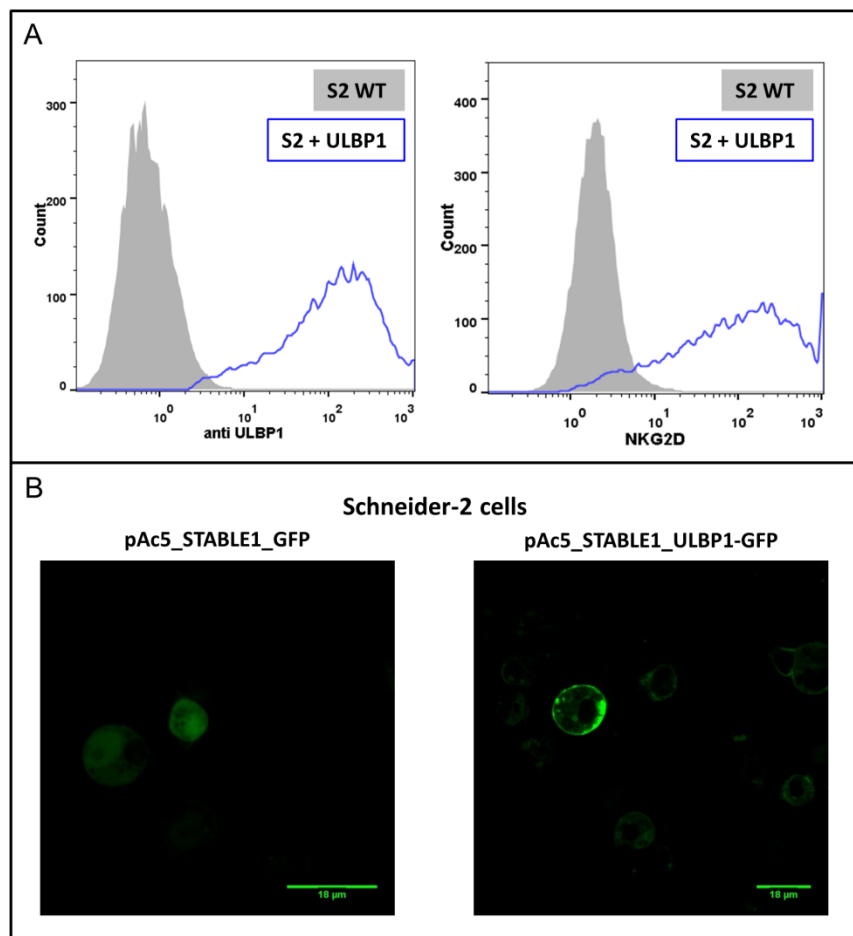


**Figure 1. ULBP1 is expressed in Schneider-2 cells and localizes on the cell membrane.** (A) ULBP1 expression on Schneider-2 cells (WT or ULBP1 transfected) as detected by anti-ULBP1 (left) or NKG2D receptor. (B) Schneider-2 cells transfected by either empty GFP vector (left) or ULBP1-GFP fused vector (right) and visualizing ULBP1-GFP localization by confocal microscopy.

As shown in figure 1, ULBP1 expressed on Schneider-2 cells could be detected by flow cytometry using anti-ULBP1 antibody as well as recombinant human NKG2D receptor. Moreover, confocal images could further confirm the presence of ULBP1 (GFP-tagged) on the surface of Schneider-2 cells as opposed to diffused and cytoplasmic GFP expression in control transfection. The nature of glycosylation in *Drosophila* system is similar but not identical to mammalian glycosylation. Despite having a less complex glycosylation system, ULBP1 expressed in Schneider-2 cells was able to locate to the cell surface and further to interact with NKG2D receptor, an important prerequisite for further functional assays.

Using ULBP1 positive Schneider-2 (S2-ULBP1<sup>+</sup>) cells as target cells, important NK cell functions such as activation, degranulation and cytokine secretion were studied by flow cytometry (FACS). NK cells were purified by negative selection from PBMC of healthy blood donors and were pre-treated with different cytokines as indicated for each experiment. Figure 2 shows the gating strategies for such FACS based experiments using the Schneider-2 system or later, human cancer cell lines. At the end of the incubation, BV421-labeled anti-CD56 antibody was used to stain the typical NK cell marker CD56 in order to efficiently discriminate NK cells from broad types of target cells used in this thesis. First, the ability of ULBP1 expressing Schneider-2 cells to activate and degranulate resting NK cells was assessed. NK cells were considered as “resting” when purified NK cells were incubated with 10 U/ml IL2 overnight. IL2 at such low concentration only keeps primary NK cells alive and in healthy state but does not activate them. Upregulation of the activation marker CD69 on NK cells was checked after 6 hours of co-incubation. The degranulation marker CD107a/LAMP-1 is exposed on the surface of NK cells for short duration when they degranulate and then is quickly re-internalized. Therefore, PE-labeled anti-CD107a antibody was present throughout the 6 hours of co-incubation to maximize the staining. Moreover, 2  $\mu$ M Monensin was added for the last 4 hours to prevent degradation of the CD107a-bound internalized anti-CD107a antibody. Figure 3 shows that NKG2D stimulation on resting NK cells by ULBP1 is not sufficient to activate or degranulate resting NK cells in 6 hours.

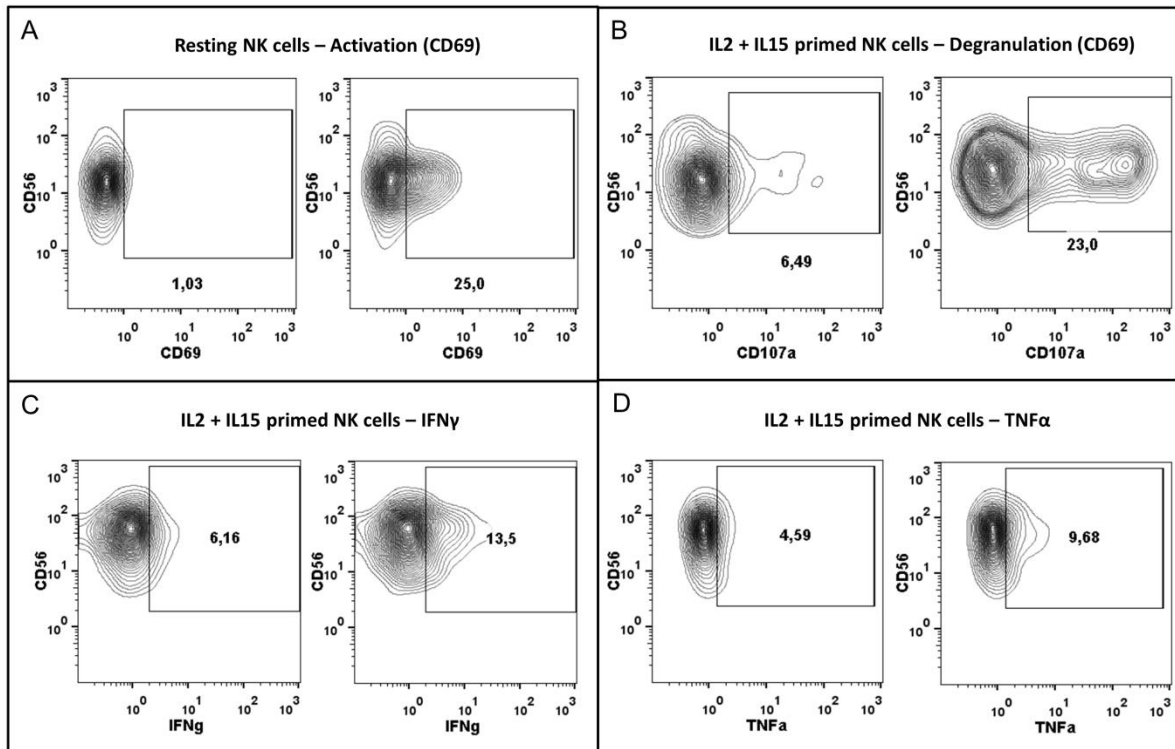
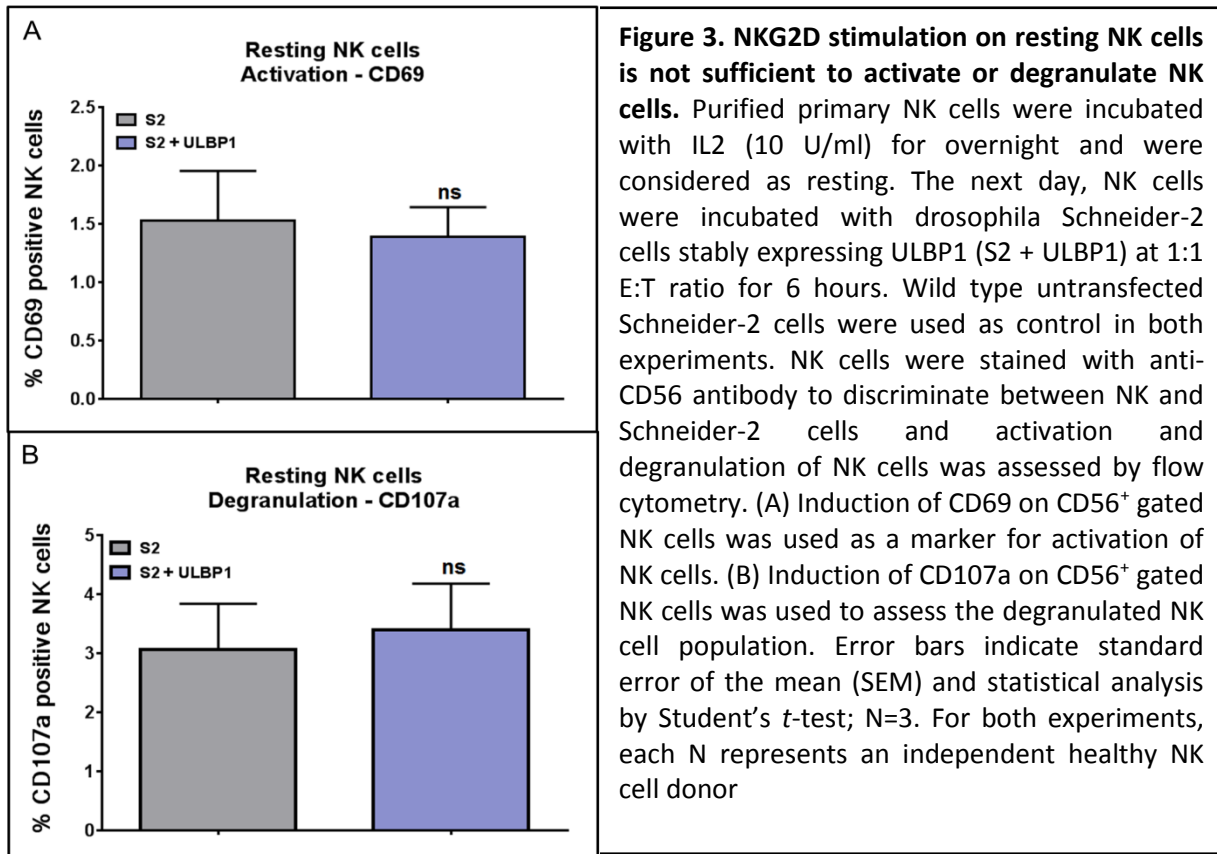


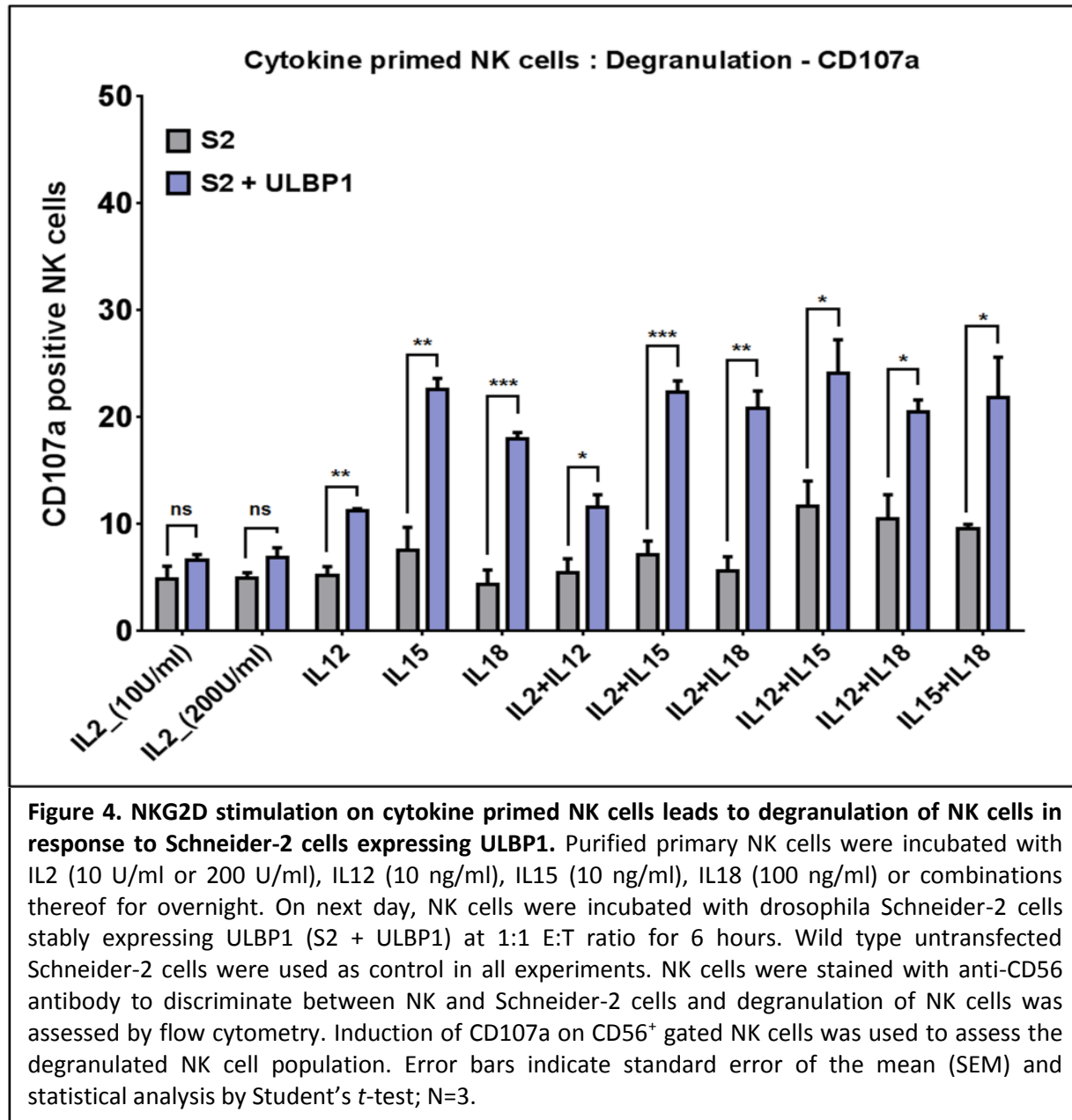
**Figure 2. Flow cytometry based gating strategies to assess various NK cell effector functions.**

NK cells were purified from PBMC of healthy donors and were cultured in presence of cytokine(s) as indicated in each experiment. Next day, NK cells were co-incubated with the target cells for indicated duration. At the end of the incubation, NK cells were stained with BV421-labeled anti-CD56 antibody to discriminate them from target cells. Different markers were analyzed to assess various NK cell effector functions in response to particular target cells. (A) Upregulation of CD69 (stained by FITC-labeled anti-CD69) within CD56 positive NK cell population indicated activation of NK cells. Left: NKG2D stimulation on resting (IL2 10 U/ml primed) NK cells fails to activate them. Right: CD16 stimulation upregulates CD69 on 25% of the resting NK cells (B) Cell surface expression of CD107a/LAMP-1 on NK cells is an accurate marker to assess degranulation of NK cells. PE-labeled anti-CD107a staining within CD56 positive NK cell population indicated degranulated NK cells. For example, NKG2D signaling on IL2 + IL15 primed NK cells leads to NK cell degranulation (right) in 23% of the population which was 6.49% in the absence of NKG2D signaling (left). (C & D) Intracellular staining of cytokines such as IFN $\gamma$  and TNF $\alpha$  in fixed and permeabilized CD56-stained NK cells was performed. AF647-labeled anti IFN $\gamma$  and FITC-labeled anti TNF $\alpha$  antibodies were used for the experiments. For example, NKG2D stimulation on IL2 + IL15 primed NK cells led to around 2-fold increase in both, IFN $\gamma$  and TNF $\alpha$  positive NK cell population.



Purified NK cells were primed with IL2 (10 U/ml or 200 U/ml), IL12 (10 ng/ml), IL15 (10 ng/ml), IL18 (100 ng/ml) or pair-wise combinations thereof for overnight to check whether this can prime NK cells to deliver effector functions in response to NKG2D stimulation. The NK cell degranulation assay was performed as described above; however, utilizing cytokine primed NK cells as effector cells (Figure 4). Increasing the concentration of IL2 from 10 U/ml (resting) to 200 U/ml did not enhance NK cell degranulation in response to S2-ULBP1<sup>+</sup>. Priming by IL12, IL15 or IL18 could significantly increase degranulating NK cell population in response to NKG2D stimulation when compared to wild-type (WT) Schneider-2 cells. Combination of IL2 with IL12, IL15 or IL18 cytokines did not have any additive effects in terms of degranulation. Although, pairwise combinations of IL12, IL15 and IL18 could significantly increase NK cell degranulation compared to WT Schneider-2 cells, these cytokines already provided the

stronger priming signals to NK cells which was evident by high degranulation in response to WT target cells.



Next, interleukin primed NK cells were also assessed for their ability to produce and secrete IFN $\gamma$  and TNF $\alpha$  in response to NKG2D triggering by ULBP1. NK cells were co-incubated with target cells for 6 hours in presence of Brefeldin-A (last 4 hours) which blocks protein transport to the Golgi complex and rather

accumulates them in endoplasmic reticulum (ER). Detection of intracellular cytokines including IFN $\gamma$  and TNF $\alpha$  can be enhanced when they accumulate in ER. Following 6 hours of incubation, cells were stained with BV421-labeled anti-CD56 antibody to detect NK cells. Cells were then fixed and permeabilized to enable intracellular staining of cytokines by AF647-labeled IFN $\gamma$  and FITC-labeled TNF $\alpha$  antibodies in the same well. Depicted are the IFN $\gamma$  (AF647 $^+$ ) and TNF $\alpha$  (FITC $^+$ ) populations within NK cells (CD56 $^+$ ) based on the gating strategy shown in figure 2.

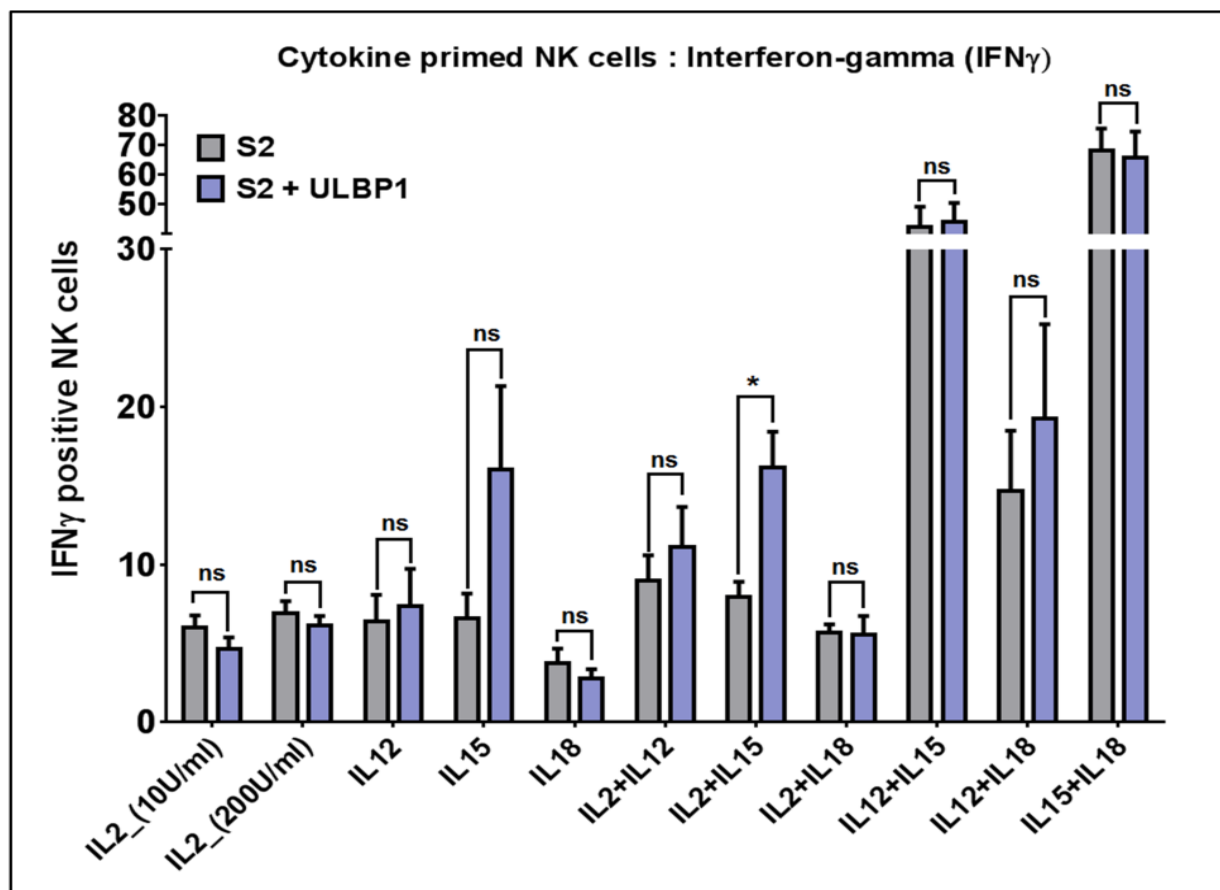


**Figure 5. NKG2D stimulation on cytokine primed NK cells leads to IFN $\gamma$  secretion in response to Schneider-2 cells expressing ULBP1.** Purified primary NK cells were incubated overnight with IL2 (10 U/ml or 200 U/ml), IL12 (10 ng/ml), IL15 (10 ng/ml), IL18 (100 ng/ml) or combinations thereof. The next day, NK cells were incubated with S2-ULBP1 $^+$  at 1:1 E:T ratio for 6 hours. Untransfected wild type Schneider-2 cells were used as control in all experiments. NK cells were stained with anti-CD56 antibody to discriminate between NK and Schneider-2 cells. Cells were fixed and permeabilized to stain intracellularly for IFN $\gamma$ . Flow cytometry analysis identified IFN $\gamma$  $^+$  cells within the CD56 $^+$  gated NK cell population. Error bars indicate standard error of the mean (SEM) and statistical analysis by Student's *t*-test; N=3.

Cytokine requirement for IFN $\gamma$  and TNF $\alpha$  secretion upon NKG2D stimulation on NK cells was more stringent. As shown in figure 5, only IL15 or the combination of IL2 and IL15 could prime NK cells to secrete more IFN $\gamma$  in response to NKG2D stimulation by S2 + ULBP1 (compared to WT Schneider-2 cells) which in case of IL2 + IL15 was also statistically significant. Similar to degranulation assay, pairwise combinations of IL12, IL15 and IL18 were activating themselves and could not be further enhanced by NKG2D stimulation.

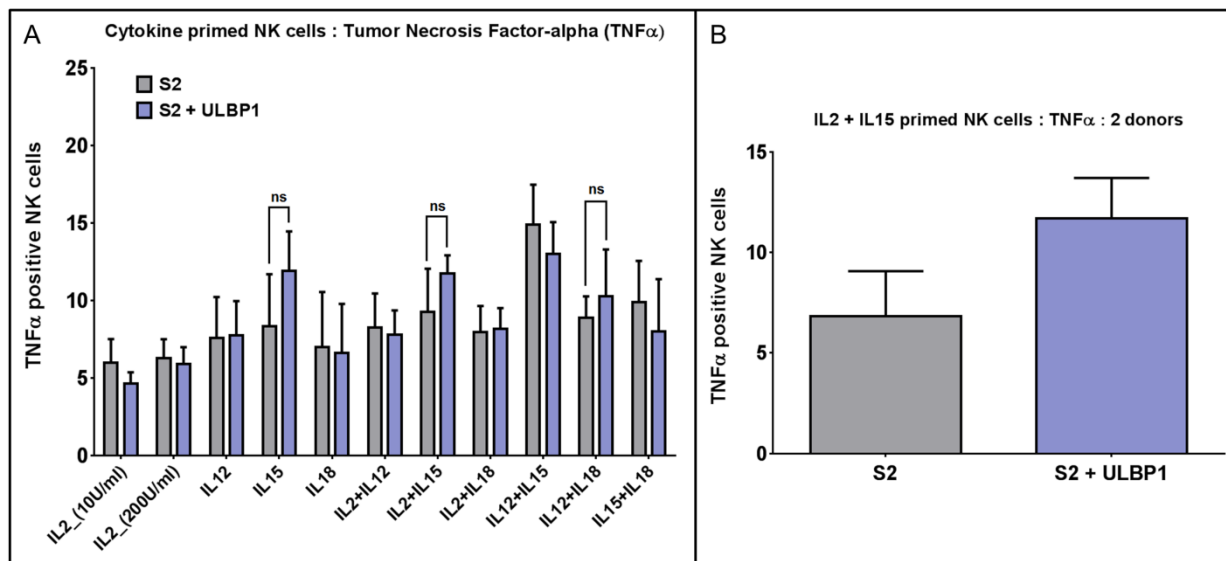


**Figure 6. NKG2D stimulation on cytokine primed NK cells leads to TNF $\alpha$  secretion in response to Schneider-2 cells expressing ULBP1.** (A) Purified primary NK cells were incubated with IL2 (10 U/ml or 200 U/ml), IL12 (10 ng/ml), IL15 (10 ng/ml), IL18 (100 ng/ml) or combinations thereof for overnight. On next day, NK cells were incubated with drosophila Schneider-2 cells stably expressing ULBP1 (S2-ULBP1<sup>+</sup>) at 1:1 E:T ratio for 6 hours. Wild type untransfected Schneider-2 cells were used as control in all experiments. NK cells were stained with anti-CD56 antibody to discriminate between NK and Schneider-2 cells. Cells were fixed and permeabilized to stain intracellularly for TNF $\alpha$ . TNF $\alpha$ <sup>+</sup> cells in CD56<sup>+</sup> gated NK cells indicated NK cell population that secreted TNF $\alpha$  by flow cytometry. Error bars indicate standard error of the mean (SEM) and statistical analysis by Student's *t*-test; N=3. (B) IL2 + IL15 primed NK cells from 2 out of 3 donors showed 2-fold increase in TNF $\alpha$  positive NK cells in response to S2 + ULBP1. Error bars indicate standard error of the mean (SEM); N=2.

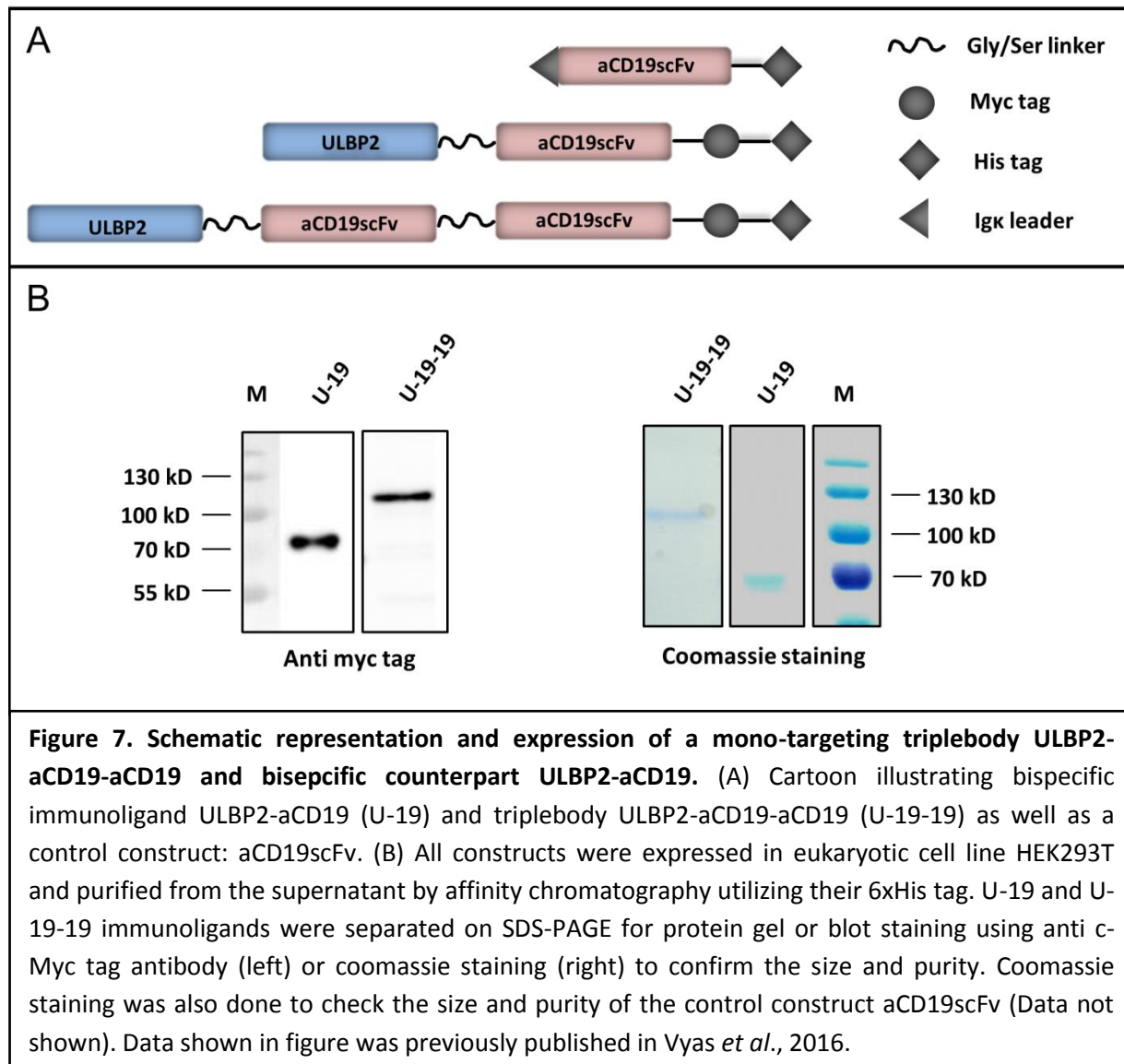
Figure 6(A) shows that ULBP1-NKG2D axes induced TNF $\alpha$  secretion by IL15 or IL2 + IL15 primed NK cells was increased compared to that by wildtype target cells but was not significant. This assay was repeated with 3 independent NK cell donors and 2 out of which showed almost 2-fold increase in TNF $\alpha$  secretion

at least by IL2 + IL15 primed NK cells (Figure 6(B)) suggesting donor dependent variability. Taken together, cytokine requirement for NKG2D-dependent NK cell degranulation was less stringent compared to IFN $\gamma$  secretion and was most stringent for TNF $\alpha$  secretion. However, IL15 or combination of IL2 + IL15 could prime NK cells most efficiently to respond to NKG2D stimulus.

## **5.2. A mono-targeting triplebody ULBP2-aCD19-aCD19 enhances NK cell dependent killing of CLL cell line – MEC1**

Successful cloning of pL(ULBP2-aCD19), pL(ULBP2-aCD19-aCD19) and pL(aCD19scFv) was confirmed by restriction digestions and sequencing of the complete reading frame. All of these three constructs were transfected into HEK293T cells and stable clones were selected with Zeocin™ as the plasmids also expressed Zeocin-resistance gene. Stable clones (polyclonal) were subsequently cultured in serum free CD293 medium and SN was collected every 2-3 days over a period of a month. As shown in figure 7(A), triplebody ULBP2-aCD19-aCD19 and bispecific counterpart ULBP2-aCD19 carried ULBP2 in front and the N-terminal sequence of ULBP2 facilitated secretion of both of these immunoligands into the SN of transfected cells. In contrast, Igk leader sequence was placed 3' of the control construct (aCD19scFv) to facilitate its secretion. A Gly/Ser linker of total 20 amino acids—(GGGGS) $_4$ x was used to link each moiety (figure 7(A)) as well as VH and VL domains of an scFv (not shown in the figure) to confer flexibility to the immunoligands. All three constructs consisted of a 6xHis (HHHHHH) tag at the C-terminus, which was used for purification. While U-19 and U-19-19 carried a c-Myc tag for detection purpose, it was omitted from a blocking construct aCD19scFv. Between 400  $\mu$ g to 700  $\mu$ g of U-19 and U-19-19 and around 1 mg of aCD19scFv was purified from around 1 liter of cell culture SN. Figure 7(B) shows that the purified immunoligands were of high purity, expected size and monomeric in nature as verified by c-Myc tag specific immunoblotting (left) and coomassie staining (right). U-19 and U-19-19 had the expected molecular weight of 64 kDa and 91 kDa, respectively. Purity and size for a blocking construct aCD19scFv

were also verified by coomassie staining (data not shown). It was found to be of high purity and according to the expected molecular weight.



Once the immunoligands were purified with high purity, next was the assessment for their binding ability and specificity. Both aspects are important prerequisites for further functional testing and preclinical development. A CD19<sup>+</sup> CLL cell line MEC1 was used for this evaluation. MEC1 cells were incubated with ULBP2-aCD19 and ULBP2-aCD19-aCD19 at 10  $\mu$ g/ml concentration and its binding was subsequently detected by c-Myc tag specific antibody or recombinant NKG2D receptor (Fc tag fused).

Both, ULBP2-aCD19 and ULBP2-aCD19-aCD19 bound to MEC1 cells and this binding was specific to CD19 antigen as pre-blocking of CD19 antigen by aCD19scFv construct completely blocked the binding of immunoligands as depicted as dotted line in histograms (figure 8).

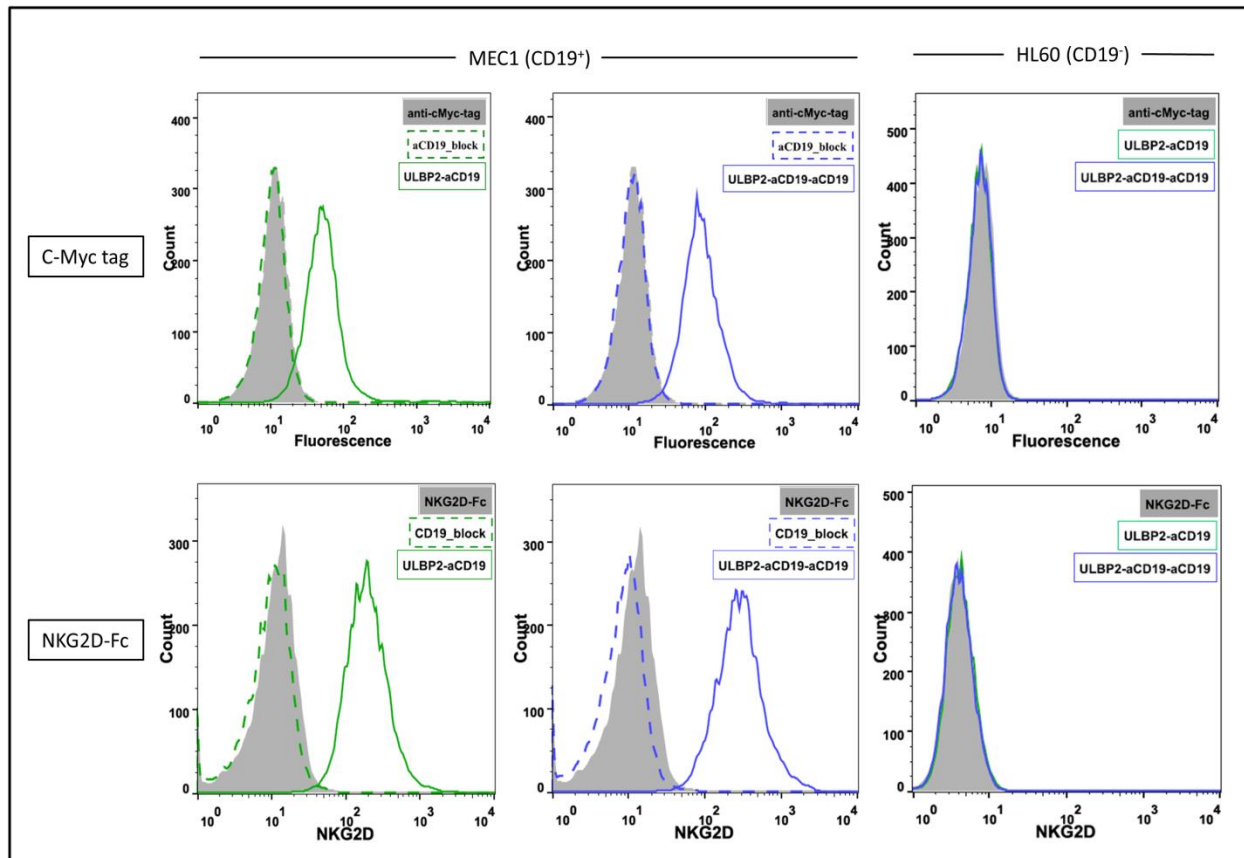
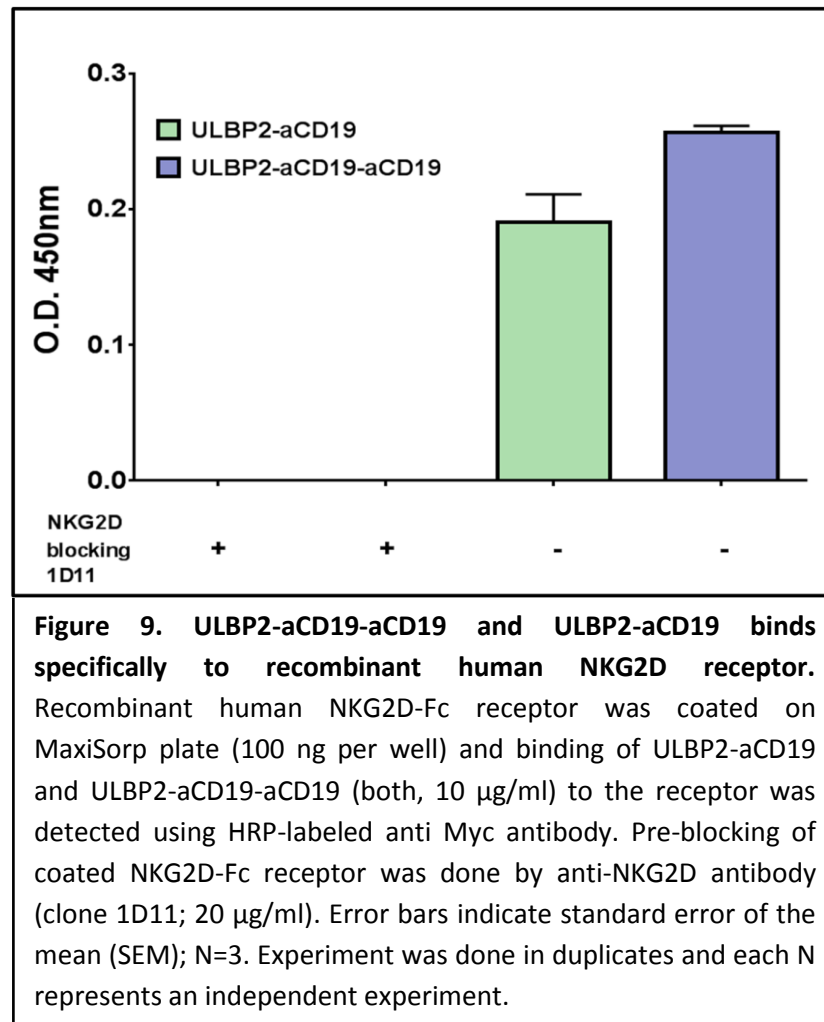


**Figure 8. ULBP2-aCD19-aCD19 and ULBP2-aCD19 binds specifically and simultaneously to both target antigens CD19 and NKG2D.** Binding of both immunoligands (10  $\mu\text{g}/\text{ml}$ ) to CD19<sup>+</sup> MEC1 cells was detected indirectly by anti-Myc tag antibody (upper panel “C-Myc-tag” - MEC1) and by recombinant human NKG2D-Fc receptor (lower panel “NKG2D-Fc” - MEC1). Specificity of both immunoligands to CD19 was confirmed by pre-blocking of CD19 antigen by a blocking construct aCD19scFv (20  $\mu\text{g}/\text{ml}$ ) as depicted by dotted line and also by performing binding assays with CD19 negative cell line HL60 (right column – “HL60”). Data shown in figure was previously published in Vyas *et al.*, 2016.

Specificity was further proven as both immunoligands failed to bind to HL60 cell line, which is CD19 antigen negative (figure 8). Detection of immunoligands by NKG2D-Fc receptor also confirmed that both, ULBP2-aCD19 and ULBP2-aCD19-aCD19 are able to bind simultaneously to both of their target moieties

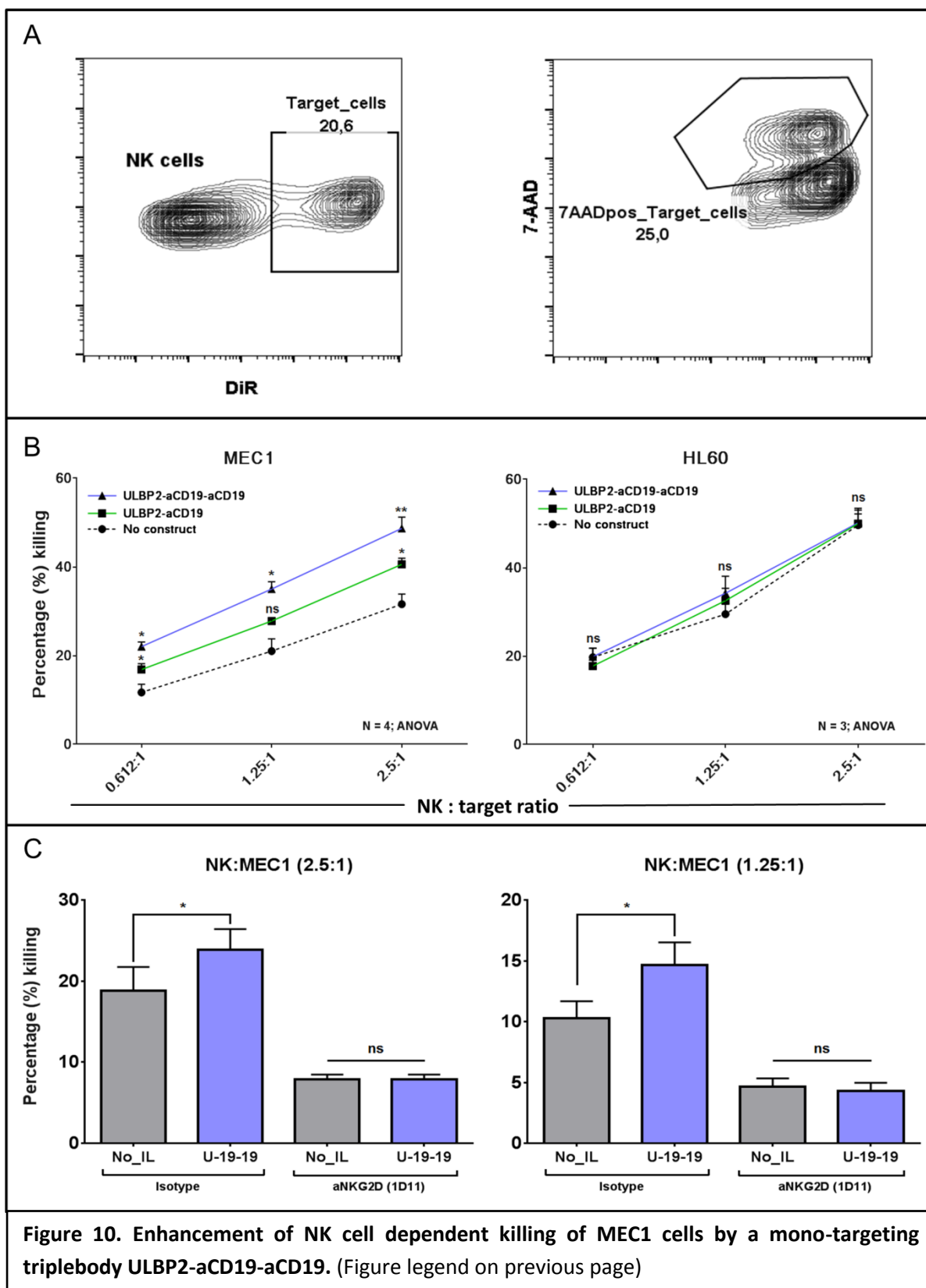
(CD19 antigen and NKG2D receptor) and therefore will be able to crosslink CLL and NK cells. Binding of immunoligands to coated NKG2D receptor additionally assured that they can bind to NKG2D receptor specifically as pre-blocking of NKG2D receptor by a blocking antibody (anti-NKG2D, clone 1D11) abolished the signal (figure 9).



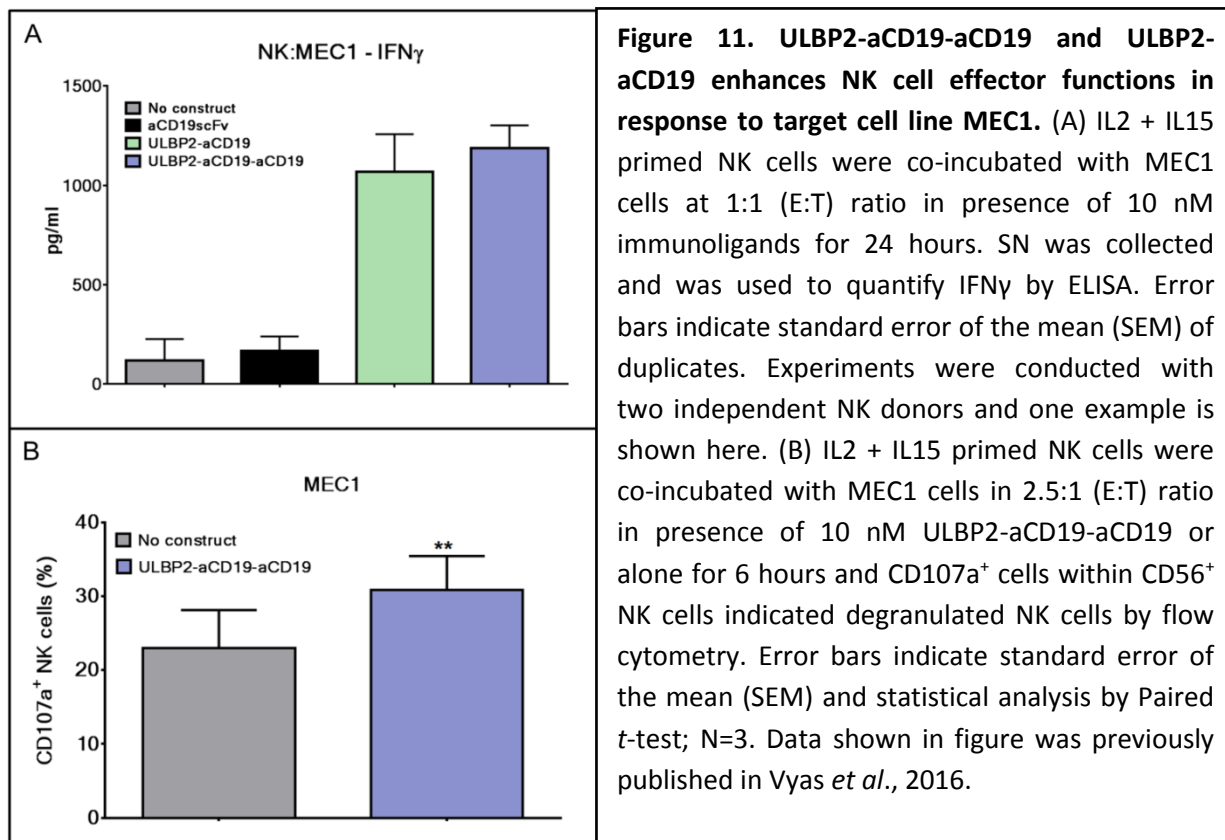
Following specific and simultaneous binding of immunoligands, I wanted to investigate their functional activity and tested whether they can also enhance NK cell-dependent killing of the CLL cell line MEC1. Another specific aspect of utmost interest was to check, whether addition of a second antiCD19 scFv to the bispecific ULBP2-aCD19 confers any advantage in terms of target cell killing. For this set of

experiments, NK cells were purified from PBMC of healthy donors, primed with IL2 (200 U/ml) and IL15 (10 ng/ml) and were then used as effector cells in a FACS based toxicity assay. NK cell preparations from different donors were routinely stained for surface markers to characterize NKG2D expression, NK cell activation status (CD69 expression) and purity (by CD56 and CD16 co-expression as well as Nkp46 expression) and preparations with  $\geq 98\%$  purity were used for experiments. NK cells were co-incubated with DiR-labeled MEC1 cells at indicated effector to target (E:T) ratios and 7-AAD was used to discriminate live and dead cells (figure 10(A)). Both immunoligands at 10 nM concentration could significantly enhance NK cell dependent killing of CD19<sup>+</sup> MEC1 cells in an E:T ratio dependent manner. This toxicity was not seen against CD19<sup>-</sup> HL60 cells, which suggested that this effect was antigen specific and immunoligands did not induce NK cell degranulation in (target cell) unbound state (figure 10(B)). Interestingly, at all E:T ratios, mono-targeting triplebody (ULBP2-aCD19-aCD19) induced killing of MEC1 cells was higher compared to the bispecific counterpart (ULBP2-aCD19). When NKG2D receptor was blocked (by anti-NKG2D antibody, clone 1D11) on NK cells prior to the toxicity assay, triplebody failed to induce any killing of MEC1 cells (figure 10(C)). In addition, NKG2D blocking also lowered the background killing of MEC1 cells by NK cells. This was most likely because it blocked the interaction between the endogenous ligands for NKG2D receptor on MEC1 cells and NKG2D receptor on NK cells.

**Figure 10. Enhancement of NK cell dependent killing of MEC1 cells by a mono-targeting triplebody ULBP2-aCD19-aCD19.** (A) Gating strategy for flow cytometry based toxicity assay. Target cells (MEC1) were labeled with DiR and were incubated with purified IL2 + IL15 primed NK cells either alone or in presence of 10 nM triplebody or bispecific ULBP2-aCD19 at various E:T ratios (left). The incubation was continued for 3 hours and 7-AAD was added to detect dead cells within the DiR positive gate (right). (B) NK cells were incubated with CD19<sup>+</sup> MEC1 cells or CD19<sup>-</sup> HL60 cells at 0.612:1, 1.25:1 and 2.5:1 E:T ratios. Both immunoligands enhanced the NK cell dependent killing of antigen positive MEC1 cells but not of antigen negative HL60 cells in E:T ratio dependent manner. Error bars indicate standard error of the mean (SEM) and statistical analysis by One-way ANOVA; N=4 (MEC1) and N=3 (HL60). Each N represents an independent healthy NK cell donor. (C) Immunoligand mediated killing of MEC1 cells is via NKG2D receptor on NK cells. NK cells were incubated with 10  $\mu$ g/ml of mouse anti-human NKG2D receptor antibody (clone 1D11) or mouse isotype control (IgG1) for 30 min on ice. Excess antibody was washed away after 30 min and toxicity assay was setup as described above. Error bars indicate standard error of the mean (SEM) and statistical analysis by Paired *t*-test; N=3. \* represents  $P < 0.05$ . Data shown in figure was previously published in Vyas *et al.*, 2016.



NK cell cytotoxicity was also independently assessed by FACS based degranulation assay against MEC1 cells. In line with the toxicity assay, ULBP2-aCD19-aCD19 could increase the degranulating NK cell population up to 1.5-fold in response to MEC1 (figure 11(B)). In addition, the ability of ULBP2-aCD19-aCD19 to induce IFN $\gamma$  production was assessed in IL2 and IL15 primed NK cells. IFN $\gamma$  release into the supernatant was measured following 24 hours co-culture of NK and MEC1 cells, either alone or in presence of 10 nM immunoligands at an E:T ratio of 1:1. Assessment with two independent NK cell donors showed comparable enhancement of IFN $\gamma$  production by NK cells by ULBP2-aCD19 and ULBP2-aCD19-aCD19 (one representative shown; figure 11(A)). A blocking construct aCD19scFv failed to induce IFN $\gamma$  production indicating that immunoligands required ULBP2 for this effect. Co-incubation in absence of any construct served as a control. IFN $\gamma$  secretion by MEC1 cells (with or without immunoligand) was carefully controlled and was found to be negative (data not shown).



### 5.3. ULBP2-aCD19-aCD19 mediates NK cell dependent killing of primary CLL cells in allogeneic setting

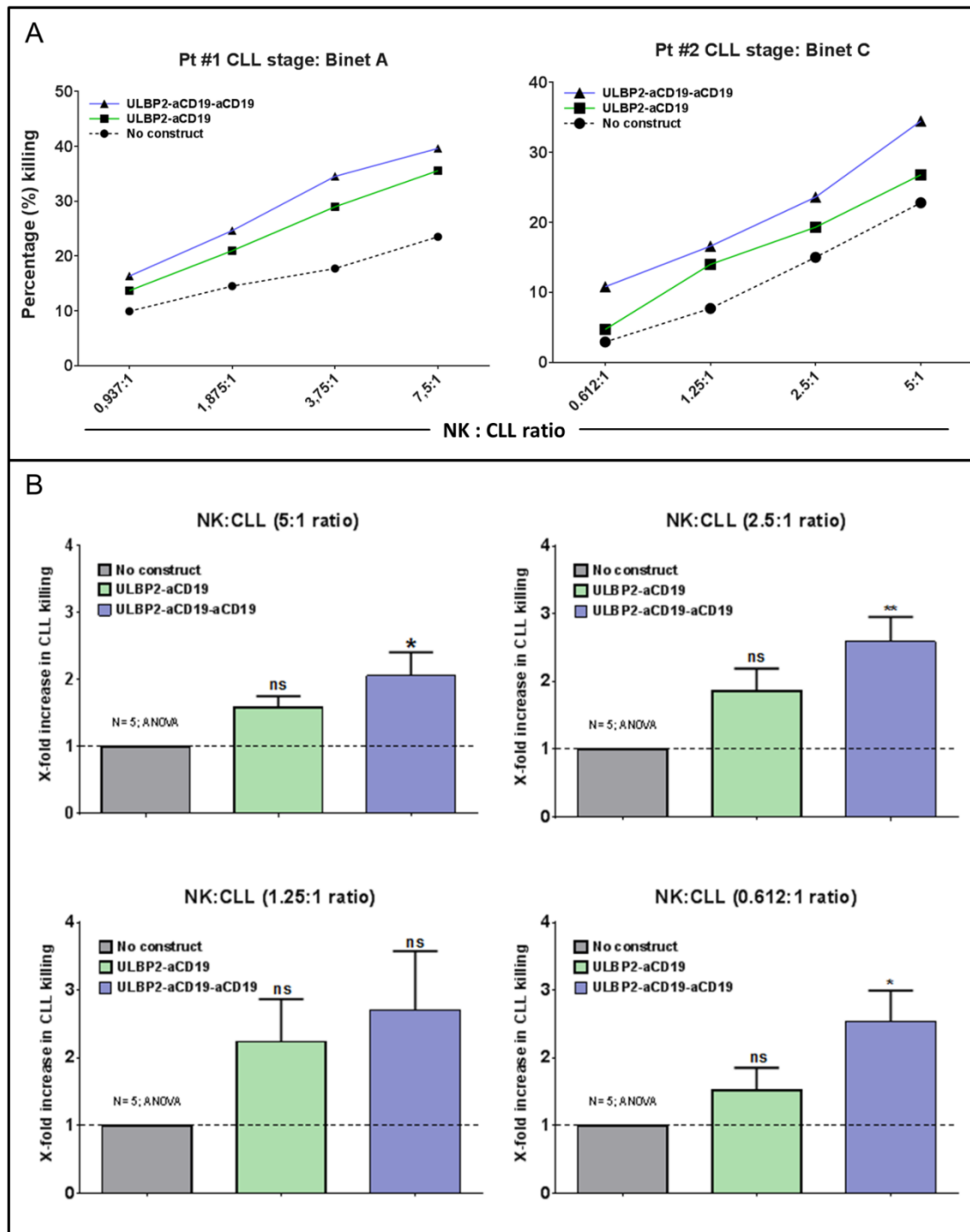


Figure 12. Enhancement of NK cell dependent killing of primary CLL cells by a mono-targeting triplebody ULBP2-aCD19-aCD19 in allogeneic setting. (Figure legend on next page)

**Figure 12. Enhancement of NK cell dependent killing of primary CLL cells by ULBP2-aCD19-aCD19 and ULBP2-aCD19 in allogeneic setting.** (A) Purified and IL2 + IL15 primed NK cells from healthy donors were co-incubated with DiR labeled primary CLL cells either alone or in presence of 10 nM indicated immunoligands. The incubation was continued for 3 hours and dead CLL cells were measured by 7-AAD staining on FACS. Two representative results from Binet A and C stage CLL patients (Pt #1 and Pt #2) are shown from total five independent experiments with different CLL patients. NK cells for each experiment were obtained from different healthy donors. (B) Data from total 4 independent tox assays were used for statistical evaluation at each E:T ratio. Error bars indicate standard error of the mean (SEM) and statistical analysis by One-way ANOVA (\*P < 0.05; \*\*P < 0.01). N= 4 where each N represents an independent CLL patient and healthy NK cell donor. Data shown in figure was previously published in Vyas *et al.*, 2016.

Following encouraging results with MEC1 cell line, toxicity assays were also performed in both allogeneic and autologous settings using malignant B cells from CLL patients. In allogeneic experiments, purified NK cells from healthy unrelated (to CLL patients) blood donors were used as effector cells while target cells comprised of freshly isolated malignant B cells from CLL patients. Apart from that, the general protocol and FACS gating strategy was similar to MEC1 toxicity assays.

In allogeneic experiments, presence of ULBP2-aCD19-aCD19 increased NK-cell-dependent killing of primary CLL cells from early (Binet A—Pt #1) and late stage (Binet C—Pt #2) CLL patients in the range of 1.5-fold–2-fold at all E:T ratios (figure 12(A)). Due to high donor-dependent variability, percentage killing of CLL cells by immunoligands were standardized to the background NK cell mediated killing of CLL cells in that particular experiment to generate x-fold increase in CLL killing. As shown in figure 12(B), cumulative analysis of four CLL patients (including Pt #2) showed that the effect mediated by ULBP2-aCD19-aCD19 was significantly higher than background killing (NK) at all but one E:T ratio (1.25:1). Even in these allogeneic experiments, ULBP2-aCD19-aCD19 showed higher NK-cell-dependent killing of CLL cells than ULBP2-aCD19, which, although not significant, is in line with the previous results with MEC1 cell line.

#### 5.4. ULBP2-aCD19-aCD19 overcomes soluble inhibitory factors in the serum of CLL patients

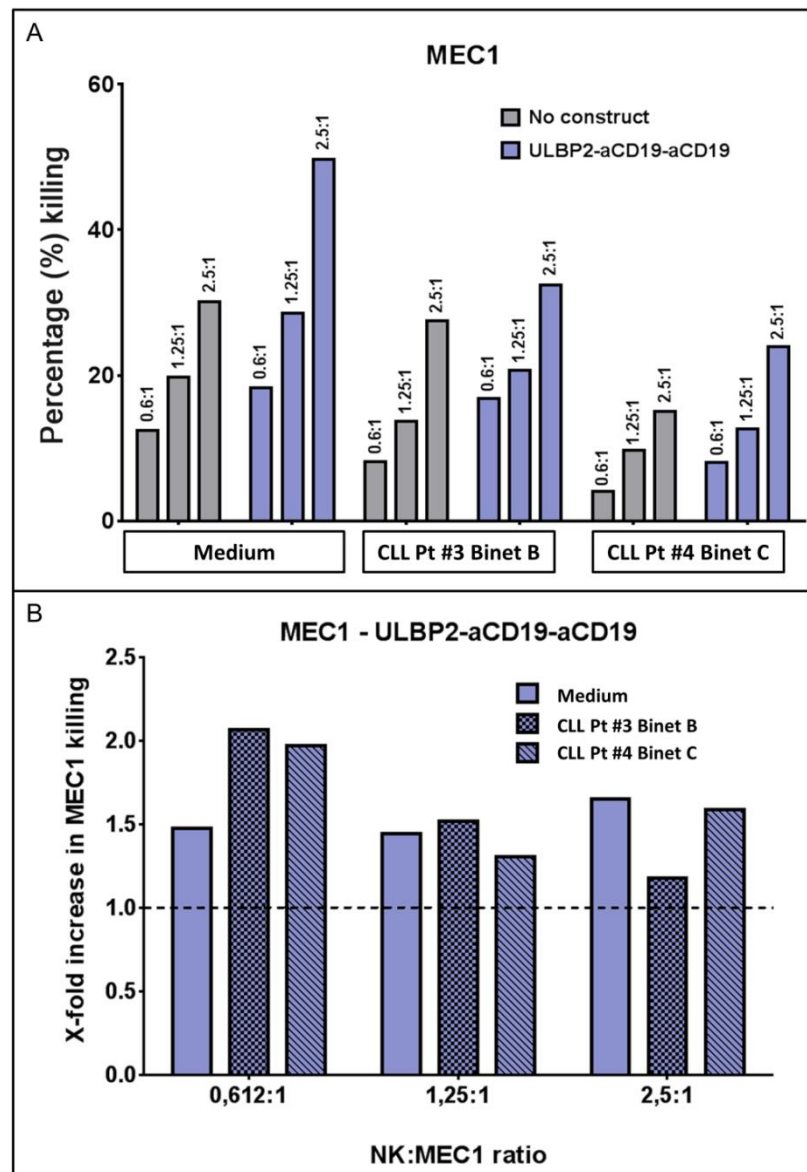


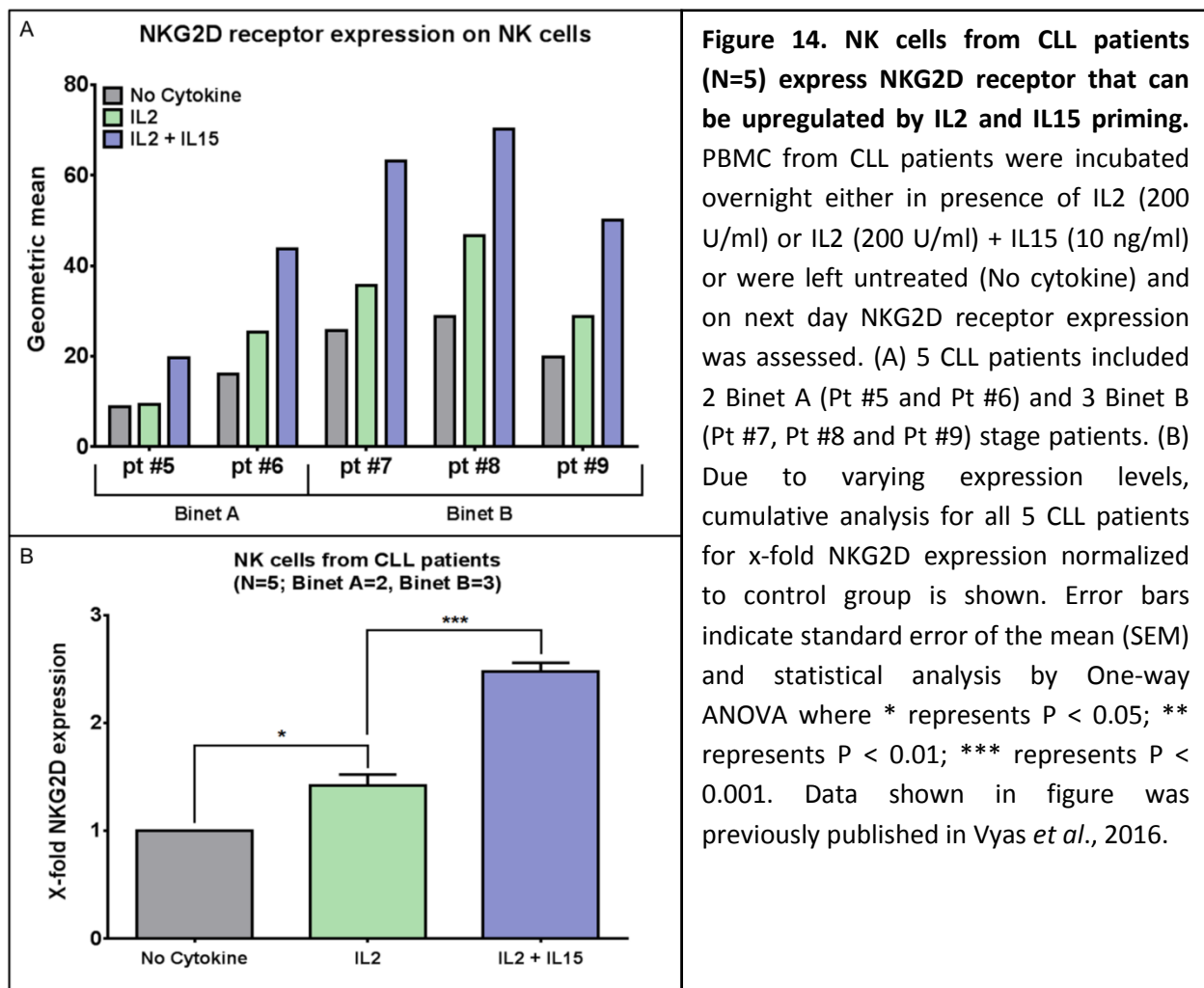
**Figure 13. ULBP2-aCD19- aCD19 overcomes the inhibitory effects of CLL serum samples to enhance NK cell dependent killing of MEC1 cell.** (A) The toxicity assay was carried out in presence of 20% serum from indicated CLL patients or same volume of IMDM medium. Dead cells were measured by 7-AAD staining in DiR positive target cells after 3 hours of co-incubation. The serum from CLL Pt #3 (Binet B) contained 537 pg/ml and from CLL Pt #4 (Binet C) contained 670 pg/ml soluble NKG2D ligands. E:T ratio written at top of each bar. (B) ULBP2-aCD19-aCD19 induced killing of MEC1 cells was normalized to the background killing by NK cells to calculate ULBP2-aCD19-aCD19 specific x-fold killing of MEC1 cells. Data shown in figure was previously published in Vyas *et al.*, 2016.

Serum from CLL patients contains high levels of soluble ligands for NK cell receptors as well as other soluble immune-inhibitory factors that can counteract any NK cell therapeutic approach. For example, soluble ligands for NKG2D can block this receptor and in turn prevent triplebody to bind and recruit NK cells. Therefore, toxicity assays were performed in presence of serum from CLL patients to check if ULBP2-aCD19-aCD19 can overcome the inhibition to mediate NK cell dependent killing of MEC1 cells (figure 13).

IL2 and IL15 primed NK cells from healthy donors were used with MEC1 cells in a 3 hour toxicity assay in absence or presence of 20% serum from two CLL patients. The serum from CLL Pt #3 (Binet B) contained 537 pg/ml soluble NKG2D ligands (ULBP2 – 12 pg/ml; MICA – 525 pg/ml); and from CLL Pt #4 (Binet C) contained 670 pg/ml soluble NKG2D ligands (MICB – 89 pg/ml, ULBP2 – 41 pg/ml; MICA – 540 pg/ml). It is possible that these serum samples also contained other NKG2D ligands or other inhibitory factors that were not quantified. As shown in figure 13(A), background killing of MEC1 cells by NK cells (No construct/immunoligand) was also reduced for all E:T ratios by serum from CLL pt #3 (Binet B) and even further by serum from CLL pt #4 (Binet C). Presence of ULBP2-aCD19-aCD19 could still enhance NK cell dependent killing of MEC1 cells in each group despite the presence of soluble NKG2D ligands and other inhibitory factors in serum samples from CLL patients which is further clarified in figure 13(B). Normalized values show that at higher NK:MEC1 ratios (2.5:1 and 1.25:1), triplebody induced MEC1 killing in presence of serum samples was in similar range to the control group, however, at E:T – 0.612:1, triplebody induced MEC1 killing was higher in presence of serum from both patients compared to without serum. Of note, this was due to stronger inhibition of NK cell mediated background killing rather than higher triplebody-specific killing at 0.612:1 ratio.

### 5.5. ULBP2-aCD19-aCD19 mediates NK cell dependent killing of primary CLL cells in autologous setting

In allogeneic setting, killer cell immunoglobulin-like receptors (KIR) mismatch between donor NK and patient CLL/MEC1 cells can contribute towards NK cell dependent target cell killing. In autologous setting, patient NK cells are less responsive towards the cancer cells from the same patient due to complete KIR matching. In addition, whether NK cells in CLL patients express NKG2D receptor and if these can be primed by IL2 and IL15 cytokines were two major concerns for feasibility of my therapeutic approach.



To test this, PBMC from 5 CLL patients (at Binet A and B stages) were stained with AF647-labeled anti-NKp46 and FITC-labeled anti-NKG2D antibodies to assess the expression level of NKG2D receptor on NK cells (figure 14). While, NK cells from all CLL patients expressed NKG2D endogenously at varying level, overnight incubation with IL2 alone significantly upregulated NKG2D expression on NK cells from all CLL patients ( $p=0.03$ ). Combination of IL2 + IL15 further enhanced the NKG2D expression on NK cells compared to “no cytokine” ( $p=0.0001$ ) and IL2 alone ( $p=0.0002$ ) groups. Similarly, NKG2D expression on CD8 T cells was also found to be upregulated by IL2 + IL15 (data not shown).

These findings encouraged to study whether ULBP2-aCD19-aCD19 can overcome KIR inhibition to retarget patient’s own effector cells against tumor cells in autologous setting. First, toxicity assays in autologous setting were performed utilizing patient’s innate or unaltered NK to CLL (E:T) ratio. PBMC were isolated from peripheral blood of CLL patients and were stained by AF647-labeled anti-NKp46 (NK cells), PB-labeled anti-CD3 (T cells) and AF647-labeled anti-CD20 + PB-labeled anti-CD5 (CLL cells) antibodies to characterize NK, T and CLL cell populations. For example, of total two analyzed Binet A patients in this study, Pt #10 had higher percentage of NK and T cells (3.61% and 15.5%) compared to Pt #11 (NK: 0.81% and T: 4.28%), shown in figure 15(A). This led to the different endogenous NK:CLL ratio in both patients with 0.05:1 – NK:CLL in Pt #10 and 0.009:1 – NK:CLL in Pt #11. For toxicity assay, PBMC from both CLL patients were cultured alone or in presence of 10 nM ULBP2-aCD19-aCD19 for 48 hours and absolute CLL count was calculated at the end of the incubation. Dead CLL cells were excluded by addition of 7-AAD dye. Figure 15(B) shows that in correlation with innate NK:CLL ratio, Pt #10 (with higher NK:CLL ratio) had lower viable CLL cells compared to Pt #11 (with lower NK:CLL ratio) and this also correlated with higher 7-AAD positive (dead) CLL cells in Pt #10 then in Pt #11 (shown in figure 15(C)).

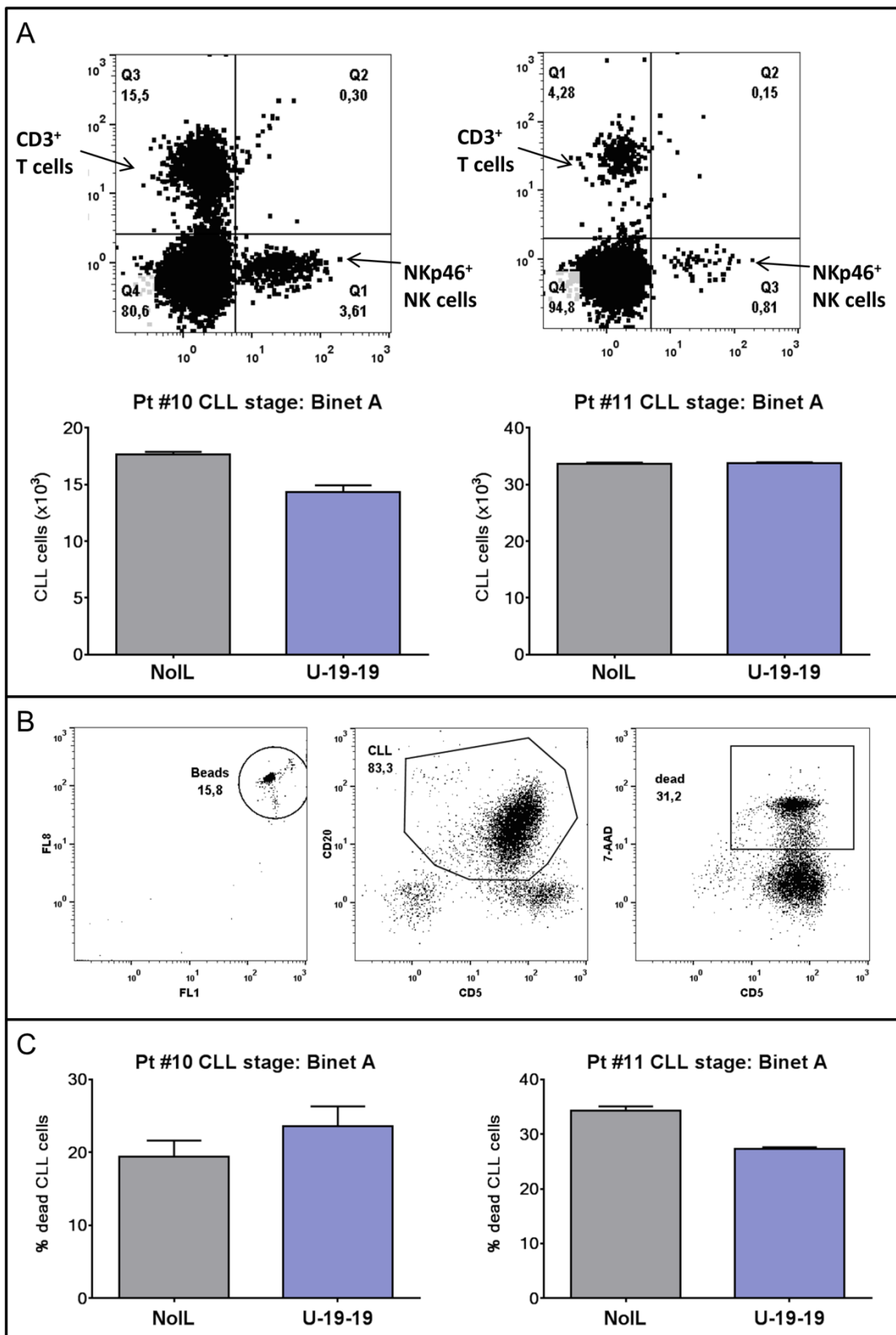
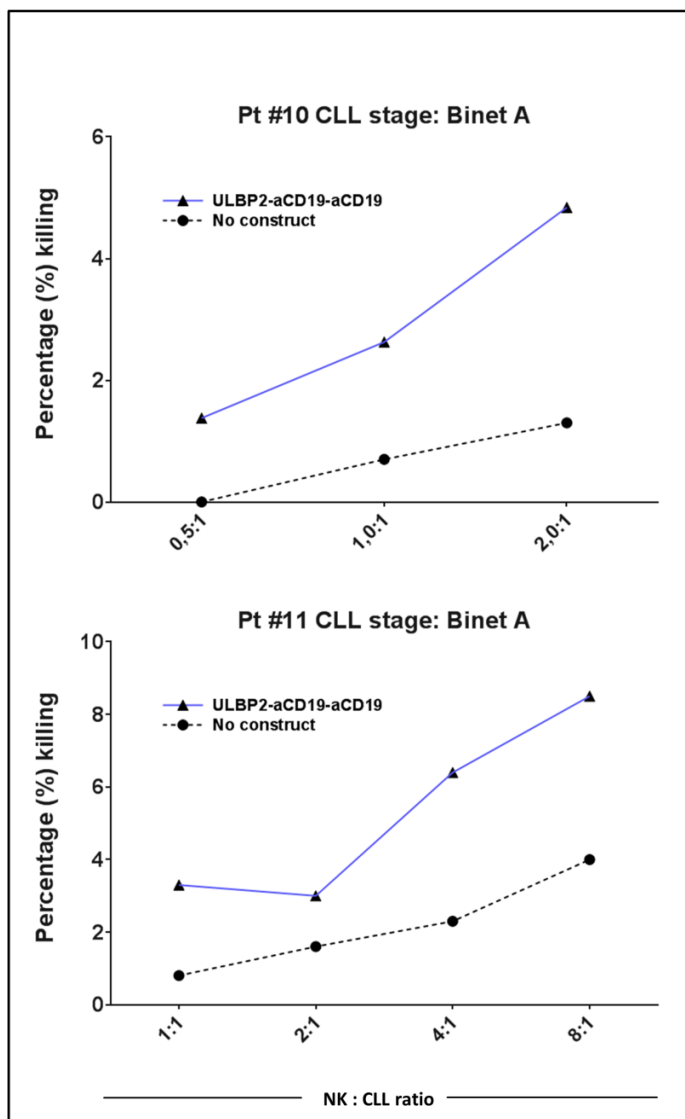


Figure 15. ULBP2-aCD19-aCD19 induced and autologous NK cell mediated killing of CLL cells depends on endogenous NK:CLL ratio. (Figure legend on next page)

**Figure 15. ULBP2-aCD19-aCD19 induced and autologous NK cell mediated killing of CLL cells depends on endogenous NK:CLL ratio.** (A) PBMC were isolated from peripheral blood of CLL patients and were stained by anti-NKp46 (NK cells), anti-CD3 (T cells) and anti-CD20 + anti-CD5 (CLL cells) antibodies to characterize NK, T and CLL cell populations. Both CLL Binet A patients, Pt #10 and Pt #11, had varying innate NK:CLL ratios (0.05:1 and 0.009:1, respectively). Isolated PBMC were incubated alone or in presence of 10 nM ULBP2-aCD19-aCD19 for 48 hours and absolute CLL cell count was measured. In addition, 7-AAD was added to exclude any dead cells (Gating strategy in (B) and results shown in (C)). Error bars indicate standard error of the mean (SEM) of duplicates. Data shown in figure was previously published in Vyas *et al.*, 2016.



**Figure 16. ULBP2-aCD19-aCD19 enhanced autologous NK cell mediated killing of CLL cells in effector to target ratio dependent manner.** NK cells were purified by negative selection from PBMC of both patients and were primed with IL2 + IL15 overnight. The following day, NK cells were co-incubated with DiR-labeled purified CLL cells from the same patient for 3 hours either alone or in presence of 10 nM ULBP2-aCD19-aCD19 and dead CLL cells were analyzed by 7-AAD gating. For both patients, triplebody enhanced NK cell dependent killing of CLL cells with increase in NK:CLL ratio. Data shown in figure was previously published in Vyas *et al.*, 2016.

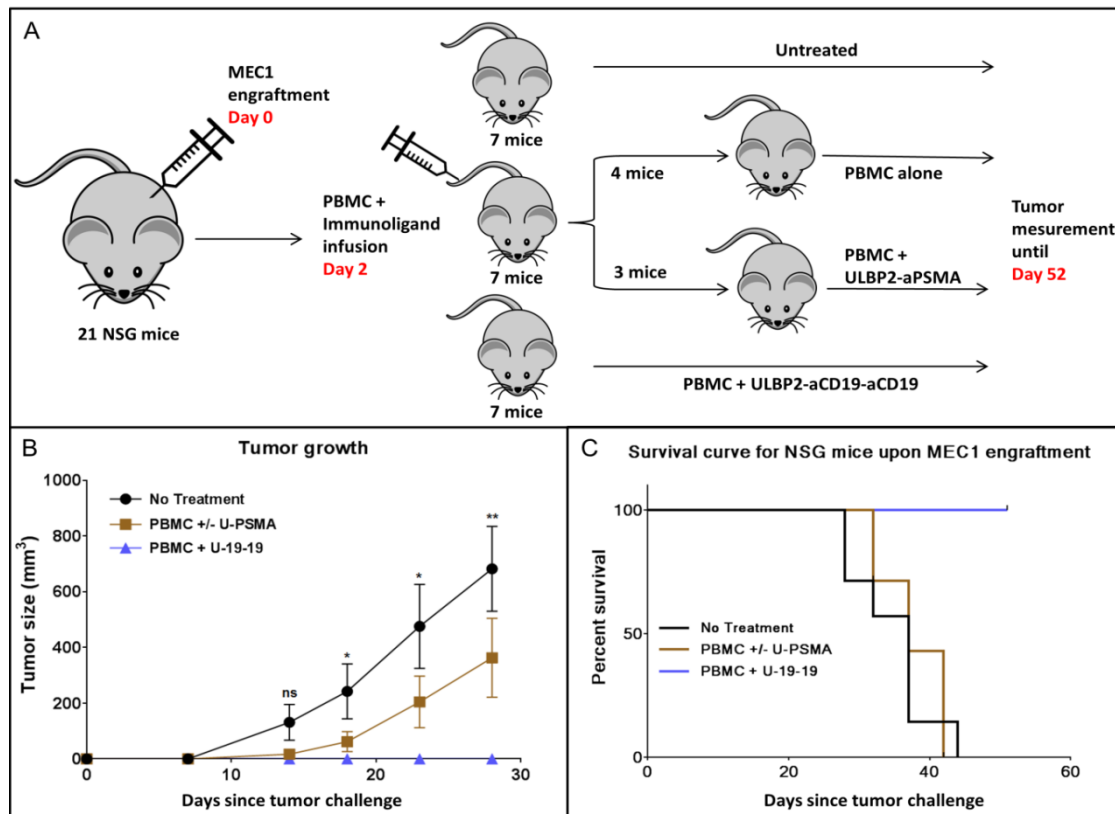
Next, NK cells were purified from the peripheral blood of the same patients (Pt #10 and Pt #11), were primed overnight IL2 and IL15 and were incubated with purified malignant B cells from the same patients to test the effect of the triplebody. The main idea was to check whether increasing the innate NK:CLL ratio can improve the triplebody mediated killing of CLL cells. Presence of ULBP2-aCD19-aCD19 enhanced NK cell dependent killing of CLL cells from both patients in merely 3 hours despite KIR inhibition. The killing capacity became more evident with increase in NK cell proportion and Pt #11 which was resistant to triplebody induced NK cell response during earlier toxicity assay now turned susceptible.

#### **5.6. ULBP2-aCD19-aCD19 shows promising anti-tumor activity in immuno-deficient mouse model (NSG)**

Finally, the ability of ULBP2-aCD19-aCD19 to restrict tumor growth was assessed in MEC1 xenografted immunodeficient mice. In total 21 female NOD *scid* gamma (NSG™) mice, aged around 5-6 weeks, were utilized in this study. NSG strain carries severe combined immunodeficiency (*scid*) and IL2 receptor deficiency on NOD/ShiLtJ background and is the most immunodeficient strain described to date. The NOD/ShiLtJ background already represents reduced innate immune system to which *Prkdc<sup>scid</sup>* or *scid* mutation results in almost complete elimination of mature B and T cells (adaptive immune system). The null mutation in IL2 receptor gamma chain (IL2R $\gamma$ ) completely blocks NK cell differentiation and enables efficient engraftment of xenografts.

Figure 17(A) shows the experimental plan and time line of the study. On day 0, MEC1 cells ( $5 \times 10^6$ ) were injected into the flank of all 21 NSG mice by a subcutaneous (s.c.) injection and mice were randomly distributed into 3 groups. Two days later,  $4 \times 10^5$  PBMC (freshly isolated from a healthy donor) together with 15  $\mu$ g of ULBP2-aCD19-aCD19 were transplanted intravenously (tail vein) in 7 mice. The control group consisting of 7 mice was left untreated. Remaining 7 mice in the second group were further

divided in two groups and 4 out of 7 mice were treated with  $4 \times 10^5$  PBMC alone while 3 mice were treated with  $4 \times 10^5$  PBMC along with 15  $\mu\text{g}$  of ULBP2-aPSMA (non-relevant immunoligand). However, for initial analysis (figure 17), both subgroups (4 + 3 mice) were combined in the same group considered as a “PBMC  $\pm$  U-PSMA” control group. Tumor growth was monitored by measuring the tumor volume regularly until the end of the study on day 52.



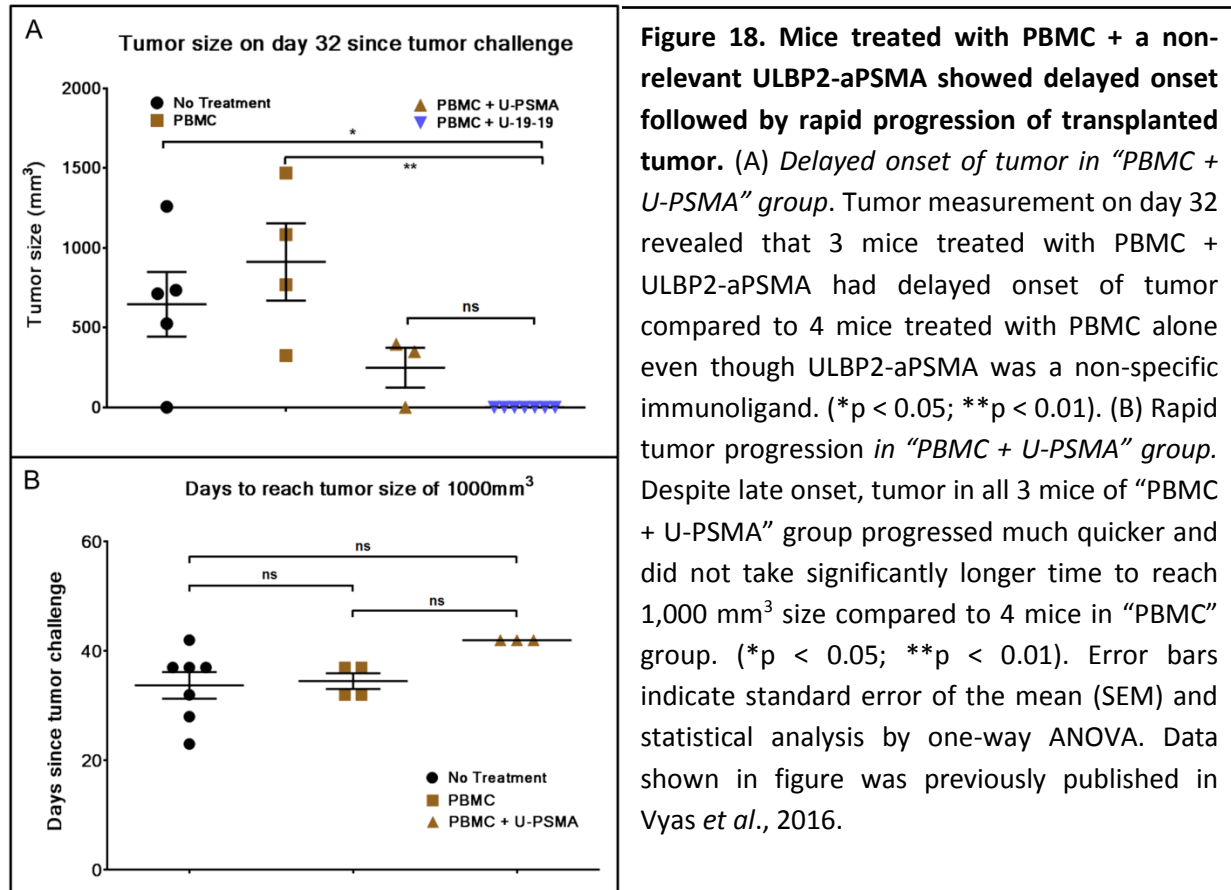
**Figure 17. ULBP2-aCD19-aCD19 restricts tumor growth in MEC1 xenotransplanted NOD™ scid gamma (NSG) mice.** (A) Subcutaneous engraftment of MEC1 cells to 21 NSG mice on day 0 followed by human PBMC transplantation alone or together with ULBP2-aPSMA (non-relevant immunoligand) (7 mice); or together with 15  $\mu\text{g}$  of ULBP2-aCD19-aCD19 (7 mice). Tumor growth was monitored regularly until the end of the study on day 52. (B) Tumor growth was assessed by measuring the tumor size on each mouse at regular intervals using the formula for tumor volume ( $L \times W \times H/2$ ). The graph shows the measurements until day 28 which was the last time point when all 21 mice were alive. Error bars indicate standard error of the mean (SEM) and statistical analysis by one-way ANOVA,  $N=7$  in each group. For simplicity, statistical significance between “No treatment” and “PBMC + U-19-19” groups are shown. (\* $p < 0.05$ ; \*\* $p < 0.01$ ). (C) During the total duration of the study (52 days), mice were sacrificed when the tumor volume reached 1,000 mm<sup>3</sup>. Data shown in figure was previously published in Vyas *et al.*, 2016.

Figure 17(B) compares the mean of tumor volume in each group until day 28 as this was the last day when all 21 mice were alive and 2 mice in the control “no treatment” group had to be sacrificed after this time point due to tumor volume larger than 1,000 mm<sup>3</sup>. The tumor occurrence was first observed in 7 mice in “no treatment” group, while the PBMC transplantation, either alone or with an irrelevant construct (PBMC + U-PSMA), delayed the tumor occurrence in “PBMC ± U-PSMA” group. However, the tumor growth between both control groups (“no treatment” and “PBMC ± U-PSMA”) was not significantly different at any given time point. On the other hand, transplantation of PBMC with ULBP2-aCD19-aCD19 (PBMC + U-19-19) completely restricted the tumor occurrence in these mice and this effect was significant compared to the “no treatment” group.

According to ethical regulations, mice were sacrificed upon the tumor volume reaching 1,000 mm<sup>3</sup>. The study was continued for 52 days and as shown in figure 17(C) all mice in both “no treatment” and “PBMC U-PSMA” groups had to be sacrificed due to large tumor volume while all 7 mice treated with ULBP2-aCD19-aCD19 remained tumor free and were censored at the end of the study. Kaplan Meier survival curve of “PBMC + U-19-19” group was significantly different from “PBMC ± U-PSMA” ( $p = 0.0003$ ) and “No treatment” group ( $p = 0.0002$ ) while there was no significant difference between “PBMC ± U-PSMA” and “no treatment” groups ( $p = 0.568$ ). (Two tailed  $p$  value  $< 0.0167$  was considered as significant; 0.0167 was Bonferroni-corrected threshold).

Interestingly, the initial tumor growth among mice treated with PBMC alone or along with a non-relevant immunoligand ULBP2-aPSMA showed discrepancy. The tumor occurrence and initial progression in 3 mice treated with PBMC + ULBP2-aPSMA was delayed compared to 4 mice treated with PBMC alone (figure 18(A)). This was surprising as ULBP2-aPSMA immunoligand was not expected to retarget NK cells to PSMA negative transplanted human cells (PBMC or MEC1). However, in the

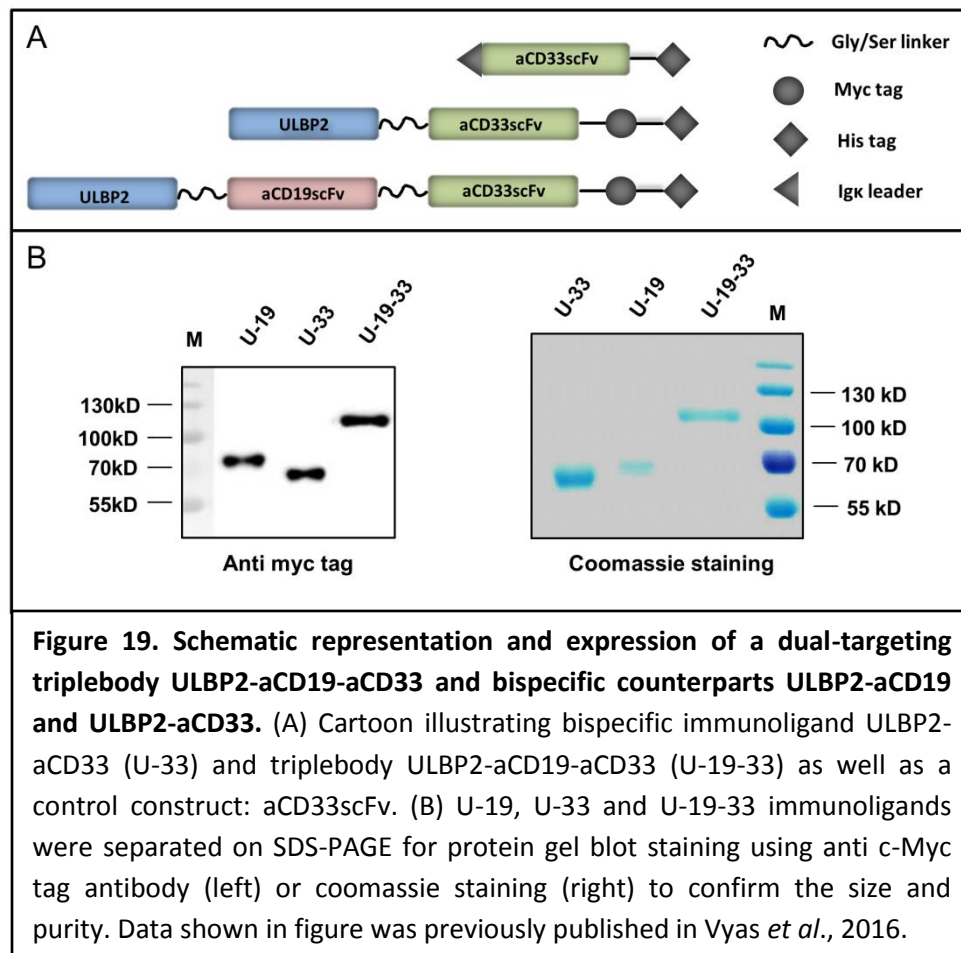
following weeks tumor started progressing rapidly in all 3 mice in “PBMC + U-PSMA” group and took similar duration to reach 1,000 mm<sup>3</sup> compared to 4 mice in “PBMC” group (figure 18(B)).



### 5.7. A dual-targeting triplebody ULBP2-aCD19-aCD33 can simultaneously bind to all three target antigens and retains specificity for antigen loss variants

Expression vectors pL(ULBP2-aCD19-aCD33), pL(ULBP2-aCD33) and pL(aCD33scFv) were successfully cloned and complete reading frame was sequenced. Expression vectors for CD19 targeting bispecific counterpart (pL(ULBP2-aCD19)) and blocking construct (pL(aCD19scFv)) were generated for CLL project and is described previously in section 2 of results. Similar to previous constructs, three new constructs in this project were also transfected into HEK293T cells and stable clones were selected with Zeocin™ as the plasmids also expressed Zeocin-resistance gene. Stable clones (polyclonal) were subsequently

cultured in serum free CD293 medium and SN was collected every 2-3 days over a period of month. As shown in figure 19(A), triplebody ULBP2-aCD19-aCD33 and bispecific counterpart ULBP2-aCD33 were secreted into the SN of transfected cells by innate secretion signal carried at the N-terminus of ULBP2. In contrast, secretion of a blocking construct aCD33scFv was enabled by Igk leader sequence at the N-terminus. A Gly/Ser linker of total 20 amino acids—(GGGGS)<sub>4</sub>x was used to link each moiety (figure 19(A)) as well as VH and VL domains of an scFv (not shown in the figure) to confer flexibility to the immunoligands. C-terminus 6xHis (HHHHHH) tag was used for purification of all constructs while an additional c-Myc tag at the C-terminus of U-33 and U-19-33 was used for their detection purposes. Between 400 µg to 700 µg of U-33 and U-19-33 and around 1 mg of aCD33scFv was purified from around 1 liter of the culture SN.



Once purified, immunoligands were separated by SDS-PAGE for c-Myc tag specific immunoblotting (figure 19(B), left) and coomassie staining (figure 19(B), right). Triplebody U-19-33 and bispecific immunoligands U-19 and U-33 were found to be pure, according to the expected molecular weight and monomeric in nature. U-19 and U-33 had the expected molecular weight of  $\approx 64$  kDa and  $\approx 58$  kDa and U-19-33 was, as expected, of  $\approx 89$  kDa, respectively. Purity and molecular weight for blocking constructs aCD19scFv and aCD33scFv were also verified by coomassie staining (data not shown).

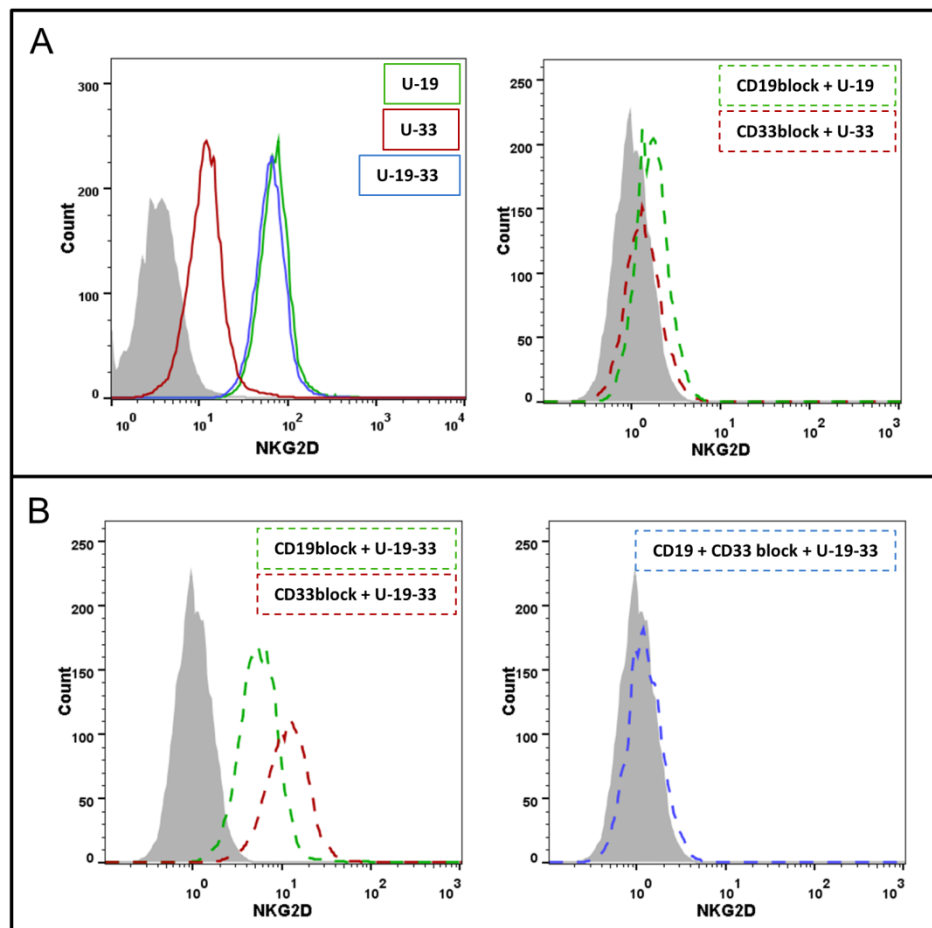


**Figure 20. ULBP2-aCD19-aCD33 and bispecific counterparts ULBP2-aCD19 and ULBP2-aCD33 bind specifically to the respective target antigens.** (A) Incubation of 10  $\mu\text{g}/\text{ml}$  immunoligands with CD19<sup>+</sup>/CD33<sup>+</sup> BV173 cell line as detected by recombinant NKG2D-Fc receptor (left graph). Pre-blocking of CD19 or CD33 antigens by aCD19scFv or aCD33scFv blocking constructs (both at 20  $\mu\text{g}/\text{ml}$ ) completely inhibited the binding of respective bispecific immunoligands (right graph). (B) Blocking of either CD19 or CD33 antigens by aCD19scFv or aCD33scFv (20  $\mu\text{g}/\text{ml}$ ) reduces the binding of a dual-targeting triplebody ULBP2-aCD19-aCD33, but does not abolish it (left graph). Binding can only be completely abrogated by pre-blocking of both CD19 and CD33 antigens simultaneously (right graph). Data shown in figure was previously published in Vyas *et al.*, 2016.

Whether purified immunoligands retained their binding specificities for all target moieties was the next question for assessment. In addition, ULBP2-aCD19-aCD33 was developed as a dual-targeting triplebody with specificities for two distinct antigens on cancer cells. It was developed with a rationale to target antigen loss variants of tumor. Can ULBP2-aCD19-aCD33 still bind to target cells when either CD19 or CD33 is blocked was an equally important question. To this end, CD19 and CD33 double positive cell line BV173 was used for FACS based binding assay. Binding of triplebody (U-19-33) and both bispecific immunoligands (U-19 and U-33) to CD19<sup>+</sup>CD33<sup>+</sup> BV173 cells could be detected by recombinant NKG2D receptor suggesting that simultaneous binding to BV173 cells and NKG2D receptor is possible for all three immunoligands (figure 20(A)). As BV173 cells express several-fold less molecules of CD33 than CD19, the signal intensity for ULBP2-aCD33 binding was low compared to the other two immunoligands.

As shown in figure 20(A), pre-blocking of CD19 or CD33 antigen prevented ULBP2-aCD19 and ULBP2-aCD33 to bind, respectively. Blocking of either CD19 or CD33 by respective blocking construct could mimic CD19 or CD33 antigen loss variants of BV173 cells: CD19<sup>+</sup>CD33<sup>block</sup> or CD19<sup>block</sup>CD33<sup>+</sup> BV173 cells. NKG2D mediated detection revealed that ULBP2-aCD19-aCD33 could retain its specificity for these variants even when one of the antigen was blocked. Only simultaneous blocking of CD19 and CD33 antigens on BV173 cells could completely abolish the binding of ULBP2-aCD19-aCD33 (figure 20(B)).

Individual specificities of a triplebody ULBP2-aCD19-aCD33 was also checked on CD19<sup>+</sup> MEC1 cells. For comparison both bispecific immunoligands were also used. Immunoligands were incubated with MEC1 cells and their CD19-specific binding was detected using recombinant CD33 (with FLAG tag) and NKG2D (with Fc tag) receptors. AF647-labeled anti-Fc and PE-labeled anti-FLAG antibodies could detect the bound receptors. As shown in figure 21 ("U-19-33"), dual signal in FITC and AF647 channel confirmed that ULBP2-aCD19-aCD33 could simultaneously bind to CD19, CD33 and NKG2D through individual specificity. Similarly, CD19 antigen bound ULBP2-CD19 could bind to NKG2D receptor as it lacked CD33

specific scFv (“U-19”). ULBP2-aCD33 served as a negative control and could not bind to CD19<sup>+</sup> but CD33<sup>-</sup> MEC1 cells (“U-33”).

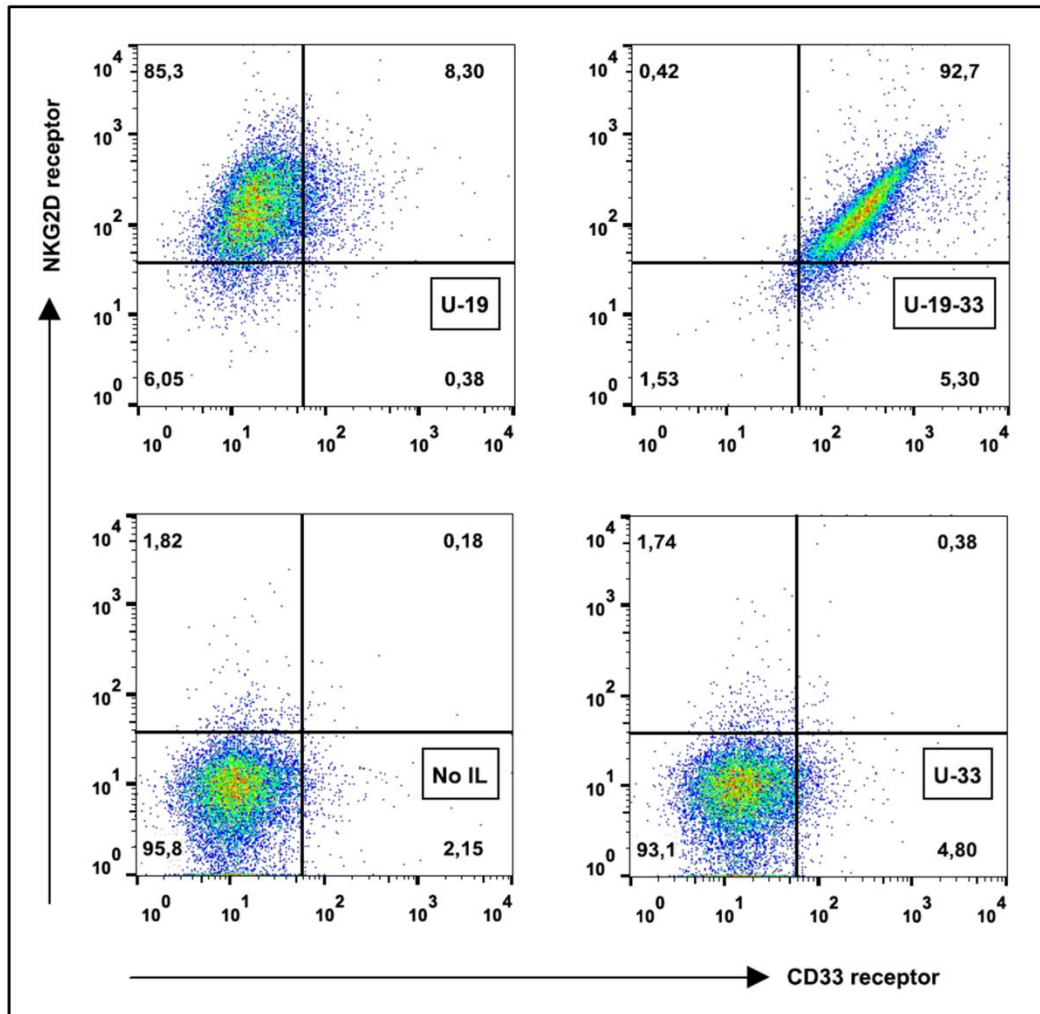


**Figure 21. Simultaneous and antigen specific binding of a triplebody ULBP2-aCD19-aCD33.** CD19<sup>+</sup> MEC1 cell line was incubated with ULBP2-aCD19-aCD33 (U-19-33), ULBP2-aCD19 (U-19) or ULBP2-aCD33 (U-33) binding was detected using recombinant human NKG2D-Fc and CD33-FLAG receptors followed by AF647-labeled anti-Fc and PE-labeled anti-FLAG antibodies, respectively. NKG2D-Fc and CD33-FLAG background binding was minimal (No IL – lower left). Data shown in figure was previously published in Vyas *et al.*, 2016.

### **5.8. ULBP2-aCD19-aCD33 enhances NK cell dependent killing of CD19/CD33 double positive cell lines as well as antigen loss variants**

To investigate the role of a dual-targeting triplebody in NK cell dependent killing of CD19 and CD33 double positive cells, two B cell precursor leukemia cell lines BV173 and SEM were utilized. NK cells were purified from healthy donors and were primed with IL2 (200 U/ml) and IL15 (10 ng/ml). NK cells were also routinely characterized for NKG2D expression, activation status and purity and only preparations  $\geq$  98% purity were used for experiments.

ULBP2-aCD19-aCD33 and both bispecific immunoligands enhanced NK cell dependent killing of BV173 and SEM cell lines (figure 22(A)). Triplebody induced increase in the killing of both cell lines was at least 2-fold at all E:T ratios and as with ULBP2-aCD19-aCD19, was also more potent than both bispecific counterparts in NK cell retargeting. The difference in killing by ULBP2-aCD19 and ULBP2-aCD33 seems to be dependent on antigen density on the surface of target cells. ULBP2-aCD33 induced killing was less compared to ULBP2-aCD19 for both BV173 and SEM cell lines as the expression of CD33 is several folds less than CD19 on the surface of both cell lines. Pre-blocking of NKG2D receptor on NK cells by anti-NKG2D antibody (clone 1D11) completely abolished the triplebody induced toxicity against both cell lines (figure 22(B)). The results of these toxicity assays were supported by independent FACS based degranulation assay in response to SEM cells. As shown in figure 22(C), ULBP2-aCD19-aCD33 induced around 1.5-fold more NK cells to degranulate in response to SEM.

In addition, the ability of immunoligands to induce IFN $\gamma$  production by IL2 and IL15 primed NK cells was assessed. NK cells were cultured for 48 hours in the plate pre-coated by immunoligands and SN was used to quantify IFN $\gamma$  by ELISA. Both, bispecific immunoligands and triplebody could augment the secretion of IFN $\gamma$  by NK cells. This was strictly dependent upon the NKG2D and ULBP2 interaction as blocking constructs lacking ULBP2 could not induce IFN $\gamma$  secretion (figure 22(C)).

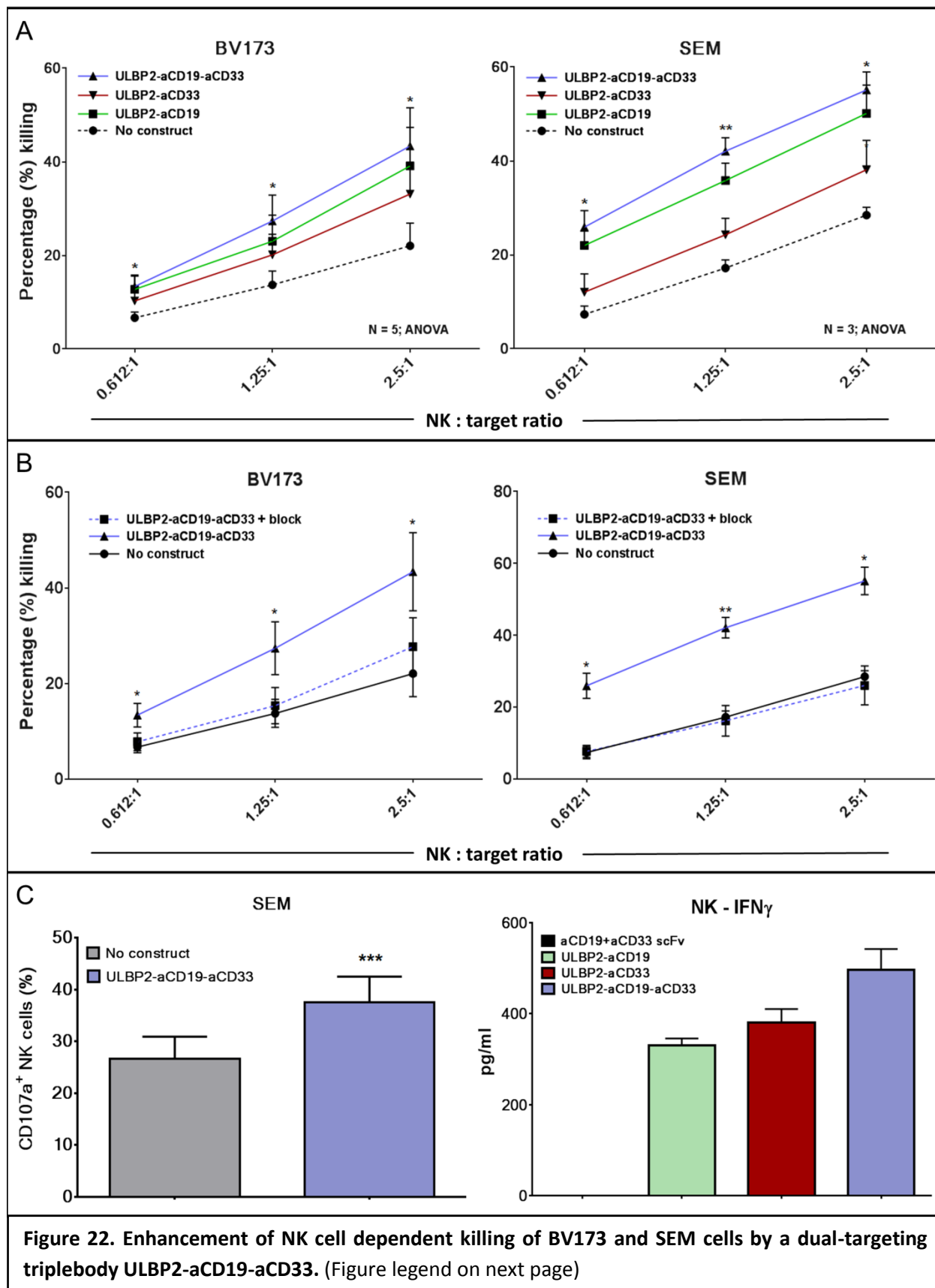


**Figure 22. Enhancement of NK cell dependent killing of BV173 and SEM cells by a dual-targeting triplebody ULBP2-aCD19-aCD33.** (A) Target cells (BV173 or SEM) were labeled with DiR and were incubated with IL2 + IL15 primed NK cells either alone or in presence of 100 nM immunoligands at 0.612:1, 1.25:1 and 2.5:1 E:T ratios. (B) NK cells were incubated with 10 µg/ml of mouse anti-human NKG2D receptor antibody (clone 1D11) for 30 min on ice to block NKG2D. Excess antibody was washed away after 30 min and toxicity assay was set up as described above. For (A) and (B), error bars indicate standard error of the mean (SEM) and statistical analysis by One-way ANOVA; N=5 (BV173) and N=3 (SEM). Each N represents an independent healthy NK cell donor and \*P < 0.05; \*\*P < 0.01. (C) For FACS based degranulation assay (left), IL2 + IL15 primed NK cells were co-incubated with SEM cells in 2.5:1 (E:T) ratio alone or in presence of 100 nM ULBP2-aCD19-aCD33 for 6 hours and CD107a stained cells within CD56<sup>+</sup> NK cells indicated degranulated NK cells by flow cytometry. Error bars indicate standard error of the mean (SEM) and statistical analysis by Paired *t*-test; N=5. Each N represents an independent healthy NK cell donor. For ELISA based IFN $\gamma$  assay (right), IL2 + IL15 primed NK cells were cultured in presence of coated indicated immunoligands (10 µg/ml) for 48 hours and SN was collected to quantify IFN $\gamma$  by ELISA. Error bars indicate standard error of the mean (SEM) of duplicates. Experiments were conducted with three independent NK donors and one example is shown here. Data shown in figure was previously published in Vyas *et al.*, 2016.

It was revealed that ULBP2-aCD19-aCD33 could retain binding ability to CD19<sup>+</sup>CD33<sup>+</sup> BV173 cells even when one of the antigens was blocked. Whether this retained specificity could retarget NK cells against antigen loss variants was also checked by FACS based toxicity assay. Similar to binding assay, CD19 or CD33 antigen was blocked on BV173 cells to generate single antigen loss variants of otherwise CD19<sup>+</sup>CD33<sup>+</sup> BV173 cells: CD19<sup>block</sup>CD33<sup>+</sup> BV173 and CD19<sup>+</sup>CD33<sup>block</sup> BV173. CD19<sup>block</sup>CD33<sup>block</sup> BV173 represented a variant which lost both antigens from the surface. Toxicity assays with these target cells were repeated with IL2 and IL15 primed NK cells from 4 individual healthy donors and one representative analysis is shown in figure 23 and a cumulative analysis at 2.5:1 E:T ratio is shown in figure 24.

When both antigens were accessible on BV173 (CD19<sup>+</sup>CD33<sup>+</sup>), all three immunoligands (100 nM) significantly enhanced the NK-cell dependent killing of BV173 cells in the same trend as previous toxicity assays. When CD19 antigen was blocked (CD19<sup>block</sup>CD33<sup>+</sup>) by pre-incubation with molar excess of aCD19scFv construct, BV173 killing induced by ULBP2-aCD19 was completely abolished while ULBP2-

aCD33 and ULBP2-aCD19-aCD33 retained their toxic effects. Similarly, CD33 blocking on BV173 ( $CD19^+CD33^{block}$ ) by molar excess of aCD33scFv could abolish killing by ULBP2-aCD33 but not by ULBP2-aCD19 and the triplebody. Only, complete blocking of both CD19 and CD33 could abolish the killing induced by the dual-targeting triplebody.

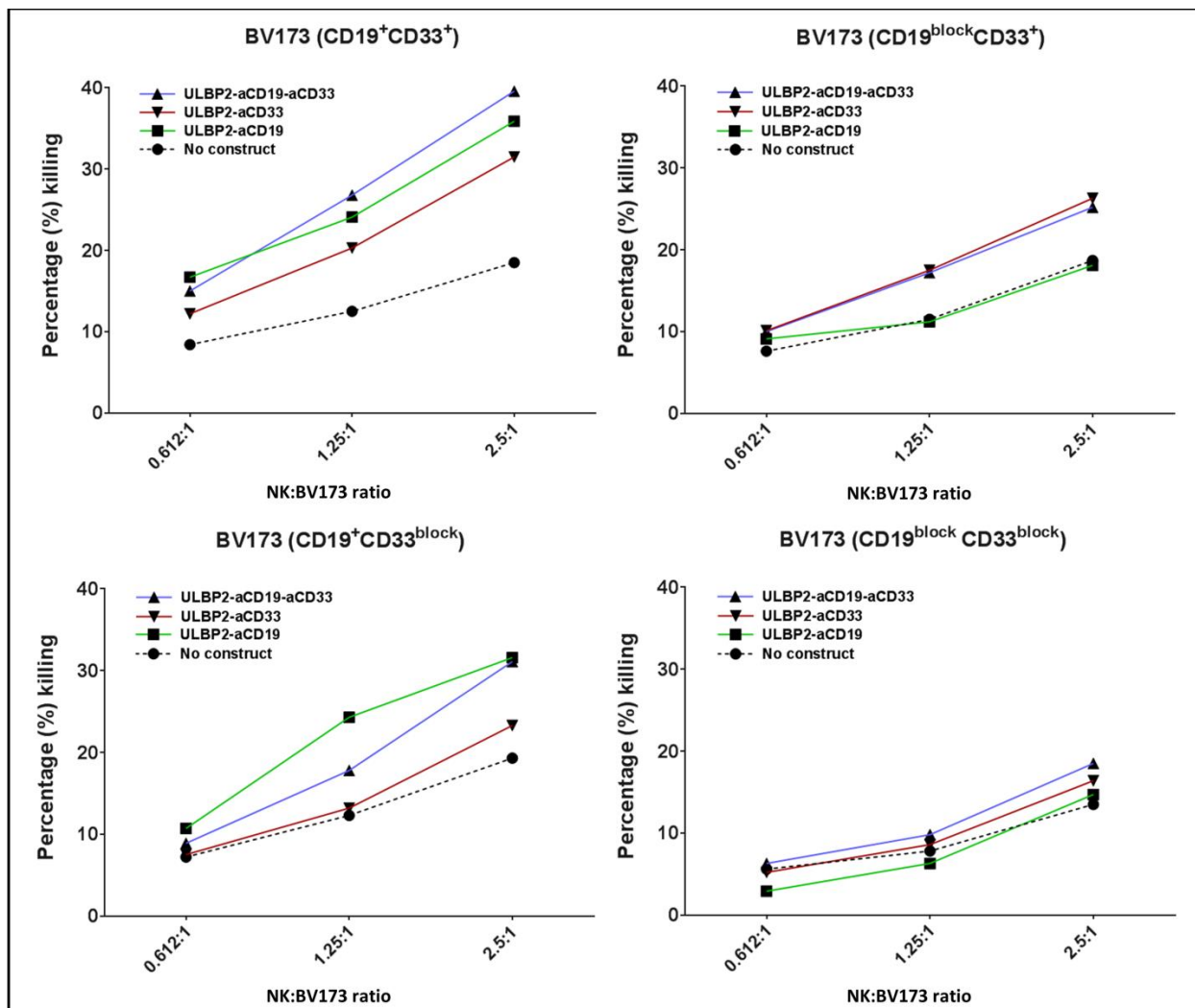


**Figure 23. A dual targeting triplebody ULBP2-aCD19-aCD33 mediates NK cell dependent killing of antigen loss variants.** IL2 + IL15 primed NK cells were incubated with DiR-labeled BV173 cells at indicated E:T ratio for 3 hours. After incubation, 7-AAD was added and 7-AAD positive cells within DiR-positive gate indicated dead target cells. (BV173 -  $CD19^+CD33^+$ ): As shown in the upper left quadrant, when both antigens were accessible on BV173. (BV173 -  $CD19^{block}CD33^+$ ): As shown in the upper right quadrant, when CD19 antigen was blocked by pre-incubation with molar excess of aCD19scFv construct. (BV173 -  $CD19^+CD33^{block}$ ): Similarly, CD33 blocking by molar excess of aCD33scFv (lower left quadrant). (BV173 -  $CD19^{block}CD33^{block}$ ): As shown in lower left quadrant, simultaneous blocking of both, CD19 and CD33 antigens by respective blocking constructs. One representative of 4 independent experiments is shown here (cumulative analysis of N=4 is shown in figure 24).

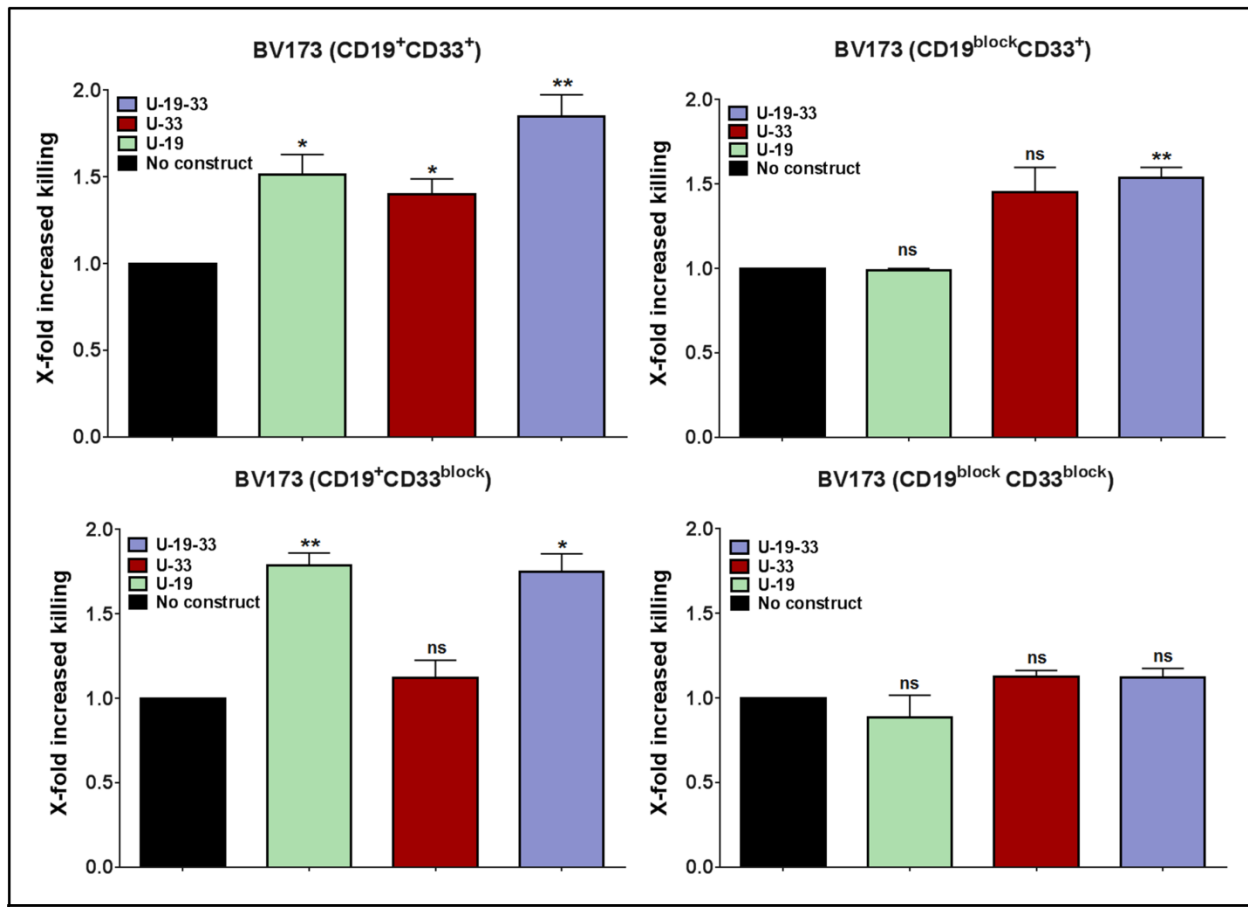


**Figure 24. A dual targeting triplebody ULBP2-aCD19-aCD33 mediates NK cell dependent killing of antigen loss variants (cumulative analysis; N=4).** This figure is a cumulative analysis of a toxicity assay at 2.5:1 (E:T) ratio shown in figure 23 (please refer to the figure legend for detailed explanation). Error bars indicate standard error of the mean (SEM) and statistical analysis by One-way ANOVA; N=4. Each N represents an independent healthy NK cell donor.

### 5.9. Resting NK cells can be activated by CD16 stimulation which can be further enhanced by NKG2D co-stimulation

Similar to initial experiments assessing NKG2D stimulation, here CD16a stimulation on NK cells was analyzed using *Drosophila* Schneider-2 cells as “target cell system”. The typical ligand for human CD16a (FcγRIIIa) receptor includes Fc part of a human IgG1 antibody, which upon binding to CD16a receptor induces antibody dependent cell-mediated cytotoxicity (ADCC). In addition, the Fc part of rabbit IgG antibody can also bind and activate CD16a receptor on human NK cells. Here, rabbit polyserum raised

against Schneider-2 cells was used for stimulation of CD16a receptor. Schneider-2 cells were incubated with 1:10,000 dilution of rabbit polyserum for 30 min at room temperature. These rabbit antibody coated Schneider-2 cells were used as target cells against IL2 (10 U/ml) cultivated resting human NK cells to assess activation via CD69 and degranulation via CD107a markers by flow cytometry. The detailed protocol is explained in section 1 (S2 + ULBP1 – NKG2D assays) and gating strategies are in figure 2.

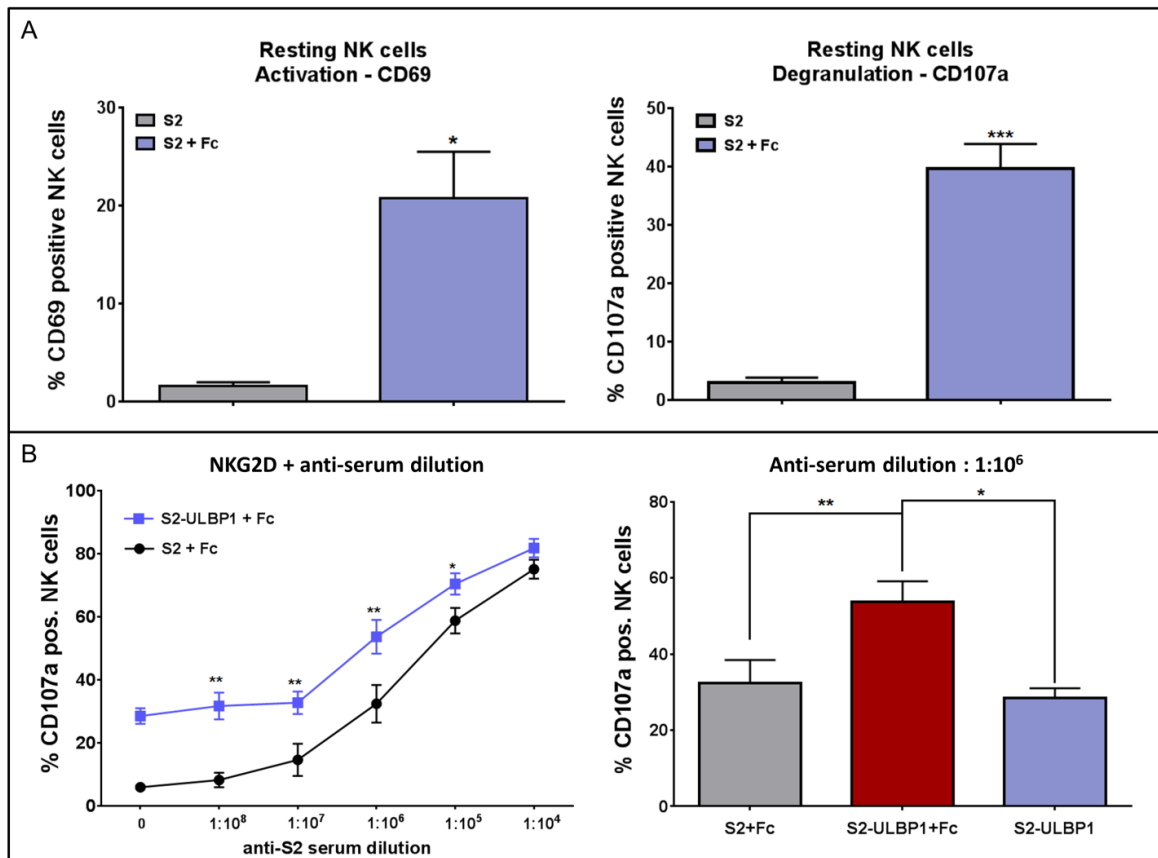


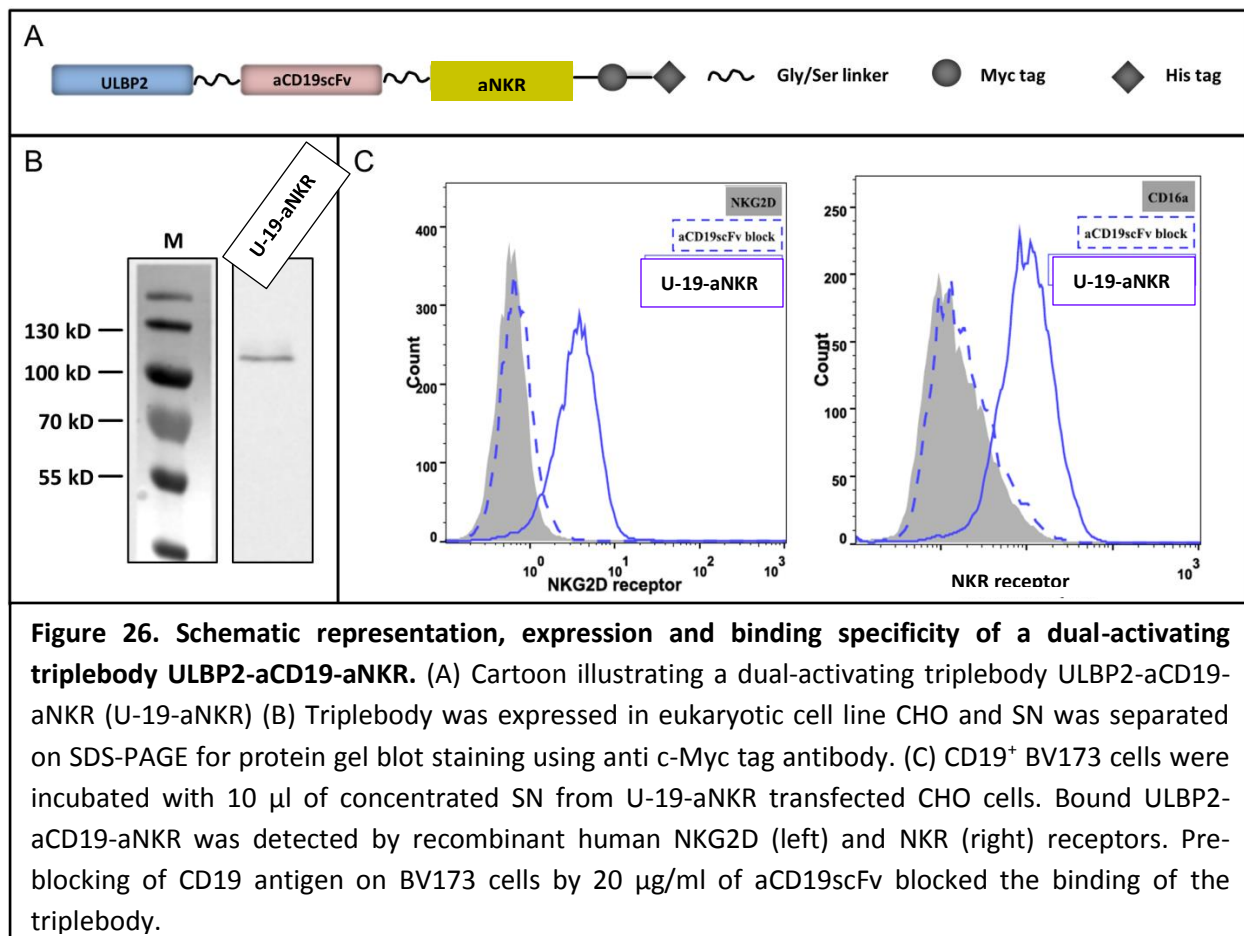
**Figure 25. Activation and degranulation of resting NK cells by CD16 stimulation can be further enhanced by co-stimulation of NKG2D receptor on IL2 + IL15 primed NK cells.** (A) Resting NK cells (10 U/ml IL2) were incubated with drosophila Schneider-2 cells coated with 1:10,000 dilution of anti-S2 polyserum (S2 + Fc) at 1:1 E:T ratio for 6 hours. NK cell activation (left graph) and degranulation (right graph) was assessed by flow cytometry by staining for CD69 or CD107a, respectively. Wild type un-coated Schneider-2 cells (S2) were used as control in both experiments. Error bars indicate standard error of the mean (SEM) and statistical analysis by Student's *t*-test; N=3. (B) Schneider-2 cells transfected with ULBP1 (S2-ULBP1<sup>+</sup>) and WT (S2) were coated with 10-fold dilutions of anti-S2 polyserum (Fc) and were co-incubated with IL2 + IL15 primed NK cells for 6 hours and NK cell degranulation was assessed as described above. Error bars indicate standard error of the mean (SEM) and statistical analysis by Student's *t*-test; N=4.

As shown in figure 25(A), only CD16a stimulation by coated Schneider-2 cells activates and degranulates a significantly, several-fold higher proportion of resting NK cells compared to incubation with uncoated WT Schneider-2 cells. Previously, I could show that NK cell degranulation through NKG2D receptor by ULBP1 on Schneider-2 cells required IL2 and IL15 priming. Therefore, co-stimulation of NKG2D and CD16a receptors on IL2 + IL15 primed NK cells were studied in terms of NK cell degranulation. To this end, Schneider-2 cells, either transfected with ULBP1 or WT (untransfected), were incubated with 10-fold dilutions of rabbit polyserum starting at 1:10,000 dilution and were used as target cells against IL2 + IL15 primed NK cells in FACS based degranulation assay. At anti S2-serum dilution 1:10,000 or 1:10<sup>4</sup>, CD16a stimulation was more dominating and only a little enhancement of NKG2D stimulation could be observed. The additive effect of NKG2D stimulation became more pronounced with increasing anti-S2 serum dilutions. 1:10<sup>6</sup> dilution of serum showed the best additive effects of combined NKG2D and CD16a stimulation on NK cells (figure 25(B)).

#### **5.10. A dual-activating triplebody ULBP2-aCD19-aNKR can retarget resting and freshly isolated NK cells against target cells**

Cloning of a dual-activating triplebody pL(ULBP2-aCD19-aNKR) was done in similar way as previous both triplebodies and was confirmed by restriction digestions and sequencing. Although, ULBP2-aCD19-aNKR utilized the same secretion leader sequence (ULBP2) and was comparable in size to previous triplebodies, it was not readily secreted from HEK293T cells. Chinese hamster ovary (CHO) cells were slightly better in facilitating its secretion and therefore, the expression vector pL(ULBP2-aCD19-aNKR) was transfected into Chinese hamster ovary (CHO) cells and stable clones were selected with Zeocin™ as the plasmids also expressed Zeocin-resistance gene. Stable clones (polyclonal) were subsequently cultured in serum free CD293 medium and SN was collected every 2-3 days over a period of 2-3 weeks. His-tag based purification of ULBP2-aCD19-aNKR was not successful due to the low yield of triplebody in the SN of transfected CHO cells. Therefore, collected SN was filtered to remove proteins or other

contaminants smaller than 90 kDa and was concentrated around 10-fold to increase the concentration of triplebody. This concentrated SN was separated on SDS-PAGE and was stained with c-Myc tag specific antibody to find that the triplebody was of the expected molecular size (figure 26(B)). Importantly, simultaneous binding of ULBP2-aCD19-aNKR to CD19 and recombinant NKG2D or NKR receptor was detected by FACS. ULBP2-aCD19-aNKR in the form of 10  $\mu$ l concentrated SN bound to CD19 on BV173 cells as well as to recombinant human NKG2D or NKR receptors. As with previous immunoligands, binding of this triplebody was antigen specific as pre-blocking of CD19 by aCD19scFv blocked both NKG2D and NKR detections (figure 26(C)).



Next, I addressed whether the addition of an anti-NKR specific scFv to the immunoligand makes it potent to activate NK cells. Moreover, activation of NK cells should only be restricted to immunoligands that are mobilized on target cells as NK cells activation in the absence of target cells can lead to severe side effects in patients. ULBP2-aCD19-aNKR could activate NK cells significantly only in response to BV173 cells, while soluble triplebody was not capable in this regard. A dual-targeting triplebody ULBP2-aCD19-aCD33 had no effect on NK cell activation in response to BV173 cells suggesting that the activating signals were provided by aNKRscFv to NKR receptor on NK cells (figure 27).

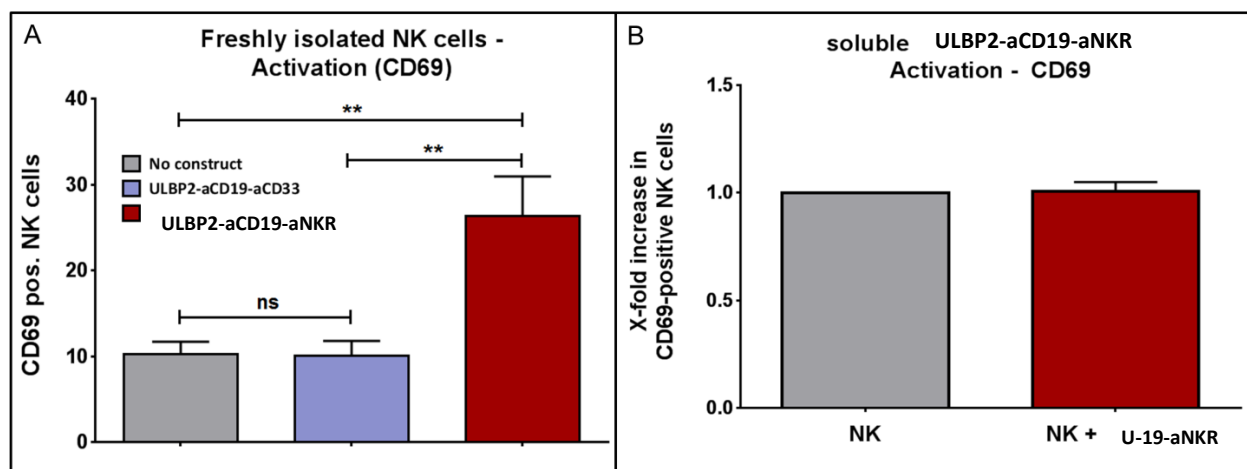


**Figure 27. ULBP2-aCD19-aNKR activates freshly isolated NK cells only when bound to target cells.**

(A) Freshly purified NK cells from healthy donors were incubated with CD19<sup>+</sup> BV173 cells alone or in presence of 100 nM ULBP2-aCD19-aCD33 or 10  $\mu$ l ULBP2-aCD19-aNKR SN for 6 hours. NK cells positive for upregulation of CD69 (stained by FITC-labeled anti-CD69) indicated activated NK cells. Error bars indicate standard error of the mean (SEM) and statistical analysis by One-way ANOVA; N=3. Each N represents an independent healthy NK cell donor. (B) In absence of BV173 cells, soluble ULBP2-aCD19-aNKR fails to activate NK cells after 6 hours of incubation. Error bars indicate standard error of the mean (SEM) of two independent NK cell donors (N=2).

Toxicity assays with MEC1 and BV173 cell lines utilized resting (IL2 - 10 U/ml) NK cells as effector cells and for comparison, respective mono- and dual-targeting triplebodies were used. Presence of ULBP2-aCD19-aNKR (as 10  $\mu$ l concentrated SN) significantly enhanced NK cell dependent killing of MEC1 cells as at all E:T ratios (figure 28(A)). As control, 10  $\mu$ l of similarly concentrated SN from untransfected CHO

cells was added. For one NK cell donor, 10 nM of ULBP2-aCD19-aCD19 was also added for comparison. As shown in figure 28(B), NKG2D stimulation alone on resting NK cells could not induce killing of MEC1 cells. Similarly, ULBP2-aCD19-aNKR could induce retargeted killing of BV173 cells at both E:T ratios by purified NK cells from two independent donors (figure 28(C)).

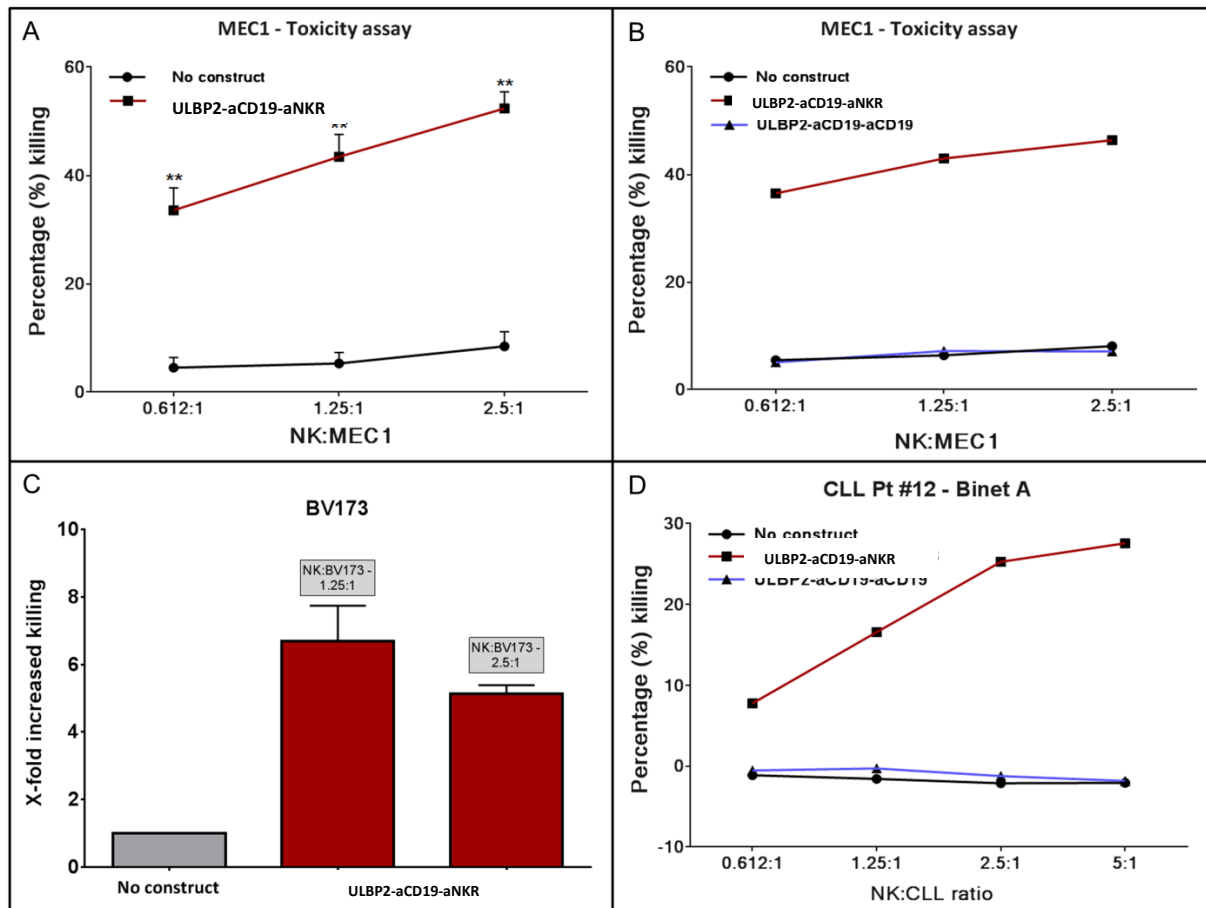


**Figure 28. Dual-activating triplebody ULBP2-aCD19-aNKR enhanced killing of target cells by resting NK cells.** Purified NK cells were either incubated with 10 U/ml IL-2 (resting; (A, B, C)) or used as freshly isolated (D) in FACS based toxicity assays. DiR-labeled target cells were incubated with NK cells with 10 nM of ULBP2-aCD19-aCD19 or 10  $\mu$ l of ULBP2-aCD19-aNKR SN. (A) ULBP2-aCD19-aNKR enhanced resting NK cell mediated MEC1 toxicity (N=3). Error bars indicate standard error of the mean (SEM) and statistical analysis by Paired *t*-test. (B) For 1 donor, NKG2D stimulation alone by ULBP2-aCD19-aCD19 could not enhance this killing. (C) ULBP2-aCD19-aNKR specific killing of BV173 cells, represented as x-fold killing. Error bars indicate standard error of the mean (SEM) of two experiments by independent healthy NK cell donors (N=2). (D) Purified CLL cells from Binet A stage CLL patients as target cells against freshly isolated NK cells from unrelated healthy donor.

To test this dual-activating immunoligand on primary CLL cells, freshly isolated NK cells from unrelated healthy donors were used as effector cells against isolated malignant B cells from a Binet A CLL patient. Neither, freshly isolated NK cells alone or in combination with 10 nM of ULBP2-aCD19-aCD19 could induce any killing of primary CLL cells. On the other hand, ULBP2-aCD19-aNKR activated freshly isolated NK cells to kill CLL cells in E:T ratio dependent manner (figure 28(D)).

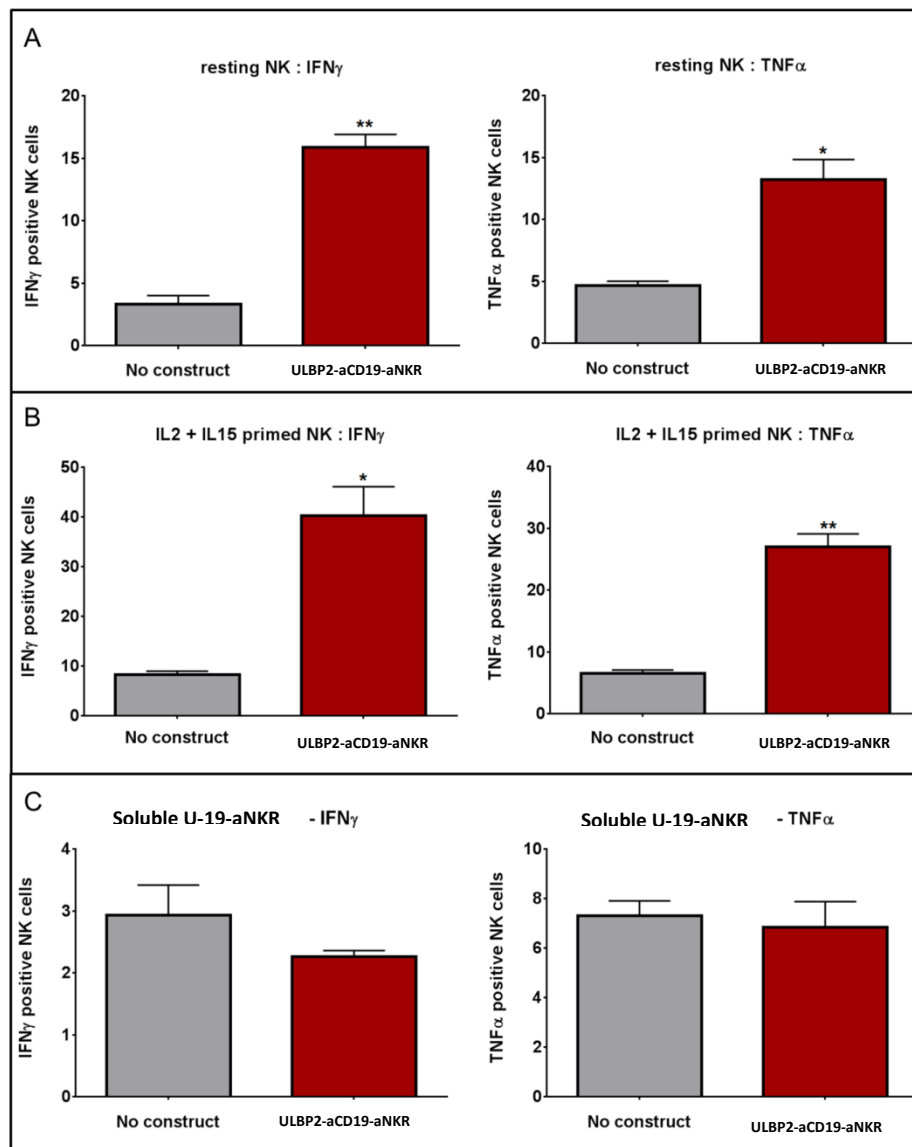


**Figure 29. ULBP2-aCD19-aNKR induces secretion of IFN $\gamma$  and TNF $\alpha$  from NK cells only in response to MEC1 cells.** NK cells were co-incubated with MEC1 cells at 1:1 ratio for 6 hours. ULBP2-aCD19-aNKR in the form of 10  $\mu$ l concentrated SN was added. NK cells were fixed and permeabilized to stain intracellularly for IFN $\gamma$  and TNF $\alpha$ . Error bars indicate standard error of the mean (SEM) and statistical analysis by Student's *t*-test; N=3.

The findings of potent and target cell specific NK cell activation and degranulation by ULBP2-aCD19-aNKR encouraged me to investigate its role in IFN $\gamma$  and TNF $\alpha$  secretion by NK cells. FACS based cytokine assay was as described before (figure 2; C & D) and involved resting and IL2 + IL15 primed NK cells. NK cells were incubated with CD19<sup>+</sup> cell lines such as MEC1 (figure 29) and BV173 (data not shown) and 10  $\mu$ l of ULBP2-aCD19-aNKR SN was added. As shown in figure 29(A), presence of ULBP2-aCD19-aNKR significantly enhanced IFN $\gamma$  and TNF $\alpha$  secreting (resting) NK cell population in response to MEC1 cells and this effect by the triplebody was further pronounced for IL2 + IL15 primed NK cells. Importantly, triplebody required binding to target cells in order mediate this effect as soluble triplebody in the absence of MEC1 cells did not induce the secretion of IFN $\gamma$  and TNF $\alpha$  (figure 29(C)).

Note: Several of the figures in this section have been published in Vyas *et al* (2016). This is currently in publishing process and is only available as online version.

**Mono- and dual-targeting triplebodies activate natural killer cells and have anti-tumor activity in vitro and in vivo against chronic lymphocytic leukemia.**

Vyas M, Schneider A, Shatnyeva O, Reiners K, Tawadros S, Kloess S, Koehl S, Hallek M, Hansen H, von Strandmann EP

Oncoimmunology. 2016 July (Online Publication: <http://dx.doi.org/10.1080/2162402X.2016.1211220>)

## 6. Discussion

The crucial role of the activating receptor NKG2D in tumor surveillance by NK cells is supported by the fact that tumor cells including CLL acquire various mechanisms to counteract NKG2D mediated NK cell recognition and activation [40]. This thesis primarily focuses on NKG2D function and restoration of the defective NK cell surveillance of the CLL cells through different formats of NKG2D triggering triplebodies.

### 6.1. IL15 priming, either alone or in combination with IL2, is required for NKG2D-dependent NK cell effector functions

In this thesis, Schneider-2 cells were transfected to express ULBP1 on the cell surface in order to study the cooperation between various cytokines (IL2, IL12, IL15 and IL18) and NKG2D stimulation. The *Drosophila* cell line Schneider-2 has been used previously to study an individual receptor-ligand interaction in T and NK cells [75, 79]. ULBP1 is a glycoprotein and serves as an activating ligand for NKG2D receptor [40]. Despite having less complex *N*-linked glycosylation machinery compared to mammals, Schneider-2 cells could express functional ULBP1 that localized on the cell surface (figure 1). Of note, the *O*-linked glycosylation in Schneider-2 cells is similar to mammalian cells [80]. NKG2D stimulation on resting NK cells by ULBP1 on Schneider-2 cells could not suffice for their activation and degranulation (figure 3). This finding is particularly contradicting to the studies that utilized antibodies for NKG2D stimulation. Indeed, IL2-primed NK cells could kill FcR<sup>+</sup> murine mastocytoma cell line P815 following NKG2D stimulation by the anti-NKG2D antibody coated on the target cells [76, 81-84]. However, the antibody mediated receptor stimulation cannot mimic the physiological interaction between a natural ligand and a receptor. Additionally, P815 cells also express ligands that can stimulate human NK cell receptors (LFA1 and NKp46), which may have contributed to the redirected lysis of P815 [83, 84]. Since Schneider-2 cells are derived from an evolutionary distant non-mammalian species, it is unlikely that some of the innately expressed molecules on Schneider-2 cells can interact with any

receptors on human immune cells [74, 79]. This assumption was tested in this thesis to confirm the previous finding that the wild type Schneider-2 cells could not enhance the basal level NK cell activation or other effector functions [76, 78].

While short (16-18 hours) priming of NK cells by IL12, IL15 or IL18, either alone or in pair-wise combinations, enabled NK cell degranulation in response to ULBP1 on Schneider-2 cells (figure 4), the regulation of IFN $\gamma$  and TNF $\alpha$  production by NKG2D stimulation seemed to be more stringent as only NK cells primed by IL15 were potent in this regard (figure 5 & 6). For all three experiments, responses of IL15 and IL2 + IL15 primed NK cells were comparable, while the resting NK cells (IL2 alone) were not responsive to the ULBP1-transfected Schneider-2 cells. The difference in the individual priming ability of IL2 and IL15 to augment NKG2D stimulation was striking since both, IL2 and IL15 share two common receptor chains (IL2R $\beta$  and IL2R $\gamma$ ) as well as downstream signaling pathways including Janus kinase [85]. Thus, increasing the concentration of IL2 (possibly 1000 U/ml or more) may lead to comparable priming by IL15. However, the more probable reason seems to be the distinct temporal expression of their respective high affinity receptor  $\alpha$  chains. The IL15R $\alpha$  chain expression reaches its peak after 18-20 hours after the stimulus (similar to the priming exposure in this thesis), while IL2R $\alpha$  expression takes around 50 hours to reach the maximum level [86].

The synergistic cooperation between IL15 priming and NKG2D stimulation in this thesis can be related to the upregulation of NKG2D receptor in response to IL15 as observed for these experiments (data not shown). This has been a consistent finding by our lab and others in the NK cell field [62, 87]. IL15 has shown to induce the transcription of NKG2D, DAP10 and cytotoxic molecules such as perforin [87, 88]. Recently, a transcription independent role of IL15 in NKG2D mediated signaling is revealed. Upon IL15 priming, Janus Kinase 3 (Jak3), a kinase downstream of IL15R, could directly phosphorylate DAP10. This

IL15-Jak3 mediated tyrosine phosphorylation of DAP10 (an adaptor molecule of NKG2D receptor) can prime the NKG2D-DAP10 complex for NKG2D stimulation [89].

Taken together, IL15 priming is necessary to induce NKG2D dependent NK cell effector functions such as degranulation and the production of IFN $\gamma$  and TNF $\alpha$ . This synergistic cooperation seems to be an IL15 mediated transcription dependent and/or independent regulation. Use of Jak3 inhibitors in above discussed experiments (figure 3-5) can help to further explore this synergy.

## **6.2. Triplebodies show better NK-cell-dependent killing of CLL and MLL target cells compared to bispecific counterparts**

To take advantage of NKG2D-dependent effector response, this thesis focused on developing mono- and dual-targeting triplebodies (ULBP2-aCD19-aCD19 and ULBP2-aCD19-aCD33, respectively) to retarget NK cells against cancer. While the *Drosophila* system utilized ULBP1 as a ligand for NKG2D, the triplebodies contained a different NKG2D ligand ULBP2. The two NKG2D ligands, ULBP1 and ULBP2 share 55-60% similarity within the amino acid sequence and are distantly related to other NKG2D ligands MICA/B (20-25% similarity) [90, 91]. There are considerable differences between the amino acid sequences of all 8 NKG2D ligands (ULBP1-6, MICA/B) which undoubtedly results in their structural differences (reviewed in [92]). Despite some minor differences in their ability to bind to NKG2D receptor, their general functions in the context of NK cell activation seem to be redundant up to some extent. This redundancy is indicated by a small Japanese population that carries MICA/MICB null haplotype, but still retains healthy NK cell immunity. This is most likely due to the other NKG2D ligands that can compensate for the loss of MICA/B [93]. In the context of immunoligands this is shown by Kellner *et al.* who compared two immunoligands MICA-7D8 and ULBP2-7D8 each consisting of a distinct NKG2D ligand (MICA or ULBP2) genetically fused with the anti-human CD20 scFv from mAb 7D8 [65]. Both, MICA-7D8 and ULBP2-7D8

triggered cytotoxicity against CD20<sup>+</sup> malignant cells where ULBP2-7D8 was more potent than MICA-7D8 with respect to the maximum lysis achieved [65].

Our group has previously developed ULBP2 containing bispecific immunoligands against multiple myeloma (ULBP2-BB4), prostate cancer (ULBP2-aPSMA) and colon cancer (ULBP2-CEA) [62-64]. Consistent with the previous immunoligands, ULBP2-aCD19-aCD19, ULBP2-aCD19-aCD33 and their bispecific counterparts in this study could also enhance NKG2D-dependent NK cell IFN $\gamma$  secretion and degranulation resulting in the target cell killing in antigen specific manner (figure 11 & 22). However, priming of NK cells with IL15 was essential, as effector functions of resting NK cells could not be triggered by immunoligands (data not shown). Additionally, for both mono-targeting and dual-targeting triplebodies, the study confirmed the superior cytotoxic potential of triplebody format over their respective bispecific counterparts and this finding was consistent for all tested cell lines as well as primary CLL patient cells. These results once again strengthened this consistent finding by Georg Fey and colleagues who developed several CD16 receptor specific trispecific immunoconstructs against typical leukemia antigens. Trispecific constructs such as aCD33-aCD16-aCD123 could induce killing of target cells (CD33<sup>+</sup>CD123<sup>+</sup>) at much lower concentration compared to their bispecific counterparts [55, 59].

This might be due to higher avidity of these triplebodies for their respective target cells, which can account for more stable and prolonged target cell coating and subsequent stronger synapse formation between NK and target cells. The firm synapse between NK and target cells can allow the interaction between other activating receptors on NK cells with their cognate ligands on the target cells, adding to the overall activation of NK cells [94]. Interestingly, we have also observed more potent NK cell mediated killing of CD19<sup>+</sup> CLL cells by a dual-targeting triplebody (ULBP2-aCD19-aCD33) compared to the bispecific ULBP2-aCD19 even though the CLL cells were negative for CD33 antigen (data not shown). This

suggests that there must be other factors associated with the format of the triplebody (such as higher affinity of ULBP2 for NKG2D) that may play a role in heightened NK cell mediated killing.

### **6.3. ULBP2-aCD19-aCD19 retargets NK cells against primary CLL cells in both, allogeneic and autologous settings**

An allogeneic setting takes advantage of incompatibility between KIRs on donor NK cells and MHC class I on target cells. Both, ULBP2-aCD19-aCD19 and ULBP2-aCD19 could induce (IL15 primed) healthy donor-derived NK cells to kill primary CLL cells. Here again, consistent with the finding on cell lines, triplebody was more potent than ULBP2-aCD19 (figure 12). For few CLL patients, the overall killing capacity by NK cells was lower than for other CLL samples and MEC1 cell line suggesting some sort of active inhibition of healthy NK cells by malignant B cells. However, this was not correlated to the Binet staging and ULBP2-aCD19-aCD19 could enhance NK cell dependent killing even for these patients. Much of the NK cell inhibition observed in this study could be attributed to the soluble factors present in the serum from CLL patients (figure 13). The strong reduction in NK cell dependent killing of MEC1 cells (figure 13) was at least in part due to the presence of high levels of soluble MICA/B and ULBP2 (NKG2D ligands) and soluble BAG6 (NKp30 ligand) [43]. Presence of soluble NKG2D ligands have been found in most CLL patients and soluble ULBP2 was considered a prognostic marker for therapy-free survival in CLL patients [45, 95]. Although, only two serum samples were analyzed in this study, there was a trend of stronger NK cell inhibition with increasing Binet stage. Irrespective of the disease progression, ULBP2-aCD19-aCD19 was able to exert its cytotoxic effect even in the presence of high levels of NK cell inhibitory factors.

KIR-dependent inhibition in autologous setting can add to the already defective NK cell activity in CLL patients. The ability of ULBP2-aCD19-aCD19 to retarget patients' own NK cells against the malignant B cells is important from the clinical application point of view. Of two CLL patients (both Binet A), ULBP2-

aCD19-aCD19 was only effective for the patient with higher NK cell number relative to the CLL cell subset (NK:CLL – 0.05:1), while the second patient with much lower NK to CLL cell ratio (0.009:1) was resistant to the triplebody effect (figure 15). Interestingly, when this innate NK:CLL cell ratio was increased by purified NK cells from these patients, the triplebody could retarget autologous NK cells against CLL cells for both patients (figure 16).

This indicates that a smaller NK cell population, outnumbered in relation to the malignant B cells in CLL patients, poses an additional limitation to the functional defects in NK and CLL cells. Indeed, in CLL patients, a high burden of malignant B cells in peripheral blood naturally reduces NK cell proportion and negatively affects the natural and antibody-dependent cytotoxicity of the latter [47]. Median NK to B cell ratio in 166 CLL patients (NK:CLL) was found to be 0.07:1 which is much lower compared to the healthy people. Moreover, NK:CLL ratio in this study was associated with CLL progression and indication to start of the treatment in newly diagnosed patients [48]. Another report also stated that a lower NK:CLL ratio (0.02:1) in CLL patients could hamper an antibody mediated NK cell induced ADCC response [47].

Taken together, NK cells in CLL patients are not totally defective but are out-numbered by malignant B cells. Further, inhibitory soluble factors along with the surface expression of inhibitory molecules on CLL cells are equally accountable for impeded NK cell responses in CLL patients.

#### **6.4. ULBP2-aCD19-aCD19 shows significant *in vivo* activity - Implications for its clinical utility against CLL**

ULBP2-aCD19-aCD19 could efficiently utilize transplanted human PBMCs to prevent the growth of xenografted MEC1 cells in immunodeficient (NSG) mice (figure 17). The triplebody (15 µg) was administered to the mice once (at the start of the study), which was enough to limit MEC1 growth throughout the study period (52 days) in all treated animals, indicating its high serum stability. Another interesting finding was that the tumor limiting activity of the triplebody was not dependent on the prior

or external priming of PBMC with IL15. T cell-derived IL2 (long exposure) or IL15 produced by monocytes may have primed the NK cells for NKG2D response. Importantly, NKG2D is a shared activating receptor on  $\gamma/\delta$  T cells and a co-activating receptor on CD8<sup>+</sup> T cells. A role of the triplebody in retargeting these T cell populations cannot be completely ruled out, as NKG2D dependent anti-tumor effector functions of CD8<sup>+</sup> T cells and  $\gamma/\delta$  T cells have been reported [64, 96, 97]. While these exciting features clearly propose ULBP2-aCD19-aCD19 for further preclinical development, there are several CLL specific challenges that need to be addressed.

First of all, due to a high burden of CLL cells and subsequent smaller compartments of CD8<sup>+</sup> T and NK cells (even smaller for  $\gamma/\delta$  T cells) in most patients for whom treatment is recommended, it is unlikely that a therapeutic strategy such as ULBP2-aCD19-aCD19 can be very effective as a single agent. However, if there are no severe side effects, it can be considered as a therapeutic option in very early stage CLL patients, who are generally classified for the “wait and watch” group. Alternatively, a strategy to expand and prime NK cell population in CLL patients can be potentially synergistic with ULBP2-aCD19-aCD19. Laprevotte *et al* used recombinant IL15 to efficiently induce NK cell killing of CLL cells and this was associated with the activation and proliferation of autologous NK cells [47]. To this end, I confirmed that NK and CD8<sup>+</sup> T cells in CLL patients express inherent NKG2D receptor which can be slightly increased by IL2 alone while IL15 addition led to the significant upregulation on both, NK (figure 14) and CD8 T cells (data not shown). Guven *et al* reported successful *ex vivo* expansion of NK and NKT cells from CLL patients using IL2 (500 U/ml) despite initial low numbers [52]. This is very exciting in view of adoptive transfer of autologous or allogeneic NK cell therapy depending upon the source of the effector population and the data of the thesis suggest that additional *ex vivo* coating of NK cells with ULBP2-aCD19-aCD19 can further overcome the inhibitory soluble factors in CLL patients and can enhance the efficacy of this strategy.

Most of the current treatment options for CLL include combinations of several approaches. ULBP2-aCD19-aCD19 may potentiate the FDA approved Rituximab (anti-CD20 Ab) or a promising immunomodulatory drug lenalidomide. Co-targeting of CD16 (receptor for rituximab) and NKG2D on NK cells was found to be synergistic (discussed later), while lenalidomide has shown to enhance the NK cell responses in CLL [98, 99]. While, FDA approved BTK inhibitor ibrutinib antagonizes CD16 receptor dependent rituximab action its effect on NKG2D induced responses are not known [100, 101].

### **6.5. Dual-targeting and dual-activating triplebodies - Novel formats to improve clinical outcome in CLL**

The clinical value of a triplebody can be further improved by modifying its format. Thus, two additional formats (dual-targeting and dual-activating) were developed to address CLL specific limitations.

#### **ULBP2-aCD19-aCD33**

A dual-targeting format of triplebody was generated to target antigen loss variants in cancer. Only a dual-targeting triplebody ULBP2-aCD19-aCD33 could efficiently kill both, CD19<sup>loss</sup> and CD33<sup>loss</sup> BV173 (MLL cell line) variants in a proof-of-principle experiment (figure 23 & 24). CD33 specific scFv can be replaced by a scFv against a second CLL antigen such as CD20. Such a CLL specific dual-targeting triplebody (ULBP2-aCD19-aCD20) would offer an additional advantage for CD19<sup>loss</sup> or CD20<sup>loss</sup> CLL patients. Two main mechanisms have been reported for CD20 loss from the CLL cells following rituximab (anti-CD20 mAb) treatment. While CD20 internalization by malignant B cells plays a minor role, the majority of CD20, along with the bound rituximab, is removed by the Fcγ receptor expressing monocytes and macrophages in a process called as trogocytosis or shaving. This does not only result in the rapid clearance of rituximab following the infusion, but also leads to selection of CD20<sup>-</sup> CLL cells that are resistant to anti-CD20 therapy. Similarly, CD19 internalization is also reported by anti-CD19 antibody XmAb5574 in CLL. Interestingly, Jones *et al* reported the loss of CD19 from the CLL cells during the

shaving (trocytosis) of anti-CD20 rituximab. It was shown that CD19 was also transferred from B cells to monocytes in Fc dependent manner.

### **ULBP2-aCD19-aNKR**

The second, dual-activating, format focused on further enhancing the NK cell activity against CLL by interacting with NKG2D and NKR receptors on NK cells. Most importantly, ULBP2-aCD19-aNKR could induce effector functions from freshly isolated or resting NK cells, a task all previous NKG2D targeting immunoligands failed to achieve. The main findings included induction of cytokines (IFN $\gamma$  and TNF $\alpha$ ) and toxicity against MEC1 and CLL primary cells using unprimed NK cells.

It is very likely that most of these potent effects were induced by NKR targeting and NKG2D receptor had little, if any, role in it. However, using IL15 primed NK cells and Schneider-2 cells as target, I confirmed that NKG2D stimulation can have additive effects even in the presence of strong NKR stimulation. Based on the convincing *in vivo* data of ULBP2-aCD19-aCD19, I believe that the dual-activating triplebody ULBP2-aCD19-aNKR may provide the initial strong NKR stimulation. But the triggering of NKG2D on NK as well as CD8<sup>+</sup> T cells in the presence of IL2 or IL15 might be just as important, since it also involves the adaptive immune response and thus results in a more dynamic immune response.

## **6.6. Future perspectives**

Further development of a dual-targeting immunoligand to target antigen loss variants in CLL is planned. To this end, a triplebody with dual, CD19 and CD20 specificity will be developed while maintaining ULBP2 for NKG2D targeting. It will be important to analyze its activity on CLL cells from patients presented with antigen loss variants following rituximab therapy as well as in a relevant mouse model. An immunodeficient mouse model engrafted with CD19<sup>loss</sup> B cell ALL blasts from a patient who relapsed

after CD19-specific chimeric antigen receptor (CAR) T cell therapy was recently used to study the effect of dual-targeting CAR T cells [102].

The production of ULBP2-aCD19-aNKR was challenging and the focus would be on modifying the system to improve its yield. Whether NKG2D and NKR receptors, both, can play a role in mounting an immune response will be of prime interest. It is also expected that this construct will be particularly effective in mounting a strong NK response and in activating adaptive immunity through NKG2D positive T cells. This idea of synergy at the cellular level has not been tested yet and would be very interesting to explore.

Finally, information on NKp30 receptor in the context of cooperation with other activating (CD16, 2B4, NKG2D) or adhesion (LFA1) receptors on NK cells is elusive. B7-H6 is recently identified as a ligand for NKp30 [37]. Therefore, Schneider-2 cells expressing B7-H6 alone or in pair-wise combinations with other ligands (ULBP1, ICAM1 etc.) have been generated and initial data showed that NKp30 has similar (to NKG2D) cytokine requirements.

## 6.7. Conclusion

IL15 priming of NK cells is required to induce NKG2D dependent NK cell effector functions, especially cytokine secretion. The synergistic cooperation between IL15 and NKG2D was efficiently exploited by the mono-targeting triplebody ULBP2-aCD19-aCD19 in retargeting NK cells against CLL cells. Surprisingly, the superior *in vivo* efficacy of this triplebody in NSG mouse model did not require external IL15 administration. Dual-targeting and dual-activating triplebody formats further extended the usefulness of this NK cell-based strategy to tackle clinically relevant CLL issues.

## References

1. Hallek, M., *Chronic lymphocytic leukemia: 2015 Update on diagnosis, risk stratification, and treatment*. Am J Hematol, 2015. **90**(5): p. 446-60.
2. Molica, S., *Sex differences in incidence and outcome of chronic lymphocytic leukemia patients*. Leuk Lymphoma, 2006. **47**(8): p. 1477-80.
3. Rozman, C. and E. Montserrat, *Chronic lymphocytic leukemia*. N Engl J Med, 1995. **333**(16): p. 1052-7.
4. Garcia-Munoz, R., V.R. Galiacho, and L. Llorente, *Immunological aspects in chronic lymphocytic leukemia (CLL) development*. Ann Hematol, 2012. **91**(7): p. 981-96.
5. Mauro, F.R., et al., *Clinical characteristics and outcome of young chronic lymphocytic leukemia patients: a single institution study of 204 cases*. Blood, 1999. **94**(2): p. 448-54.
6. Hallek, M., et al., *Guidelines for the diagnosis and treatment of chronic lymphocytic leukemia: a report from the International Workshop on Chronic Lymphocytic Leukemia updating the National Cancer Institute-Working Group 1996 guidelines*. Blood, 2008. **111**(12): p. 5446-56.
7. Rai, K.R., et al., *Clinical staging of chronic lymphocytic leukemia*. Blood, 1975. **46**(2): p. 219-34.
8. Binet, J.L., et al., *A new prognostic classification of chronic lymphocytic leukemia derived from a multivariate survival analysis*. Cancer, 1981. **48**(1): p. 198-206.
9. Jain, N. and S. O'Brien, *Initial treatment of CLL: integrating biology and functional status*. Blood, 2015. **126**(4): p. 463-70.
10. Hoellenriegel, J., et al., *The phosphoinositide 3'-kinase delta inhibitor, CAL-101, inhibits B-cell receptor signaling and chemokine networks in chronic lymphocytic leukemia*. Blood, 2011. **118**(13): p. 3603-12.
11. Herman, S.E., et al., *Bruton tyrosine kinase represents a promising therapeutic target for treatment of chronic lymphocytic leukemia and is effectively targeted by PCI-32765*. Blood, 2011. **117**(23): p. 6287-96.
12. Extermann, M., et al., *Comorbidity and functional status are independent in older cancer patients*. J Clin Oncol, 1998. **16**(4): p. 1582-7.
13. Calin, G.A., et al., *Frequent deletions and down-regulation of micro- RNA genes miR15 and miR16 at 13q14 in chronic lymphocytic leukemia*. Proc Natl Acad Sci U S A, 2002. **99**(24): p. 15524-9.
14. Dohner, H., et al., *11q deletions identify a new subset of B-cell chronic lymphocytic leukemia characterized by extensive nodal involvement and inferior prognosis*. Blood, 1997. **89**(7): p. 2516-22.
15. Hallek, M., et al., *Addition of rituximab to fludarabine and cyclophosphamide in patients with chronic lymphocytic leukaemia: a randomised, open-label, phase 3 trial*. Lancet, 2010. **376**(9747): p. 1164-74.
16. Zenz, T., et al., *TP53 mutation profile in chronic lymphocytic leukemia: evidence for a disease specific profile from a comprehensive analysis of 268 mutations*. Leukemia, 2010. **24**(12): p. 2072-9.
17. Woyach, J.A., et al., *Resistance mechanisms for the Bruton's tyrosine kinase inhibitor ibrutinib*. N Engl J Med, 2014. **370**(24): p. 2286-94.
18. Zhou, Q., et al., *A hypermorphic missense mutation in PLCG2, encoding phospholipase Cgamma2, causes a dominantly inherited autoinflammatory disease with immunodeficiency*. Am J Hum Genet, 2012. **91**(4): p. 713-20.

19. Cheng, S., et al., *Functional characterization of BTK(C481S) mutation that confers ibrutinib resistance: exploration of alternative kinase inhibitors*. *Leukemia*, 2015. **29**(4): p. 895-900.
20. Mato, A. and D.L. Porter, *A drive through cellular therapy for CLL in 2015: allogeneic cell transplantation and CARs*. *Blood*, 2015. **126**(4): p. 478-85.
21. Bachireddy, P., et al., *Haematological malignancies: at the forefront of immunotherapeutic innovation*. *Nat Rev Cancer*, 2015. **15**(4): p. 201-15.
22. Freeman, C.L. and J.G. Gribben, *Immunotherapy in Chronic Lymphocytic Leukaemia (CLL)*. *Curr Hematol Malig Rep*, 2016. **11**(1): p. 29-36.
23. Verneris, M.R., *Natural killer cells and regulatory T cells: how to manipulate a graft for optimal GVL*. *Hematology Am Soc Hematol Educ Program*, 2013. **2013**: p. 335-41.
24. Ames, E. and W.J. Murphy, *Advantages and clinical applications of natural killer cells in cancer immunotherapy*. *Cancer Immunol Immunother*, 2014. **63**(1): p. 21-8.
25. Kiessling, R., et al., *"Natural" killer cells in the mouse. II. Cytotoxic cells with specificity for mouse Moloney leukemia cells. Characteristics of the killer cell*. *Eur J Immunol*, 1975. **5**(2): p. 117-21.
26. Herberman, R.B., et al., *Natural cytotoxic reactivity of mouse lymphoid cells against syngeneic and allogeneic tumors. II. Characterization of effector cells*. *Int J Cancer*, 1975. **16**(2): p. 230-9.
27. Pross, H.F., et al., *Spontaneous human lymphocyte-mediated cytotoxicity against tumor target cells. IX. The quantitation of natural killer cell activity*. *J Clin Immunol*, 1981. **1**(1): p. 51-63.
28. Morvan, M.G. and L.L. Lanier, *NK cells and cancer: you can teach innate cells new tricks*. *Nat Rev Cancer*, 2016. **16**(1): p. 7-19.
29. Raulet, D.H. and R.E. Vance, *Self-tolerance of natural killer cells*. *Nat Rev Immunol*, 2006. **6**(7): p. 520-31.
30. Vitale, M., et al., *NKp44, a novel triggering surface molecule specifically expressed by activated natural killer cells, is involved in non-major histocompatibility complex-restricted tumor cell lysis*. *J Exp Med*, 1998. **187**(12): p. 2065-72.
31. Freud, A.G., et al., *Expression of the activating receptor, NKp46 (CD335), in human natural killer and T-cell neoplasia*. *Am J Clin Pathol*, 2013. **140**(6): p. 853-66.
32. Rosental, B., et al., *Proliferating cell nuclear antigen is a novel inhibitory ligand for the natural cytotoxicity receptor NKp44*. *J Immunol*, 2011. **187**(11): p. 5693-702.
33. Baychelier, F., et al., *Identification of a cellular ligand for the natural cytotoxicity receptor NKp44*. *Blood*, 2013. **122**(17): p. 2935-42.
34. Garg, A., et al., *Vimentin expressed on Mycobacterium tuberculosis-infected human monocytes is involved in binding to the NKp46 receptor*. *J Immunol*, 2006. **177**(9): p. 6192-8.
35. Pogge von Strandmann, E., et al., *Human leukocyte antigen-B-associated transcript 3 is released from tumor cells and engages the NKp30 receptor on natural killer cells*. *Immunity*, 2007. **27**(6): p. 965-74.
36. Simhadri, V.R., et al., *Dendritic cells release HLA-B-associated transcript-3 positive exosomes to regulate natural killer function*. *PLoS One*, 2008. **3**(10): p. e3377.
37. Brandt, C.S., et al., *The B7 family member B7-H6 is a tumor cell ligand for the activating natural killer cell receptor NKp30 in humans*. *J Exp Med*, 2009. **206**(7): p. 1495-503.
38. Matta, J., et al., *Induction of B7-H6, a ligand for the natural killer cell-activating receptor NKp30, in inflammatory conditions*. *Blood*, 2013. **122**(3): p. 394-404.
39. Wang, W., et al., *NK Cell-Mediated Antibody-Dependent Cellular Cytotoxicity in Cancer Immunotherapy*. *Front Immunol*, 2015. **6**: p. 368.
40. Hayakawa, Y., *Targeting NKG2D in tumor surveillance*. *Expert Opin Ther Targets*, 2012. **16**(6): p. 587-99.
41. Shatnyeva, O.M., et al., *DNA damage response and evasion from immunosurveillance in CLL: new options for NK cell-based immunotherapies*. *Front Genet*, 2015. **6**: p. 11.

42. Costello, R.T., et al., *Expression of natural killer cell activating receptors in patients with chronic lymphocytic leukaemia*. Immunology, 2012. **135**(2): p. 151-7.
43. Reiners, K.S., et al., *Soluble ligands for NK cell receptors promote evasion of chronic lymphocytic leukemia cells from NK cell anti-tumor activity*. Blood, 2013. **121**(18): p. 3658-65.
44. Veuillen, C., et al., *Primary B-CLL resistance to NK cell cytotoxicity can be overcome in vitro and in vivo by priming NK cells and monoclonal antibody therapy*. J Clin Immunol, 2012. **32**(3): p. 632-46.
45. Nuckel, H., et al., *The prognostic significance of soluble NKG2D ligands in B-cell chronic lymphocytic leukemia*. Leukemia, 2010. **24**(6): p. 1152-9.
46. Raulet, D.H., et al., *Regulation of ligands for the NKG2D activating receptor*. Annu Rev Immunol, 2013. **31**: p. 413-41.
47. Laprevotte, E., et al., *Recombinant human IL-15 trans-presentation by B leukemic cells from chronic lymphocytic leukemia induces autologous NK cell proliferation leading to improved anti-CD20 immunotherapy*. J Immunol, 2013. **191**(7): p. 3634-40.
48. Palmer, S., et al., *Prognostic importance of T and NK-cells in a consecutive series of newly diagnosed patients with chronic lymphocytic leukaemia*. Br J Haematol, 2008. **141**(5): p. 607-14.
49. Keir, M.E., et al., *PD-1 and its ligands in tolerance and immunity*. Annu Rev Immunol, 2008. **26**: p. 677-704.
50. Hodi, F.S., et al., *Improved survival with ipilimumab in patients with metastatic melanoma*. N Engl J Med, 2010. **363**(8): p. 711-23.
51. Chester, C., K. Fritsch, and H.E. Kohrt, *Natural Killer Cell Immunomodulation: Targeting Activating, Inhibitory, and Co-stimulatory Receptor Signaling for Cancer Immunotherapy*. Front Immunol, 2015. **6**: p. 601.
52. Guven, H., et al., *Expansion of natural killer (NK) and natural killer-like T (NKT)-cell populations derived from patients with B-chronic lymphocytic leukemia (B-CLL): a potential source for cellular immunotherapy*. Leukemia, 2003. **17**(10): p. 1973-80.
53. Becker, P.S., et al., *Selection and expansion of natural killer cells for NK cell-based immunotherapy*. Cancer Immunol Immunother, 2016. **65**(4): p. 477-84.
54. Suck, G., et al., *NK-92: an 'off-the-shelf therapeutic' for adoptive natural killer cell-based cancer immunotherapy*. Cancer Immunol Immunother, 2016. **65**(4): p. 485-92.
55. Vyas, M., et al., *Natural ligands and antibody-based fusion proteins: harnessing the immune system against cancer*. Trends Mol Med, 2014. **20**(2): p. 72-82.
56. Kellner, C., et al., *A novel CD19-directed recombinant bispecific antibody derivative with enhanced immune effector functions for human leukemic cells*. J Immunother, 2008. **31**(9): p. 871-84.
57. Singer, H., et al., *Effective elimination of acute myeloid leukemic cells by recombinant bispecific antibody derivatives directed against CD33 and CD16*. J Immunother, 2010. **33**(6): p. 599-608.
58. Stein, C., et al., *Novel conjugates of single-chain Fv antibody fragments specific for stem cell antigen CD123 mediate potent death of acute myeloid leukaemia cells*. Br J Haematol, 2010. **148**(6): p. 879-89.
59. Kugler, M., et al., *A recombinant trispecific single-chain Fv derivative directed against CD123 and CD33 mediates effective elimination of acute myeloid leukaemia cells by dual targeting*. Br J Haematol, 2010. **150**(5): p. 574-86.
60. Schubert, I., et al., *A single-chain triplebody with specificity for CD19 and CD33 mediates effective lysis of mixed lineage leukemia cells by dual targeting*. MAbs, 2011. **3**(1): p. 21-30.
61. McAleese, F. and M. Eser, *RECRUIT-TandAbs: harnessing the immune system to kill cancer cells*. Future Oncol, 2012. **8**(6): p. 687-95.

62. von Strandmann, E.P., et al., *A novel bispecific protein (ULBP2-BB4) targeting the NKG2D receptor on natural killer (NK) cells and CD138 activates NK cells and has potent antitumor activity against human multiple myeloma in vitro and in vivo*. *Blood*, 2006. **107**(5): p. 1955-62.
63. Jachimowicz, R.D., et al., *Induction of in vitro and in vivo NK cell cytotoxicity using high-avidity immunoligands targeting prostate-specific membrane antigen in prostate carcinoma*. *Mol Cancer Ther*, 2011. **10**(6): p. 1036-45.
64. Rothe, A., et al., *The bispecific immunoligand ULBP2-aCEA redirects natural killer cells to tumor cells and reveals potent anti-tumor activity against colon carcinoma*. *Int J Cancer*, 2014. **134**(12): p. 2829-40.
65. Kellner, C., et al., *Fusion proteins between ligands for NKG2D and CD20-directed single-chain variable fragments sensitize lymphoma cells for natural killer cell-mediated lysis and enhance antibody-dependent cellular cytotoxicity*. *Leukemia*, 2012. **26**(4): p. 830-4.
66. Nagorsen, D., et al., *Blinatumomab: a historical perspective*. *Pharmacol Ther*, 2012. **136**(3): p. 334-42.
67. Khong, H.T. and N.P. Restifo, *Natural selection of tumor variants in the generation of "tumor escape" phenotypes*. *Nat Immunol*, 2002. **3**(11): p. 999-1005.
68. Williams, M.E., et al., *Thrice-weekly low-dose rituximab decreases CD20 loss via shaving and promotes enhanced targeting in chronic lymphocytic leukemia*. *J Immunol*, 2006. **177**(10): p. 7435-43.
69. Awan, F.T., et al., *CD19 targeting of chronic lymphocytic leukemia with a novel Fc-domain-engineered monoclonal antibody*. *Blood*, 2010. **115**(6): p. 1204-13.
70. Beum, P.V., et al., *Loss of CD20 and bound CD20 antibody from opsonized B cells occurs more rapidly because of trogocytosis mediated by Fc receptor-expressing effector cells than direct internalization by the B cells*. *J Immunol*, 2011. **187**(6): p. 3438-47.
71. Jones, J.D., B.J. Hamilton, and W.F. Rigby, *Rituximab mediates loss of CD19 on B cells in the absence of cell death*. *Arthritis Rheum*, 2012. **64**(10): p. 3111-8.
72. Gardner, R., et al., *Acquisition of a CD19-negative myeloid phenotype allows immune escape of MLL-rearranged B-ALL from CD19 CAR-T-cell therapy*. *Blood*, 2016. **127**(20): p. 2406-10.
73. Linenberger, M.L., *CD33-directed therapy with gemtuzumab ozogamicin in acute myeloid leukemia: progress in understanding cytotoxicity and potential mechanisms of drug resistance*. *Leukemia*, 2005. **19**(2): p. 176-82.
74. March, M.E., C.C. Gross, and E.O. Long, *Use of transfected Drosophila S2 cells to study NK cell activation*. *Methods Mol Biol*, 2010. **612**: p. 67-88.
75. Schneider, I., *Cell lines derived from late embryonic stages of Drosophila melanogaster*. *J Embryol Exp Morphol*, 1972. **27**(2): p. 353-65.
76. Bryceson, Y.T., et al., *Synergy among receptors on resting NK cells for the activation of natural cytotoxicity and cytokine secretion*. *Blood*, 2006. **107**(1): p. 159-66.
77. Kwon, H.J. and H.S. Kim, *Signaling for synergistic activation of natural killer cells*. *Immune Netw*, 2012. **12**(6): p. 240-6.
78. Bryceson, Y.T., et al., *Cytolytic granule polarization and degranulation controlled by different receptors in resting NK cells*. *J Exp Med*, 2005. **202**(7): p. 1001-12.
79. Cai, Z., et al., *Transfected Drosophila cells as a probe for defining the minimal requirements for stimulating unprimed CD8+ T cells*. *Proc Natl Acad Sci U S A*, 1996. **93**(25): p. 14736-41.
80. Altmann, F., et al., *Insect cells as hosts for the expression of recombinant glycoproteins*. *Glycoconj J*, 1999. **16**(2): p. 109-23.
81. Bauer, S., et al., *Activation of NK cells and T cells by NKG2D, a receptor for stress-inducible MICA*. *Science*, 1999. **285**(5428): p. 727-9.

82. Andre, P., et al., *Comparative analysis of human NK cell activation induced by NKG2D and natural cytotoxicity receptors*. Eur J Immunol, 2004. **34**(4): p. 961-71.
83. Sivori, S., et al., *NKp46 is the major triggering receptor involved in the natural cytotoxicity of fresh or cultured human NK cells. Correlation between surface density of NKp46 and natural cytotoxicity against autologous, allogeneic or xenogeneic target cells*. Eur J Immunol, 1999. **29**(5): p. 1656-66.
84. Johnston, S.C., et al., *On the species specificity of the interaction of LFA-1 with intercellular adhesion molecules*. J Immunol, 1990. **145**(4): p. 1181-7.
85. Romee, R., J.W. Leong, and T.A. Fehniger, *Utilizing cytokines to function-enable human NK cells for the immunotherapy of cancer*. Scientifica (Cairo), 2014. **2014**: p. 205796.
86. Pillet, A.H., J. Theze, and T. Rose, *Interleukin (IL)-2 and IL-15 have different effects on human natural killer lymphocytes*. Hum Immunol, 2011. **72**(11): p. 1013-7.
87. Zhang, C., et al., *Interleukin-15 improves cytotoxicity of natural killer cells via up-regulating NKG2D and cytotoxic effector molecule expression as well as STAT1 and ERK1/2 phosphorylation*. Cytokine, 2008. **42**(1): p. 128-36.
88. Zhu, S., et al., *Transcription of the activating receptor NKG2D in natural killer cells is regulated by STAT3 tyrosine phosphorylation*. Blood, 2014. **124**(3): p. 403-11.
89. Horng, T., J.S. Bezbradica, and R. Medzhitov, *NKG2D signaling is coupled to the interleukin 15 receptor signaling pathway*. Nat Immunol, 2007. **8**(12): p. 1345-52.
90. Fernandez-Messina, L., H.T. Reyburn, and M. Vales-Gomez, *Human NKG2D-ligands: cell biology strategies to ensure immune recognition*. Front Immunol, 2012. **3**: p. 299.
91. Cosman, D., et al., *ULBPs, novel MHC class I-related molecules, bind to CMV glycoprotein UL16 and stimulate NK cytotoxicity through the NKG2D receptor*. Immunity, 2001. **14**(2): p. 123-33.
92. Eagle, R.A. and J. Trowsdale, *Promiscuity and the single receptor: NKG2D*. Nat Rev Immunol, 2007. **7**(9): p. 737-44.
93. Komatsu-Wakui, M., et al., *MIC-A polymorphism in Japanese and a MIC-A-MIC-B null haplotype*. Immunogenetics, 1999. **49**(7-8): p. 620-8.
94. Orange, J.S., *Formation and function of the lytic NK-cell immunological synapse*. Nat Rev Immunol, 2008. **8**(9): p. 713-25.
95. Hilpert, J., et al., *Comprehensive analysis of NKG2D ligand expression and release in leukemia: implications for NKG2D-mediated NK cell responses*. J Immunol, 2012. **189**(3): p. 1360-71.
96. Oberg, H.H., et al., *Novel bispecific antibodies increase gammadelta T-cell cytotoxicity against pancreatic cancer cells*. Cancer Res, 2014. **74**(5): p. 1349-60.
97. Oberg, H.H., et al., *gammadelta T cell activation by bispecific antibodies*. Cell Immunol, 2015. **296**(1): p. 41-9.
98. Huergo-Zapico, L., et al., *Expansion of NK cells and reduction of NKG2D expression in chronic lymphocytic leukemia. Correlation with progressive disease*. PLoS One, 2014. **9**(10): p. e108326.
99. Wu, L., et al., *Lenalidomide enhances antibody-dependent cellular cytotoxicity of solid tumor cells in vitro: influence of host immune and tumor markers*. Cancer Immunol Immunother, 2011. **60**(1): p. 61-73.
100. Kohrt, H.E., et al., *Ibrutinib antagonizes rituximab-dependent NK cell-mediated cytotoxicity*. Blood, 2014. **123**(12): p. 1957-60.
101. Da Roit, F., et al., *Ibrutinib interferes with the cell-mediated anti-tumor activities of therapeutic CD20 antibodies: implications for combination therapy*. Haematologica, 2015. **100**(1): p. 77-86.
102. Ruella, M., et al., *Dual CD19 and CD123 targeting prevents antigen-loss relapses after CD19-directed immunotherapies*. J Clin Invest, 2016. **126**(10): p. 3814-3826.

## Abbreviations

7-AAD	7-aminoactinomycin D
Ac5	Actin 5
ADCC	Antibody Dependent Cell mediated Cytotoxicity
AF647	Alexa Fluor 647
Amp	Ampere
ANOVA	Analysis of variance
B7-H6	Member of the B7 family of immunoreceptors
BAG6	BCL2-associated athanogene 6
B-ALL	B-cell acute lymphocytic leukemia
BAT3	HLA-B-associated transcript 3
B-CLL	Chronic Lymphocytic Leukemia of B cells
BFA	Brefeldin A
BiTE	Bispecific T-cell engager
BTK	Bruton's Tyrosine Kinase
BV421	Brilliant Violet 421
CAR	Chimeric antigen receptor
CD	cluster of differentiation
CEA	Carcinoembryonic antigen
CHO cells	Chinese hamster ovarian cells
CLL	Chronic Lymphocytic Leukemia
CTLA-4	cytotoxic T-lymphocyte-associated protein 4
DAP10	DNAX-activation protein 10
DC	Dendritic Cell
DNA	Deoxyribonucleic acid
DNAM-1	DNAX Accessory Molecule-1
DTT	Dithiothreitol
E:T	Effector to target
EGFP	Enhanced green fluorescent protein
ELISA	Enzyme linked immunosorbent assay
ER	Endoplasmic reticulum
FACS	Fluorescence-activated cell sorting (flow cytometry)
Fc	Fragment crystallizable
FcγRIIIa	Fc gamma receptor IIIa
FDA	Food and Drug Administration
FITC	Fluorescein isothiocyanate
GFP	Green fluorescent protein
Gly/Ser	Glycine / serine
Grb2	Growth factor receptor-bound protein 2
GvHD	Graft versus Host Disease

GvL	Graft versus Leukemia
HBS	Hepes Buffered Saline
HBSS	Hank's Balanced Salt Solution
HEK293T cells	Human embryonic kidney 293T cells
His	Histidine
HLA	Human Leukocyte Antigen
HRP	Horse radish peroxidase
HSCs	Hematopoietic Stem Cells
HSCT	Hematopoietic Stem Cell Transplantation
ICAM1	Intercellular Adhesion Molecule 1
IFN $\gamma$	Interferon gamma
IgG	Immunoglobulin G
Igk	Immunoglobulin kappa
IL	Interleukin
IL15R $\alpha$	Interleukin 15 receptor 15 $\alpha$ chain
IL2R $\gamma/\beta$	Interleukin 15 receptor 15 $\gamma/\beta$ chain
IMAC	Immobilized Metal Affinity Chromatography
ITAM	Immunoreceptor tyrosine-based activation motif
ITIM	Immunoreceptor tyrosine-based inhibition motif
ITSM	Immunoreceptor tyrosine-based switch motif
Jak3	Janus kinase 3
Kb	Kilobase
kDa	Kilo Dalton
KIRs	Killer-cell immunoglobulin-like receptors
LAMP-1	lysosome-associated membrane glycoprotein 1
mAb	Monoclonal antibody
MACS	Magnetic-activated cell sorting
MHC-I	Major Histocompatibility Class – I
MICA	MHC-I related chain A
MICB	MHC-I related chain B
MLL	Mixed Lineage Leukemia
MMPs	Matrix Metalloproteinases
MRD	Minimal Residual Disease
NCI	National Cancer Institute
NCRs	Natural Cytotoxicity Receptors
NK	Natural Killer
NKG2D	Natural killer group 2, member D
NKp30	Natural killer cell protein 30
NKp44	Natural killer cell protein 44
NKp46	Natural killer cell protein 46
NSG	NOD <i>scid</i> gamma
PAGE	Polyacrylamide agarose gel electrophoresis

PB	Pacific Blue
PBMCs	Peripheral blood mononuclear cells
PBS	Phosphate buffered saline
PBST	Phosphate buffered saline + Tween 20
PCNA	Proliferating cell nuclear antigen
PD-1	Programmed cell death protein 1
PE	Phycoerythrin
PI3K	Phosphatidylinositol-4,5-bisphosphate 3-kinase
PLCy1	phospholipase Cy1
PSMA	Prostate specific membrane antigen
RT	Room temperature
S/N or SN	Supernatant
S2 cells	Schneider-2 cells
scFv	Single-chain variable fragment
SDS	Sodium dodecyl sulfate
SEM	Standard error of the mean
SyK	Spleen tyrosine kinase
TGF $\beta$	Transforming growth factor $\beta$
TNF $\alpha$	Tumor Necrosis Factor alpha
TRAIL	TNF-related apoptosis-inducing ligand
U	Units
ULBP1	UL16 binding protein 1
ULBP2	UL16 binding protein 2
V	Voltage
Vav1	Vav 1 guanine nucleotide exchange factor
VH	Variable heavy chain
VL	Variable light chain
WT	Wildtype
ZAP70	Zeta-chain-associated protein kinase 70

## Acknowledgment

First and foremost, I would like to convey my deep gratitude to my PhD supervisor Prof. Dr. Elke Pogge von Strandmann for this opportunity to pursue PhD in her lab. The confidence she had shown in me was the true motivating force throughout the last four years. Most importantly, her continuous support and guidance made this PhD an exceptional learning experience and developed me to be a better scientist. She believed in me and gave me some great opportunities to develop my communication and interpersonal skills. Whether it was writing my first review article or a recent talk at the international Immunology conference, all of these experiences have been very valuable for me.

I am thankful to Prof. Peter Nürnberg for accepting to be my thesis committee member and to my GSfBS tutor Dr. Thomas Wunderlich for the helpful tips. My last four years in Innate Immunity group at University Hospital Cologne were spent with very supportive and friendly colleagues. Katrin taught me the basics of FACS and always helped me in designing and analyzing the experiments. Also thanks Katrin for proof-reading my papers and this thesis. Hinrich was always there for discussing new ideas and science in general. Also, thanks Hinrich for all the fun and friendly support in and outside the lab. Olga was always there to troubleshoot experiments and protocols. Without the support from Silke, Anne and Gisela, the clonings and protein production would have been impossible. Samir Tawadros helped and assisted me in animal experiments. A big thank you to the master students Ann-Charlott, Katharina and Gökcen for their company and help in my experiments. Daniel and Katharina were always there for the fun-filled coffee and lunch breaks, any help with the German language or while discussing science. Last but not least, thank you to all my co-PhD students and colleagues in “LFI” and “Haus 15” for nice memories and fruitful discussions.

Finally, my special gratitude goes to my parents, wife and her family for all their sacrifices, love and support. My friends and family in India always kept me motivated so that I could reach at the present stage in my life.

## Erklärung

Ich versichere, dass ich die von mir vorgelegte Dissertation selbständig angefertigt, die benutzten Quellen und Hilfsmittel vollständig angegeben und die Stellen der Arbeit - einschließlich Tabellen, Karten und Abbildungen -, die anderen Werken im Wortlaut oder dem Sinn nach entnommen sind, in jedem Einzelfall als Entlehnung kenntlich gemacht habe; dass diese Dissertation noch keiner anderen Fakultät oder Universität zur Prüfung vorgelegen hat; dass sie - abgesehen von unten angegebenen Teilpublikationen - noch nicht veröffentlicht worden ist sowie, dass ich eine solche Veröffentlichung vor Abschluss des Promotionsverfahrens nicht vornehmen werde. Die Bestimmungen der Promotionsordnung sind mir bekannt. Die von mir vorgelegte Dissertation ist von Prof. Peter Nürnberg betreut worden.

### Teilveröffentlichungen:

#### **Mono- and dual-targeting triplebodies activate natural killer cells and have anti-tumor activity in vitro and in vivo against chronic lymphocytic leukemia.**

Vyas M, Schneider A, Shatnyeva O, Reiners K, Tawadros S, Kloess S, Koehl S, Hallek M, Hansen H, von Strandmann EP

Oncoimmunology. 2016 July (Online Publication: <http://dx.doi.org/10.1080/2162402X.2016.1211220>)

#### **Antigen Loss Variants: Catching Hold of Escaping Foes.**

Vyas M, Müller R, Pogge von Strandmann E.

Front Immunol. 2017 Feb 24;8:175.

Köln, den 07 Aug 2017

.....

Maulik Vyas

## Lebenslauf

---

### Persönliches & Kontakt

---

Geboren: am 03.03.1988 in Ahmedabad (Indien)  
 Staatsbürgerschaft: Indien  
 Familienstand: Verheiratet

Adresse: Remigius Str. 24, 50937 Köln  
 Telefon: 0176/84893949  
 E-Mail: maulikkvyas@gmail.com

### Ausbildung

---

Seit August 2012	Dissertation
Nov. 2011 – Juli 2012	Wissenschaftlicher Mitarbeiter Tata Cancer Institute – Mumbai, Indien
2009 – 2010	MSc in Cancer Immunology and Biotechnology University of Nottingham, UK – 71% („Distinction“)
2006 – 2009	BSc in Biomedical Sciences University of Central Lancashire, UK – 67%
1994 – 2006	Grundschule und Gymnasium (Sharada Mandir, Ahmedabad)

### Kongressteilnahmen & Sonstiges

---

Meeting „International Congress of Immunology“ im Aug. 2016 in Melbourne, Australien  
 (Talk)

Meeting „Natural Killer Cell symposium“ im Sep. 2014 in Hannover  
 (Posterpräsentation)

Meeting „Combined International Workshop on CLL“ im März 2014 in Bonn  
 (Posterpräsentation)

„2nd Translational Immunology School – DGfi“ im März 2014 in Potsdam  
 (Student)

## Veröffentlichungen

---

### **Antigen Loss Variants: Catching Hold of Escaping Foes.**

Vyas M, Müller R, Pogge von Strandmann E.

Front Immunol. 2017 Feb 24;8:175.

### **Mono- and dual-targeting triplebodies activate natural killer cells and have anti-tumor activity in vitro and in vivo against chronic lymphocytic leukemia.**

Vyas M, Schneider A, Shatnyeva O, Reiners K, Tawadros S, Kloess S, Koehl S, Hallek M, Hansen H, von Strandmann EP

Oncoimmunology. 2016 July (Online Publication: <http://dx.doi.org/10.1080/2162402X.2016.1211220>)

### **DNA damage response and evasion from immunosurveillance in CLL: new options for NK cell-based immunotherapies. (Review)**

Shatnyeva OM, Hansen HP, Reiners KS, Sauer M, Vyas M, von Strandmann EP.

Front Genet. 2015 Feb

### **Natural ligands and antibody-based fusion proteins: harnessing the immune system against cancer. (Review)**

Vyas M, Koehl U, Hallek M, von Strandmann EP.

Trends Mol Med. 2014 Feb

### **High levels of cleaved caspase-3 in colorectal tumour stroma predict good survival.**

Noble P, Vyas M, Al-Attar A, Durrant S, Scholefield J, Durrant L.

Br J Cancer. 2013 May